Studies of the Tissues and Molecules That Regulate the Migration of Cranial Neural Crest Cells in the Chicken Embryo: Roles of Midline 1 and Retinoic Acid

Thesis

UNRESTRICTED

Studies of the tissues and molecules that regulate the migration of cranial neural crest cells in the chicken embryo: roles of Midline 1 and retinoic acid

Elizabeth Janet Latta

Thesis submitted to The Open University for the degree of Doctor of Philosophy

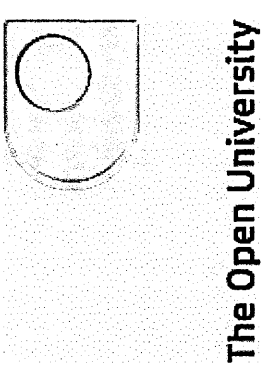

DATE OF SUBMISSION: 28 SEPT 2009

DATE OF AWARD: 18 JUN 2010

ProQuest LLC.
789 East Eisenhower Parkway
P.O. Box 1346
Ann Arbor, MI 48106 – 1346

Acknowledgements

First and foremost I would like to thank my supervisor Jon. You've always been there when I've needed help and have always been full of ideas and inspiration. Thank you for all your guidance throughout my PhD. I would also like to thank Jill, for your support over the years and your help and advice with writing this thesis.

I would like to thanks James, for having useful insights and ideas, as well as reagents. I'd like to thank Emma for taking time to teach me new methods, 'lending' me reagents and being a great role model. My thanks go to the staff of the BRU, Karen and Steve without you things would not have run as smoothly. I'd like to thank Devika and Joan for all their help in the lab over the summer. I would also like to thank the entire CMN group, for always having useful input.

I would like to thank all of the 'original office,' for always having interesting conversation, giving unwavering support and food to eat! Thank you to Kathleen for always being there, always having something to say and always cheering me up when I'm feeling down. Friday pub lunches will never be the same without you. Thank you Ya for always being such a lovely person, I can't fail to feel good around you. Thank you Leon for always making life interesting, if not food orientated, and always listening when I needed someone to talk to.

Hadassah, I'd like to thank you for, not only the help and guidance you have given me in the lab, but also for being such a wonderful friend, I'll never forget all the lunches we had at the OU. I consider myself lucky to have met you. Angie, Heather and Helen, I'd like to thank you all for providing me with much needed time away and some wonderful girly weekends, you're great friends.

Jean and Bill, thank you for your love and support, you provided me with much needed recuperation and spoiling and always taken an interest in my studies. You've always treated me like a member of the family and I can't wait to the day its made official.

Thank you to Joan, for always being there, supporting me, listening to me and taking an interest in what I do, you are the best sister anyone could ask for. Thanks to Jenni for all your love, and my little niece, Jasmine, for all your snuggles and entertainment. Thank you to Melon for always being available for a cuddle whenever I needed them.

Mum and dad, I'd like to thank you for all of the support you've given me, not only the financial kind, and not just during my PhD but my entire education, you've always believed in me and pushed me to believe in myself. I wouldn't be where I am today without you.

Tommy, I don't know what I would have done without you. You have always reminded me of what's important and kept me grounded through the tougher times. You kept me going through it all and I could not have done any of this without you. I always strive to make you as proud of me as I am of you.
I love you.

Abstract

Studies of the tissues and molecules that regulate the migration of cranial neural crest cells in the chicken embryo: roles of Midline 1 and retinoic acid

Cranial neural crest cells (cNCC) emigrate from the neuroepithelium to form the cartilaginous structures of the face and much of the peripheral nervous system of the head. Several genetic disorders and drug compounds can disrupt the patterning of cNCC-derived tissues during development.

I have studied cNCC patterning in the chick embryo, focussing on one genetic disorder (X-linked Opitz syndrome, caused by mutations in the *MIDLINE1* (*MID1*) gene) and one drug compound (retinoic acid).

I demonstrate the expression pattern of the chick orthologue of *MID1* and show that the Mid1 protein, via its effects on Protein Phosphatase 2A, controls the migration of cNCCs and regulates the timing of cranial gangliogenesis, likely by altering cNCC protease activities.

Retinoic Acid (RA) is a diffusible morphogen and well-known teratogen that causes patterning defects in cNCC migration. I provide evidence that the cranial mesenchyme adjacent to rhombomere 3 of the hindbrain is a potent responder to the presence of RA, resulting in cNCC mis-migration. Furthermore, I demonstrate that the 9-cis RA isoform is more potent than the all-trans RA isoform at causing cNCC mis-migration.

Declaration of Originality

I declare that this thesis is the result of my own individual work, except where specifically indicated in the text. This thesis, or any part of it, has not been published elsewhere, or submitted for a degree or any other qualification. All of the work described here was carried out at The Open University, Milton Keynes, between October 2005 and September 2009, under the supervision of Dr Jon Golding and Dr Jill Saffrey.

Contents

List of Figures

List of abbreviations

bHLH	basic helix loop helix
BMP	Bone morphogenic protein
cNCC	cranial neural crest cell
CNS	central nervous system
CRABP	cellular retinoic acid binding protein
DN-Mid1	Dominant negative Midline 1
EF-1	elongation factor-1
Eg	epibranchial geniculate
EMT	epithelial mesenchymal transition
En	epibranchial nodose
Ep	epibranchial petrosal
GFP	green fluorescent protein
GTPases	guanosine triphosphotases
HH	Hamburger Hamilton
mes	mesenchyme
Mid1	Midline 1
Mid1	Midline 1
Mid2	Miline 2
MMP	matrix metalloprotease
NRG	neuregulin
NT	neural tube
OA	okadaic acid
OV	Otic vesicle
PNS	peripheral nervous system
PP2A	Protein Phosphotase 2A
PPAR-gamma	peroxisome proliferator activated receptor -gamma
r	rhombomere
RA	Retinoic Acid
RAR	retinoic acid receptor
RARE	retinoic acid response element
RBCC	RING-finger, B-Box and coiled coil
RXR	retinoid X receptor
SE	surface ectoderm
Sema	Semaphorin
Shh	Sonic hedgehog
SS	Somite stage

TIMP	tissue inhibitor of metalloproteinase
Tm	trigeminal maxillo-mandibular
To	Trigeminal Opthalmic
Ub	Ubiquitin
XLOS	X-linked Opitz syndrome

1. General Introduction

This chapter introduces the development of the head, specifically focusing on the hindbrain and cranial neural crest cells (cNCC). There is particular focus on the role of retinoic acid and other molecules involved in cNCC migration patterning as a background introduction to Chapter 4. Furthermore there is also a section on development of the peripheral nervous system (PNS) involving cNCCs and the role of proteases in development as background for Chapter 3.

1.1. Craniofacial development

Formation of the body plan during development, and tissue repair and turnover in adults require that cells undertake a series of highly stereotyped migrations and cellular differentiation programs. The mechanisms controlling how cells migrate and interact with their environment are still poorly understood. This thesis is concerned with improving our understanding of the mechanisms and molecules that control the migrations of cells which give rise to the peripheral nervous system and the skeletal structures of the head. Defects in the patterning of cell migration, cell survival and cell fate choice, can all lead to craniofacial abnormalities, which account for around one third of human congenital birth defects [1]. There are several craniofacial syndromes in which cell migration patterning abnormalities are thought to be involved, such as First Arch Syndrome [1], Treacher-Collins Syndrome [1] and DiGeorge's Syndrome [2].

1.2. The Developing Head

The developing head consists of three layers: an external sheet of ectoderm, the mesoderm, and in the centre, the neuroepithelium (**Figure 1-1**). Mesenchyme is the mesoderm once the cNCCs begin to migrate into it. Along the anterior-posterior axis of the head, the developing neuroepithelium is broadly divided into three regions: the forebrain, the midbrain and the hindbrain. The hindbrain neural tube is transiently subdivided into 7 lineage restricted metameric segmented units (**Figure 1-1**) called rhombomeres (r).

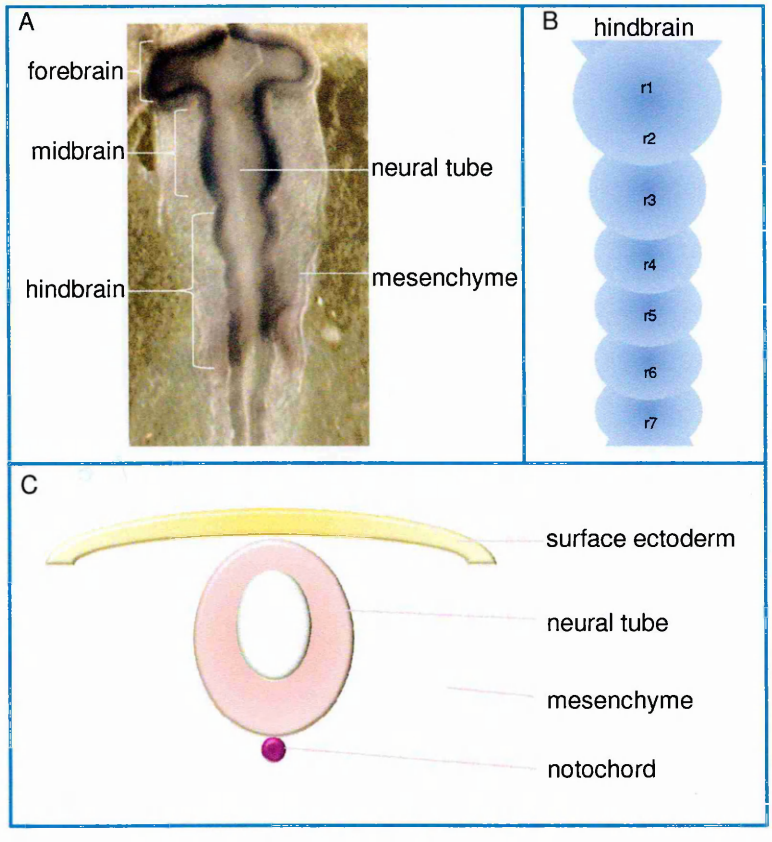

Figure 1-1. Head structure in the early developing embryo

A – a dorsal photo of a chick hindbrain at the 10 somite stage, depicting the areas of the brain and surrounding mesenchyme. B – Structure of the chick hindbrain (dorsal view), depicting the segmentation of the neuroepithelium into rhombomeres (r1-r7) C – schematic diagram of a cross section through the hindbrain portraying the major structures of the developing head, neural tube (neuroepithelium), mesenchyme and surface ectoderm.

The positional identity of each rhombomere can be defined by the expression of a combination of transcription factors (**Figure 1-2**), such as members of the Hox family [3]. For instance, Krox20 is expressed by both r3 and r5, but r5 is distinguished by the additional expression of Hoxa3 and RARα. With regards to gene expression, the cells of odd-numbered rhombomeres resemble each other more closely; r3 and r5 both express Krox20, EphA4, EphB2 and EphB3, whereas r2, r4 and r6 do not. These molecular differences and similarities generate differential cell affinities, such that neuroepithelial cells from odd- and even-numbered rhombomeres, if mixed together, will migrate to re-segregate themselves into two separate odd- and even-populations [4]. This was shown to rely on Eph-Ephrin bi-directional signalling to prevent intermingling of cells from different rhombomeres [4], as **Figure 1-2** shows EphA4, EphB2 and EphB3 receptors are expressed in r3 and r5, whereas the Ephrin ligands, Ephrin B2 and Ephrin B3 are expressed in all rhombomeres except r3 and r5.

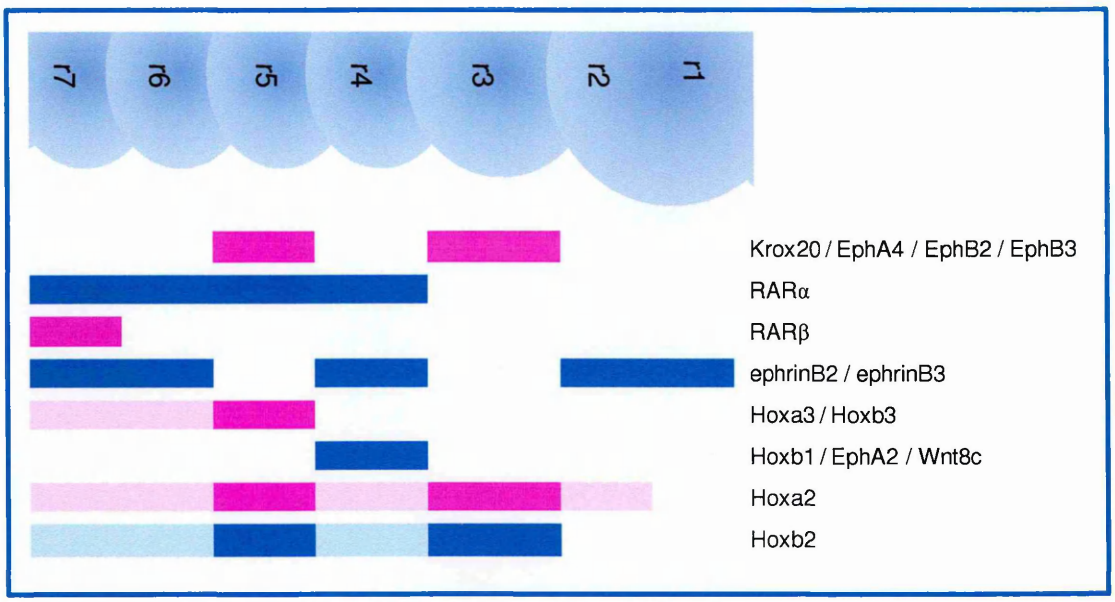

Figure 1-2. Gene expression patterns in the chick hindbrain

A schematic diagram representing the genes expressed in each rhombomere of the hindbrain. Although several genes are expressed in a repeated pattern in every other rhombomere, the combined expression pattern of these genes uniquely defines the identity of each rhombomere. Dark blue and pink represent strong expression of the gene, whereas lighter blue and pink represents weaker expression of that particular gene in the corresponding rhombomere.

1.3. The cranial neural crest

The population of cells that that is the subject of my thesis is the cranial neural crest (cNCC). cNCCs are neuroepithelial cells that can differentiate into connective tissues, glia and peripheral neurons of the cranial ganglia, cartilage and bone. Although crest is produced throughout the dorsal neuroepithelium of the neural tube, in the hindbrain crest only migrates from r2, r4 and r6 into the adjacent mesoderm (creating a mixture of epithelial and mesodermal cells, called the cranial mesenchyme). cNCC migration is constrained into three streams that do not enter mesenchyme adjacent to r3 or r5 (**Figure 1-3**). Rhombomeres 3 and 4 do not output crest directly into their mesenchyme, the

cNCCs they produce migrate rostrally or caudally to even numbered rhombomeres and join the crest streams there. Even though crest is produced by r3 and r5, there is a high level of apoptosis in these rhombomeres that limits the amount of cNCCs that they contribute to the head [5, 6], although this is not solely responsible for the formation of crest stream segregation. The r3 mesenchyme is maintained crest free by as yet uncharacterized growth inhibitory factors that rely on signals from r3 and its overlying surface ectoderm [7].

1.3.1. Neural crest cell induction and delamination of the neural crest from the neuroepithelium

There are 3 main stages the neural crest will go through before its differentiation into multiple cell types (**Figure 1-3**) (reviewed in [8] and [9]),

Induction – the process by which the production of the neural crest cells is initiated

Delamination – at this stage the neural crest cells undergo an epithelial to mesenchymal transition (EMT), leave the neural tube and enter the mesenchyme

Migration – the neural crest cells migrate along defined paths to their point of differentiation

Induction of neural crest cells begins even before the neural tube is formed. At the neural plate stage of development, signals from the non-neuronal epidermal ectoderm, specifically Bmp4, Bmp7 and Wnt6, act upon the neural plate border region and induce NCC formation. The neural plate then invaginates and both sides of the neural plate border come into contact and close to form the neural tube.

Delamination of the neural crest cells can then occur from the dorsal neural tube, this process is called an epithelial to mesenchymal transition (EMT). This involves a change in the cell-cell contacts between the NCCs and the surrounding cells of the dorsal neural tube allowing the NCCs to release themselves from the neural tube and migrate into the adjacent mesenchyme. At this point, the cell adhesion molecules N-CAM, N-cad and cadherin-6B are all down regulated, while cadherin-7 is upregulated. Studies in chick have shown that down regulation of cadherin-6B causes early emigration of NCCs from the neural tube, whereas up regulation of cadherin-6B leads to reduced EMT and cNCCs remaining in the neural tube [8].

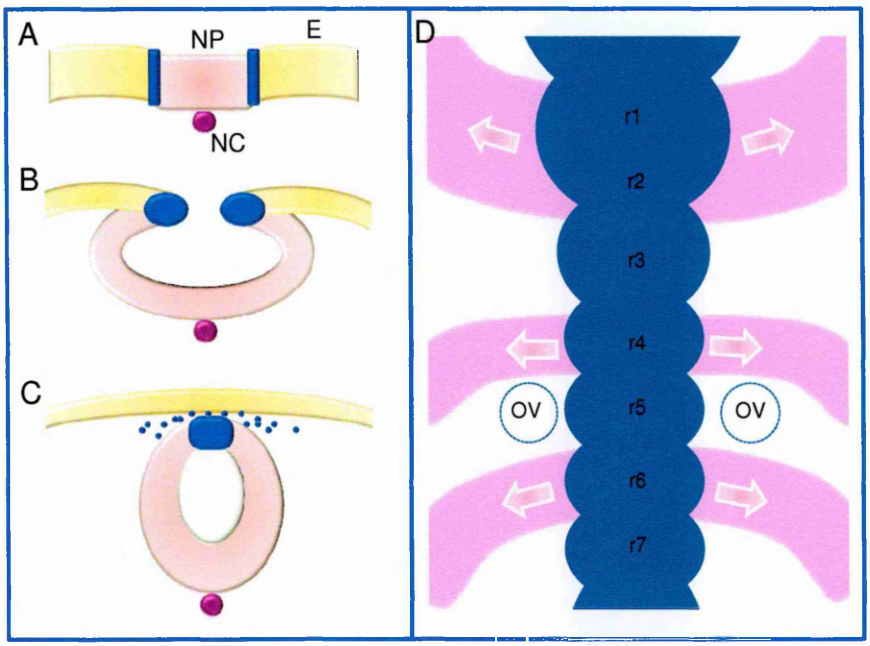

Figure 1-3. Induction, formation and migration of the cranial neural crest.
Schematic diagrams depicting the induction, formation and migration of the neural crest. A – neural plate stage, non-neural ectoderm (yellow) signals induce the production of NCCs (Blue) at the border of the neural plate (pink). B – the neural plate invaginates to form the neural tube with the NCCs meeting at the dorsal part of the forming neural tube. C – the neural tube forms and the NCCs begin to delaminate from the neural tube and migrate into the surrounding mesenchyme. D – schematic diagram showing the migration pattern of the cNCCs (pink) from the hindbrain (blue). NP – neural plate, NC – notochord, E – ectoderm, OV – otic vesicle, r – rhombomere, arrows depict the direction of migration.

The cNCCs, once having undergone EMT, migrate through the mesenchyme in highly defined streams towards the branchial arches. There are three streams of cNCCs, the trigeminal, which is adjacent to rhombomeres 1 an 2, the hyoid, adjacent to rhombomere 4 and the post-otic, adjacent to rhombomeres 6 and 7 (Figure 1-3). The cNCCs that migrate in these streams originate from the rhombomeres immediately adjacent to them and also contain a proportion of cells from r3 and/or r5. The majority of cNCCs produced by r3 and r5 undergo apoptosis; however those that do survive migrate within the neural tube towards an adjacent even numbered rhombomere and then leave the neural tube with that cNCC stream..

1.4. Neural crest and development of the face

The development and migration of the cranial neural crest cells (cNCCs) are essential processes in the early development of the head. Inadequate induction of cNCC development, delamination from the neural tube or incorrect migration of the cNCCs to their point of differentiation leads to craniofacial structural defects, such as cleft lip and palate [1, 10]. **Figure 1-4** demonstrates the origins of the lower facial region are from the maxillomandibular processes, which is cNCC derived [11].

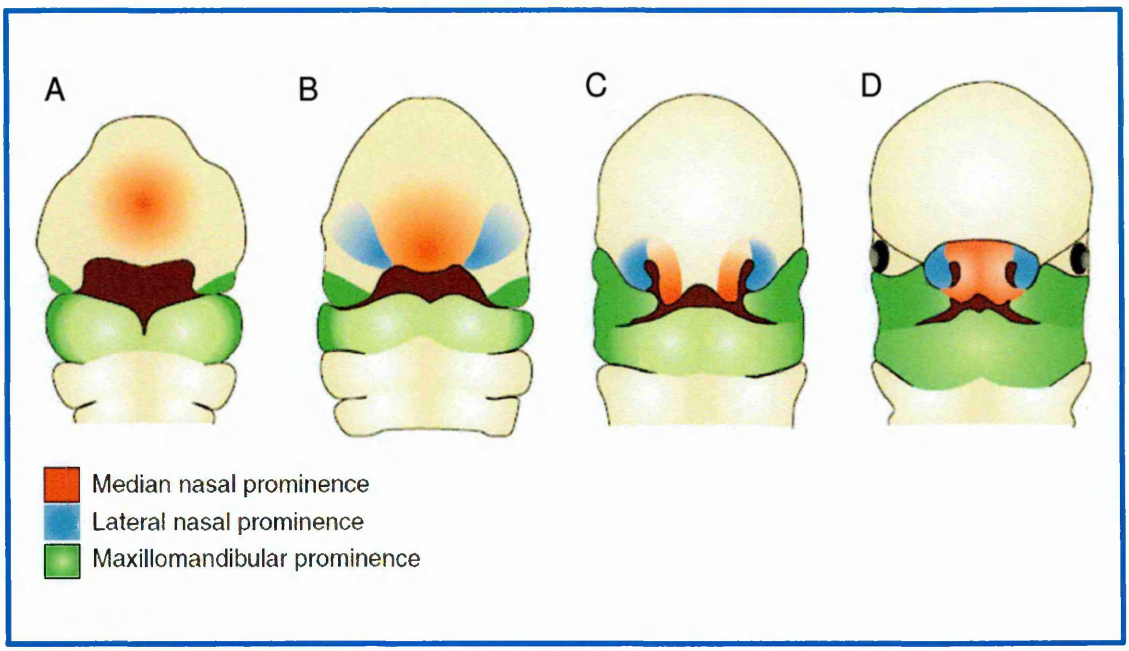

Figure 1-4. Development of facial structures.

A schematic diagram of frontal views of a developing embryo, depicting the origins of the facial prominences. The maxillomandibular processes (also known as branchial arch 1, BA1), of which the cNCCs originate from r1/r2, are highlighted in green, lateral prominences in blue and median nasal prominences in red. The work in this thesis focuses on stage A, which equates to around 3 weeks of human embryo development and 1.5 days in chick. Human embryo development progresses to stage B by about week 4, stage C by week 5 and stage D by around week 6. In comparison chick embryos reach stage B by 2.25 days, stage C by 3 days and stage D by 4.75 days in development. Adapted from Tapadia, Cordero et al. 2005 [11].

1.5. Environmental factors that control the migration pattern of cranial neural crest cells

1.5.1. Mechanisms controlling cell migration

Neural crest cells, like other migratory cell types, integrate growth promoting and growth inhibitory cues from their environment. Cell migration begins by the leading edge of the cell extending the plasma membrane, stabilized by nascent cell adhesions, which strengthen as the cell forms a point of traction over which it can move (reviewed in [12]).

Members of the intracellular second messenger Rho family of small guanosine triphosphotases (GTPases) control cell movements by regulating the formation of these adhesions (Rho) and the formation of the extensions (Rac, Cdc42), the type of extension also depends on which GTPase is activated. Rac activation causes broad extensions called lamellipodia, whereas activation of Cdc42 leads to the formation of long thin extensions called filopodia. These filopodia continuously survey their surrounding microenvironment and recognise guidance cues. There are some growth inhibitory molecules, such as the Semaphorins, that will bind to the cell surface Neuropilin1/plexinA receptor complex and affect second messenger signalling to prevent cell adhesions from forming and cause the filopodia to collapse and thereby turn away from the inhibitory source [13].

1.5.2. Cues that pattern cranial neural crest cell migration

NCCs use both lamellipodia and filopodia to pathfind, maintaining nearly constant contact with neighbouring NCCs via lamellipodia and filopodia and keep long distance contact with the local environment through use of filopodia [14]. NCCs will also often change direction to follow neighbouring cells [14] and tend to migrate in chains of cells [15]. Integration of the mechanisms that control the patterning of NCC migration have yet to be elucidated, however several tissues and genes have been shown to be involved in maintaining the segregation of cranial crest streams.

Here the observed defects in cranial NCC migration have been classified into two groups (Figure 1.5). Firstly a phenotype in which a thin stream of cells connects the r4 and r2 crest streams through r3 mesenchyme (referred to as a Type1 phenotype in this report). Secondly a phenotype that shows cells from the r4 stream disregarding the r3 crest free zone altogether and spreading throughout the r3 mesenchyme (referred to as a Type2 phenotype in this report).

The Type1 phenotype is observed in several situations (Figure 1.5): e.g. following ablation of r3 neuroepithelium or r3 surface ectoderm (SE), or interference with the signalling pathways of ErbB4 (a receptor tyrosine kinase of the EGF receptor family) or Sema3 (a ligand for Neuropilin receptors) or after over stimulation with retinoic acid (RA), (see figure 1.5 for references). The Type2 phenotype occurs in knockouts of Twist, a bHLH transcription factor [16].

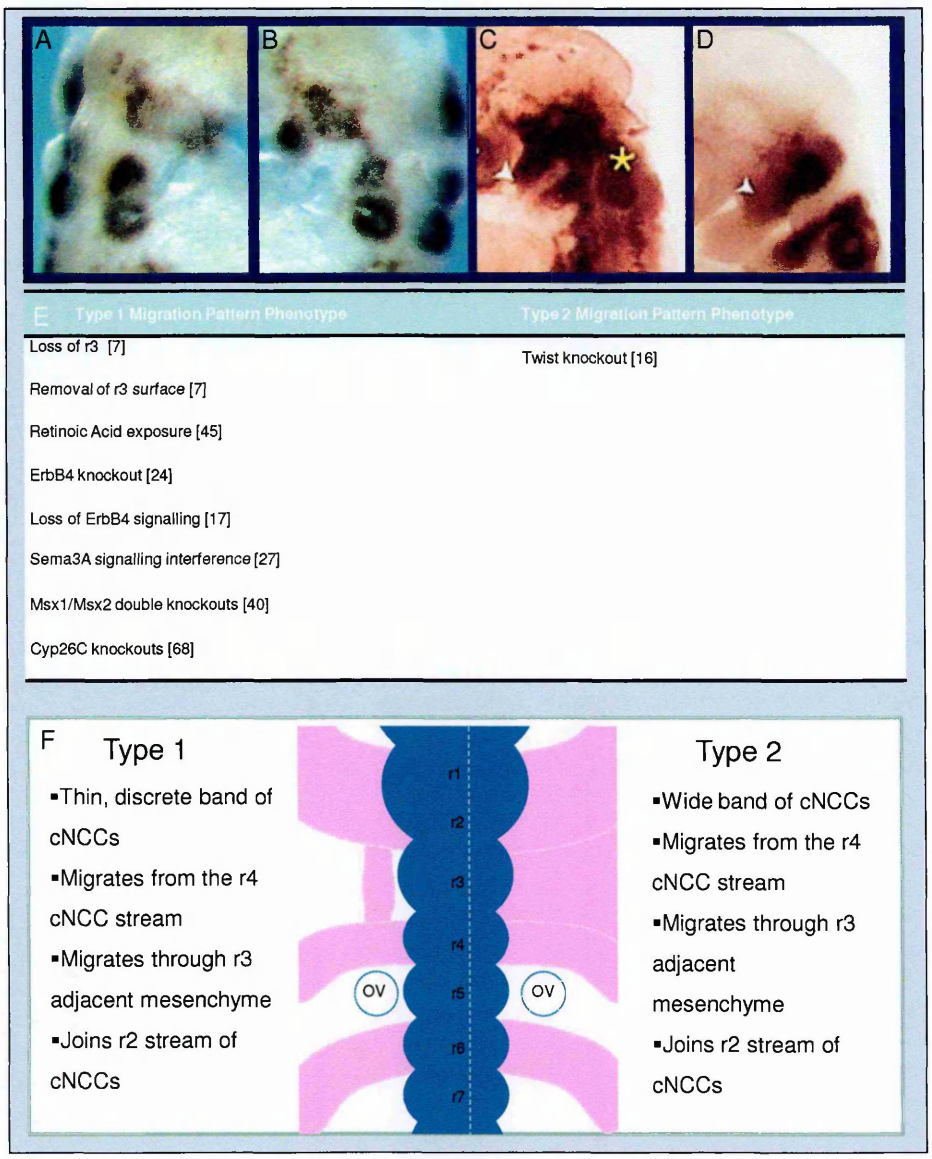

Figure 1-5. Summary and classification of cranial neural crest mismigration phenotypes.

The figures A-D show published examples of cNCC mismigration phenotypes, B shows an example of a typical Type 1 phœnotype as referred to here, showing a discrete band of cNCCs migrating through the r3 mesenchyme. A – control. A-B, sox10 staining following r3 removal [17]. C shows an example of a Type2 phenotype, consisting of a more wholesale movement of cNCCs through the r3 mesenchyme, rather than a thin band of cells. D – control, A-B sox10 staining for cNCCs in a twist knockout mouse [16]. E – table of published instances of each migration phenotype. F – schematic diagram of the cNCC migration pattern and summary of a Type1 and Type2 migration phenotype. cNCCs are shown in pink.

1.5.3. Tissues and molecules involved in patterning cranial neural crest migration

In this section the various tissues that have been found to play a role in maintaining correct cNCC migration patterning will be reviewed, followed by the specific molecules which have been identified to be involved in maintaining correct cNCC migration patterning.

One such tissue responsible for cNCC migration patterning is rhombomere 3, when removed in either mouse or chick embryos a Type 1 mismigration pattern of r4 cNCCs through the r3 adjacent mesenchyme is observed [7, 17]. Rhombomere 5 also has a cNCC free adjacent mesenchyme, however it has been shown that r3 is distinct from r5 as unlike r3, r5 is unable to maintain r3 adjacent mesenchyme cNCC-free, when transplanted in place of r3 [17]. Rhombomere 5, unlike r3, is not necessary to maintain the r5-adjacent NCC-free zone, when r5 is removed the cNCC migration pattern is not affected.

Another tissue found to be important in the maintenance of correct cNCC migration patterning is the surface ectoderm (SE) at the level of r3. When removed from chick embryos the cNCCs migrated through the r3 adjacent mesenchyme towards the r2 cNCC stream, in a Type1 phenotype [7]. Interestingly when the same experiment is repeated with the r5 SE, cNCC mismigration is observed [17]. Thus, it appears that r3 and its SE cooperate to maintain the r3-adjacent cNCC-free zone, whilst the r5-adjacent cNCC-free zone is maintained primarily by the SE over r5.

Eph receptors and their Ephrin ligands are membrane bound proteins involved in bi-directional signaling, transducing both repulsive and attractive growth signals, depending on the cellular context. It has been shown previously that Eph and Ephrin signaling is involved in axon growth cone repulsion, and it has been suggested that a similar

mechanism may be responsible for cNCC guidance, ensuring migration of cNCCs to their appropriate branchial arch and preventing intermingling of cNCCs from different streams [18, 19]. In support of this, chick and *Xenopus* cNCCs express EphrinB2, while either side of the cNCC streams the mesenchymal cells express EphB2 [19, 20]. Furthermore EphB2 and EphrinB2 signaling prevents cNCCs of the second and third branchial arch from intermingling and also correctly targets third arch cNCCs [19].

Ephrin-B1 null mutants exhibit cNCC migration defects, including aberrant neuronal development and abnormal skeletal structures, the cNCCs themselves exhibit a 'wandering' pattern of migration. Although this might be a Type1 like phenotype, as the EphrinB1 null mice show cNCCs from the r6 and r7 joining in a thin stream across the mesenchyme adjacent to r6/r7, it is unclear if this happens through the r3 adjacent mesenchyme [21].

The signaling between ErbB4 and Neuregulin (NRG) is essential to maintain the r3-adjacent cNCC-free zone. Neuregulin 1 (NRG1) is expressed in r4 in chick embryos and in r2 and r4 in mice [22, 23]. The receptor for NRG1, ErbB4, is found expressed in r3. When ErbB4 signaling activity is suppressed in chick, or knocked out in ErbB4 null mice, the cNCCs from r4 show a Type1 migration pattern [17, 24]. Moreover when WT r4 cNCCs are transplanted into an ErbB4 null mouse embryo, the same Type1 mis-migration pattern is observed, conversely if ErbB4- r4 cNCCs are transplanted into a WT embryo the cells migrate normally [24]. Therefore in this case the effect seen is not cNCC autonomous, but is environmental.

Semaphorin (Sema) 3A and 3F also contribute to correct positioning of the cNCC migration pattern. Semaphorins were initially characterized for their importance in axon guidance and nervous system development and act through binding to neuropilins (NRP)

and plexin [25]. It has recently been shown that loss of either SEMA3A or NRP1 causes incorrect migration of cNCCs to the point of differentiation, which leads to ectopic nerve development [26]. Sema3A and Sema3F are found expressed in r1, r3 and r5 in chick hindbrain at 11ss [27]. Sema3F additionally is found expressed strongly in r3 alone at 9ss [27]. Therefore at the stage when the r3 cNCC free zone is important, Sema3A and Sema3F are expressed in r3, making them candidates for maintenance of correct cNCC migration patterning. Indeed when their signaling is impaired, via use of a Neuropilin-Fc or in SEMA3A or NRP1 knockout chicks, a Type1 migration phenotype occurs [27] [28].

The Msx proteins, Msx1 and Msx2, are involved in cell proliferation, differentiation and survival [29-34]. They are downstream effector proteins in the Bmp pathway and in addition are effectors for the Fgf and Wnt siganlling pathways in some tissues [32, 35-38]. In models where defects of Msx1 or Msx2 are present, a variety of NCC development defects have been observed, including cleft palate and cranial skeletal abnormalities [39]. Thus Msx function in cNCCs was investigated; both Msx1 and Msx2 are expressed in premigratory and migratory cNCCs, moreover Msx1/Msx2 double knockout mice the cNCCs exhibit a Type1 phenotype [40]. Therefore the Msx proteins play a vital role in correct cNCC migration patterning.

1.6. Retinoic acid

Retinoic acid (RA) and the Cyp26 group of retinoic acid metabolizing enzymes, are also involved in maintaining correct cNCC patterning.

Retinoic acid is a potent teratogen and was first realized to have an important role in development when rat pups were born with severe congenital deformations to mothers fed on a Vitamin A deficient diet [41]. Correct RA signaling during development is vital for correct formation of an embryo, gradients of RA in the neural tube are used to define antero-posterior patterning, increased local concentrations of RA lead to more posterior cell fates [42]. Furthermore in the hindbrain region RA directly regulates patterning genes, such as the Hox family of transcription factors (reviewed in [42]).

RA has a number of possible isoforms, of these all-trans RA and 9-cis RA receive much attention due to their ability to mediate gene regulation [43]. Endogenous RA is produced from Vitamin A by ADH, producing Retinaldehyde, which is then acted on by RALDH to produce RA (Figure 1-6).

1.6.1.1. Retinoic acid and cranial neural crest migration patterning

It has long been known that overexposure of developing embryos to retinoic acid leads to a range of birth defects, called retinoic acid embryopathies, consistent with NCC mismigration [44]. In line with these early observations, exposure of whole embryos to all-trans RA leads to a Type1 cNCC phenotype, further studies have shown that this can be caused by specifically targeted exposure of r4 to all-trans RA [45]. A study by Gale and Prince [45] showed that injections of all-trans RA into r4 gave a Type1 phenotype, and also altered rhombomere gene expression patterns. Rhombomere 4 showed ectopic Krox20 and a loss of Hoxb1, perhaps indicating a change in r4 to being more r3/r5 like

(**Figure 1-2**). The study also showed that RA injections into r2 or r6 gave no cNCC mismigration, as well as injections of RA into the r2, r3 and r4 adjacent mesenchyme.

1.6.2. Cellular retinoic acid binding proteins (CRABPs)

Cellular retinoic acid binding proteins (CRABPs) are involved in regulating the localisation of RA within the cell. CRABPII is most likely responsible for transporting RA into the nucleus, when RA binds to the CRABPII protein it causes a change in conformation, exposing a nuclear localization signal [46]. Another finding to further support this function of CRABPII is the observation that over-expression of xCRABP in *xenopus* leads to a loss of anterior structures, such as that seen in *xenopus* following RA treatment [47]. This suggests that when more CRABPII is available, transport of RA to the nucleus is more efficient and therefore mimics the effect of having more available RA.

Conversely CRABPI has been shown to have the opposite effect on RA transport, by binding RA and remaining in the cytoplasm, therefore preventing RA signalling. A study in F9 murine carcinoma cells reports that when CRABPI is overexpressed cells become less sensitive to treatment with RA, however when CRABPI expression is reduced, cells become more sensitive to RA [48, 49].

1.6.3. Retinoic Acid Receptors

The retinoids have two known receptors; the retinoic acid receptors (RAR) and the retinoid X receptors (RXR). Both the RAR and RXR have three isotypes, α, β and γ, which are each encoded by separate genes [50-52]. These RAR and RXR receptors have been shown to form both RAR-RXR heterodimers and homodimers [53], additionally RXR has been shown to also form heterodimers with other nuclear receptors, including peroxisome

proliferator- activated receptor (PPAR-γ), thyroid hormone receptor (TR), vitamin D3 receptor (VDR) and the liver X receptor (LXR)[54-58].

RAR has been shown to mainly bind all-trans RA, whereas 9-cis RA binds to both the RAR and RXR receptors, however 9-cis RA has a much lower binding affinity, around 40 times less, to the RAR receptor than the RAR receptor [59]. A study by Shulman and Larson [60] showed that the RXR receptor when dimerised with RAR cannot on its own initiate responses unless the RAR receptor has also been activated. They also show that the RXR receptor under different conditions, such as when dimerised with PPAR-γ, is sensitive to ligand on its own.

1.6.3.1. Retinoic Acid Response Elements

Retinoic Acid Response Elements (RAREs) are binding domains located in the promoter region of target genes. The RARs and RXRs can bind as either hetero or homodimers to the RAREs and repress or enhance transcription of the targeted gene when activated by RA [61]. RAR and RXR hetero or homodimers bind to the RAREs and in the absence of RA binding act to repress gene transcription. This is achieved by the binding of a transcriptional repression complex, which includes a histone deacetylase that represses transcriptional activity [62, 63]. In the event that RA binds to the RA receptors, the transcription repression complex is released and replaced by a transcriptional activator complex, which contains histone acetyltransferase activity, thus allowing a conformational change in chromosomes allowing promoter activation and transcription of the gene [64]. RAREs play a role in early development; both Hoxa1 and Hoxb1 have been shown to have RARE sites in their promoter region, due to the importance of Hox genes in the correct development of the hindbrain, this indicates the significance of correct RA signaling during these processes.

1.6.3.2. Cyp26s and retinoic acid metabolism

The RA metabolizing enzymes, Cyp26A, Cyp26B and Cyp26C are all expressed in embryo hindbrain and mesenchyme during early development. Cyp26A is upregulated by RA and acts to inhibit the metabolism of RA into its metabolites, including 5,6 Epoxy RA, 4-OH RA and 4-oxo RA. These metabolites promote upregulation of Cyp26A and Cyp26B in a positive feedback loop. Conversely Cyp26C is down regulated by RA.

At the 10 somite stage Cyp26A is expressed in the r3 and the r6 adjacent mesenchyme, Cyp26B is expressed in r4 and the r6 adjacent mesenchyme and Cyp26C is expressed in r2/r3 and the r2/r3 adjacent mesenchyme [65-67]. Therefore Cyp26 proteins are expressed in the correct areas and at the stages of development when cNCCs are migrating and their guidance can be affected.

Cyp26A/Cyp26C double knockouts show r4 cNCCs exhibiting a Type1 phenotype [68]. The Cyp26 inhibitor, Fluconazole, when applied globally to rat embryos, also causes a Type1 phenotype, further supporting their importance in cNCC guidance.

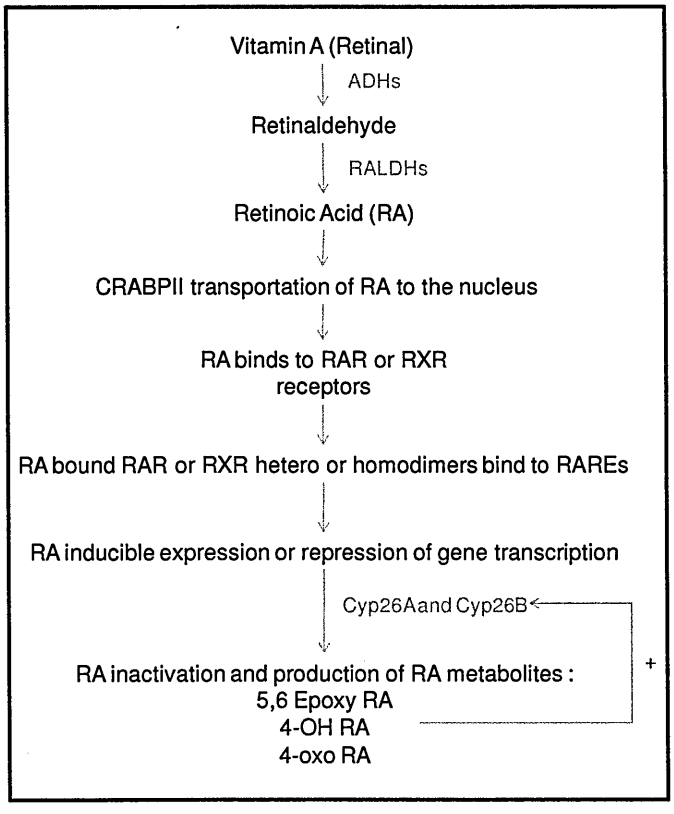

Figure 1-6. Metabolism and function of Vitamin A

Flow chart of the metabolism of Vitamin A into RA and the function of RA before its degradation into its metabolites. Blue text indicates enzymes, red arrow indicates positive upregulation. ADHs – alcohol dehydrogenase, RALDHs –retinaldehyde dehydrogenase

1.7. Development of the cranial Peripheral Nervous System

The cranial neural crest is a pluripotent group of cells that have the ability to form melanocytes, connective tissues, cartilage and bone and also form the neurons and glia of the cranial ganglia. The first cell type to differentiate from cNCCs are the cranial ganglia. Thus, the cranial ganglia are the first "victim" of cNCC patterning defects. The peripheral nervous system in the developing head of an embryo receives contributions from two progenitor cell types. First, there are the cranial neural crest cells, which give rise to neurons and glia of the cranial ganglia. Secondly there are the cells of the neurogenic placodes, these cells contribute neurons to some of the cranial ganglia, the ratio of neurons originating from a cNCC or placode progenitor varies depending on the particular ganglion (Figure 1-7).

1.7.1. The ectodermal placodes

The placodes are recognized as transient focal thickenings in the cranial ectoderm (Figure 1-7). Whilst the neural crest develops both in the head and the trunk of an embryo, the neurogenic placodes develop exclusively in the cranial region. Placodes can also be recognized by their increased cell proliferation rate, in comparison to the surrounding ectoderm [69, 70]. In addition when placodal cells delaminate from the placode, unlike neural crest cells, they do not undergo EMT [70].

The cranial placodes identified to date include the adenohypophyseal, olfactory, lens, trigeminal, profundal, otic, lateral line and epibranchial and hypobranchial placodes [71]. Of these, many are found in vertebrates, with the exception of the hypobranchial placodes which have only been identified in amphibians [71].

The trigeminal placode, in chick, has two subdivisions, the maxillomandibular and ophthalmic placode [72]. These produce migratory placodal cells, which convene with neural crest cells from the r1 /r2 stream, and form the sensory neurons of the trigeminal placode, the maxillomandibular placode contributing to the maxillomandibular processes of the trigeminal and the ophthalmic placode contributing to the ophthalmic processes [73]. One distinct difference observed between the two trigeminal placodes is that the maxillomandibular, like many other placodes, outputs mitotically active cells, whereas the ophthalmic placode produces cells which are post-mitotic [73]. The two trigeminal placodes can also be distinguished by their expression of different neurogenin genes, the maxillomandibular trigeminal placode, along with all the other placodes, expresses neurogenin-1, whereas the ophthalmic trigeminal placode expresses neurogenin-2 [73].

The epibranchial placodes include the geniculate, nodose and the petrosal placodes. Each of these produce neural progenitors that migrate away from the placode and differentiate into sensory neurons that form part of the geniculate ganglion, vagal nerves (nodose) and the glossopharageal (petrosal) ganglion respectively [74]. The development of the epibranchinal placodes are induced by the nearby pharangeal endoderm [75]. In particular BMP7 and FGF signaling have been shown to play an important role in placode initiation, loss of FGF3 and FGF8 function leads to a block in the development of the otic and epibranchial placodes [76-79].

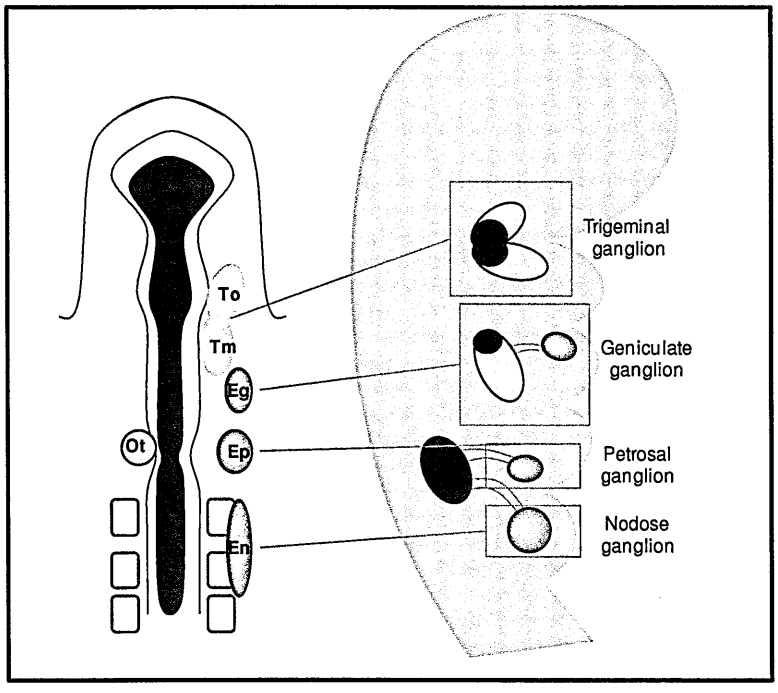

Figure 1-7. Location of the ectodermal neurogenic placodes and contribution of cNCC and placodal cells to the cranial ganglia.

Schematic diagram showing the location of the otic, trigeminal and epibranchial placodes in a developing chick head and their contributions to subsequent development of the cranial ganglia. The locations of the placodes within the embryo head are shown on the right. Green portions of ganglion represent cells that originated from the neural tube, ie cNCCs and other sections of ganglia are colour coded according to the placode from which the cells originated. Eg – Epibranchial geniculate, En – Epibranchial nodose, Ep – Epibranchial petrosal, Ot – Otic, Tm – Trigeminal Maxillomandibular, To – Trigeminal Ophthalmic.

In order for the placodal cells to begin delaminating from the placode and migrating into the mesenchyme to the point of ganglion development, the placode requires contact from the neural crest in order to initiate detachment from the placode [70] (Figure 1-8). In the absence of cNCCs placodal cells do not migrate from the placode, however if the cNCCs make contact with the placode but the stream of cNCCs is discontinued then the neuronal projections from the ganglion that innervate the hindbrain overshoot their destination [80]. Furthermore once the cells of the placode have detached from the placode they use the

neural crest as a scaffold, using them to migrate up the stream of cNCCs, in the opposite direction to the general stream of cNCCs to the point of ganglion development [80].

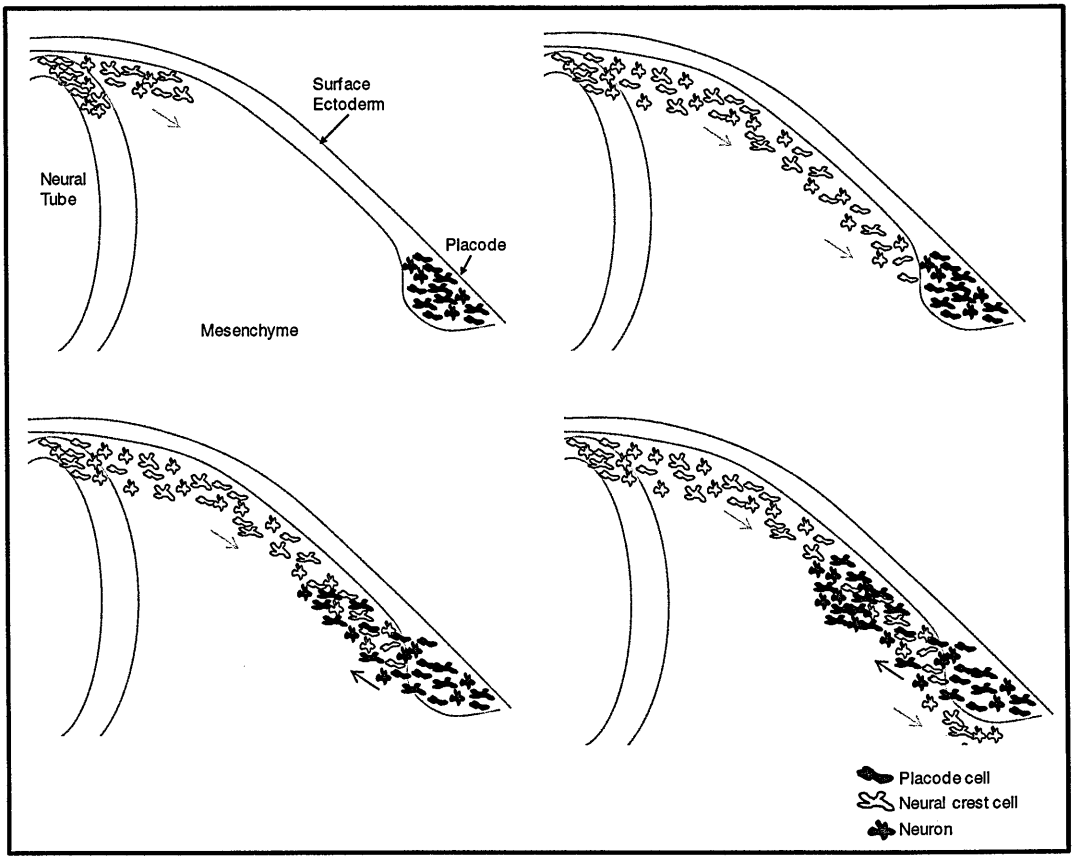

Figure 1-8. Initiation of placodal cell migration by neural crest cells.
Schematic diagram depicting the initiation of placodal cell migration following cNCC migration to the placode location and the subsequent differentiation of the placodal cells at the site of ganglion development. Arrows indicate migration direction of cells, pink cells represent cNCCs, blue cells represent placodal cells and green cells represent neurons.

1.8. Proteases in development

Proteases are enzymes which have the ability to degrade proteins and play a role in development processes, including cNCC EMT and migration (Figure 1-9). Matrix metalloproteinases (MMP's) are a family zinc-dependent proteases, they have the capability of degrading many types of extracellular matrices and make up a subgroup of the metalloprotease(MP) protein superfamily. The MP super family includes several subgroups, including the ADAMs (A Disintegrin And Metalloprotease), ADAMTs (A Disintegrin-like and Metalloprotease with Thrombospondin motifs), membrane bound MMPs (MT-MMPs), and the 'classical' MMPs. Many are expressed during hindbrain development and some have been shown to be not only expressed in neural crest cells but also necessary for their migration.

MMP2, MMP8, Adam10, Adam13, MT1-MMP and Timp2 have all been shown to be expressed by neural crest cells [81-86]. MMP2 has been shown to be expressed in NCCs in chick [82, 87, 88] and MMP8 in NCCs in mice [84]. MMP2 has also been found to be essential for EMT, inhibition of MMP2 leads to failed EMT of NCCs from the neural tube [88], MMP2 is also required for correct migration/delamination of the NCCs from the neural tube [87].

Adam10 is expressed in avian NCCs *in vitro* [85] and Adam13 is expressed in *xenopus* NCCs [81]. Work to date has shown that when defective Adam13 NCCs are transplanted into a normal embryo the NCCs do not migrate, furthermore when normal NCCs are transplanted into a Adam13 defective embryo the WT NCCs can migrate correctly [89].

The expression pattern of MT1-MMP (also recently referred to as MMP14) in *xenopus* has shown it to be expressed in cranial NCCs [86], in chick however the findings are that MT1-MMP is found in the cardiac NCCs [83]. One activity of MT1-MMP is to activate MMP2

[90], therefore it is possible that MT1-MMP is required for NCC EMT and migration as it is upstream of MMP2. Tissue inhibitor of metalloproteinases, (TIMPs) act as regulators of MMP activity, one of these, Timp2, can be found expressed in chick cardiac NCCs. High levels of Timp2 will prevent activation of MMP2 by stopping MTI-MMP action, whereas low levels of Timp2 actually promotes formation of active MMP2 through the promotion of a MMP2-Timp2-MT1-MMP complex [91-93]. Therefore the correct regulation of Timp2 protein levels is most likely important for correct NCC EMT and migration due to its role in both complex formation for activation of MMP2 and also its inhibitive role for MT1-MMP.

Protease	Expression in development	Substrates	Reference
MMP2 (Gelatinase A)	Head and cardiac region (10ss+)	Gelatin, Collagens, laminin-5	[82,87,88]
MMP3 (Stromelysin 1)	-	Collagens, laminin-1, fibronectin	[152]
MMP8 (Neutrophil Collagenase)	Mice NCCs	Collagens	[84]
MMP10 (Stromelysin 2)	-	Collagens, laminin-1, fibronectin	[152]
MT1-MMP (MMP14)	Xenopus cNCCs, Avian cardiac NCCs	Pro-MMP2, gelatin, collagens, laminin-5	[86]
Adam10	Avian NCCs in vitro	N-cadherin	[85]
Adam 13	Xenopus NCCs, Avian head mesenchyme		[81]

Figure 1-9. Table of proteases involved in development

A table of some proteases available during development, particularly those relevant to NCCs and head development, and their known substrates.

1.9. General Aims

The work presented in this thesis aims to further elucidate the mechanisms involved in correct cNCC migration patterning. Particular focus is on identifying if there is a possible common mechanism behind the Type1 mismigration phenotype as described here. At the centre of this query is the role of retinoic acid in cNCC migration patterning.

Furthermore the role of Mid1 in the cNCC cell migration, formation and patterning of the cranial ganglia forms a major part of this research work. Mid1 is the gene found mutated in X-linked Opitz Syndrome, patients present with craniopfacial birth defects, including cleft lip and palate and widely spaced eyes (hypertelorism). This is further explained in section 3.1. A spatio-temporal study of the gene expression pattern of the *MID* genes during development aims to elucidate the presence of Mid1 during cNCC emigration. In addition, the role of Mid1 during early development, with focus on cNCCs, will be investigated by use of expression constructs for Mid1, PP2A (a Mid1 target) and a dominant-negative Mid1 and Okadaic acid (a PP2A inhibitor). Finally the role of Mid1 in the formation of the cranial ganglia will be investigated.

2. Materials and methods

2.1. Materials

2.1.1. Sources of reagents

Reagent (listed alphabetically)	Manufacturer	Catalogue Number
9-cis retinoic acid	Sigma	R4643
Agar	Fisher Scientific	A/1080/48
Agarose	Invitrogen	15510-019
All-trans retinoic acid	Sigma	R2625
Ammonium acetate	Sigma	A1542
Ampicillin	Sigma	A9518
B27 Supplement 100x	Gibco	17504
Beads (Bio-Rad AG 1-X2 resin, 200-400 mesh, hydroxide form)	BioRad	143-1255
Beads affi-gel blue (100-200 mesh)	BioRad	153-7302
Blue/Orange Loading dye 6x	Promega	G1881
BM Purple (alkaline phosphotase substrate)	Roche	11 442 074 001
Boehringer blocking reagent	Roche	1 096 176
Cell tracker CM-DiI	Molecular Probes	C7000

Cell tracker CM-FDA	Invitrogen	C2925
CO2 Independent Medium	Gibco	18045-054
Diethyl pyrocarbonate (DEPC)	Sigma	D5758
Dimethyl sulfoxide (DMSO)	Sigma	D5879
ECL Western Blotting analysis system	Amersham	RPN2109
EDTA	Sigma	E5134
Ethanol (EtOH)	VWR	20 819.298
Ethidium Bromide	Fisher Scientific	E/P800/03
Fast Red tablets (alkaline phosphotase substrate)	Roche	11 496 549 001
Fetal bovine serum	Sigma	F-7524
Fibronectin	R&D systems	1030-FN
Fluorescent Mounting Medium	DakoCytomation	S3023
Formamide	Aldrich	22,119-8
Glycerol	Sigma	G9012
Hybond nitrocellulose membrane	Amersham	RPN303F
Ipegal CA-630 detergent	Sigma	18896
L-Glutamine	Sigma	G8540
Lipofectamine LTX reagent	Invitrogen	15338-100
Magic Mark	Invitrogen	LC5602

Marval skimmed milk	Tescos	
Methanol (MeOH)	BDH	101586B
Molecular Weight ladder 1kb	NEB	N3232S
Molecular weight ladder –low	NEB	N3233S
N2 Supplement 50x	Gibco	17502048
Okadaic Acid – sodium salt	Calbiochem	459620
Paraformaldehyde (PAF)	Sigma	P6148
Phosphate Buffered Saline (PBS) Tablets	Sigma	P4417-100TAB
PLUS reagent (lipofection reagent)	Invitrogen	11514-015
Potassium chloride (KCl)	Sigma	P9541
Ready Gel 10% Tris-HCL	BioRad	161-1155
RNaseOUT™ (Ribonuclease Inhibitor)	Invitrogen	10777-019
Sheep serum	Sigma	S3772
Sodium chloride (NaCl)	Sigma	SS7653
Sodium citrate-tribasic dihydrate	Sigma	C8532
Sodium Deoxycholate	Sigma	D6750
Sodium dodecyl sulfate (SDS)	Sigma	L4390
Sodium hydroxide (NaOH)	Fisher Scientific	S/4920/53
Sucrose	Fisher Scientific	S/8600/60

SureClean (DNA cleanup kit)	Bioline	BIO-37042
Tris-Borate-EDTA buffer 10x Concentrate	Sigma	T4415
Triton X 100 detergent	Sigma	T8787
tRNA from baker's yeast	Sigma	R5636
Tryptone	Fisher Scientific	BPE1421
Tween 20 detergent	Sigma	P9416
Yeast extract	Fisher Scientific	BPE1422

2.2. Antibodies

2.2.1. Primary antibodies

Antibody	Species	Immunogen / Clone	Application* and dilution	Company	Catalogue Number
Actin	Mouse	β-actin N-terminus	WB – 1:2000	Sigma	A1978
BrdU	Rat	BrdU (clone BU1/75)	IF – 1:500	Abcam	Ab6326
DIG-alkaline phosphotase (AP) conjugated	Sheep	Digoxigenein (DIG)	ISH – 1:1500	Roche	11 093 274 910
FITC	Goat	FITC	IF – 1:1000	Abcam	ab19224
FITC- alkaline phosphotase (AP) conjugated	Sheep	Fluorescine (FITC)	ISH – 1:1500	Roche	11 426 338 910
GFP	Rabbit	whole GFP molecule	IF – 1:3000	Abcam	ab290
HNK-1	Mouse	Clone VC1.1	IF – 1:2000	Sigma	C0678

Laminin	Mouse		IF -		
Neurofilament	Mouse	phosphate independent epitope in carboxy terminus (Clone RMO-270)	IF – 1:100	Zymed	13-0700
Pax2	Rabbit	aa 188-385 of Pax2	IF – 1:100	Abcam	ab37129
Pax3	Mouse	C-terminal region (aa298-481)	IF – 1:1000	Developmental Studies Hybridoma Bank	
PP2A	Rabbit	PP2A catalytic subunit (A and B forms)	WB -1:1000	Cell Signalling Technologies	2038

*IF – Immunofluorescence, ISH – In-situ hybridisation, WB – western blot

2.2.2. Secondary antibodies

Antibody	Species	Immunogen / Clone	Application* and dilution	Company	Catalogue Number
Alexa Fluor 488	Goat	Anti mouse	IF – 1:200	Molecular probes	A11029
Alexa Fluor 488	Goat	Anti rabbit	IF – 1:200	Molecular Probes	A11034
Alexa Fluor 488	Goat	Anti rat	IF – 1:200	Molecular Probes	A11006
Alexa Fluor 594	Goat	Anti mouse	IF – 1:200	Molecular Probes	A11032
Alexa Fluor 594	Goat	Anti rabbit	IF – 1:200	Molecular Probes	A11037
HRP conjugated	Goat	Anti mouse	WB – 1:15000	Pierce	E7756556
HRP Conjugated	Goat	Anti rabbit	WB – 1:15000	Pierce	E7756789

*IF – Immunofluorescence, WB – western blot

2.2.3. Kits

Kit	Company	Catalogue Number
ApopTag Red *In Situ* Apoptosis Detection kit	Chemicon	S7165
DC assay	BioRad	500-013, 500-014, 500-015
HiSpeed Plasmid Maxi kit	Qiagen	12662
QIAprep Spin Miniprep kit	Qiagen	27106
Spin Prep Gel DNA kit	Novagen	70852-3AT

2.2.4. In-situ hybridisation mRNA probes

Probe target	Plasmid vector	Restriction Enzyme for linearisation	Polymerase for antisense probe	Reference
cCyp26A	pGEM-T Easy vector	*Bam*HI	T7	[94]
cCyp26B	pGEM-T Easy vector	*Kpn*I	T7	[66]
cCyp26C	pGEM-T Easy vector	*Sal*I	T7	[67]
cErbB4	pCR-Script SK +	*Hind*III	T3	[23]

cKrox20		*Hind*III	T7	[95]
cMid1	pCAβ	*Not*I	T3	[96]
cMid2	pCAβ	*Not*I	T3	[97]
cSox10	pBluescript SK-	*Hind*III	T3	[98]

2.2.5. Expression constructs

Recombinant proteins	Vector	Reference
cMid1 - IRES eGFP	pCAβ	[96]
dN.cMid1/2 – IRES eGFP	pCAβ	[97]

2.2.6. Enzymes

Enzyme	Buffer	Company	Catalogue Number
*Eco*RI	Roche Buffer H	Roche	10 703 737 001
*Hind*III	NEB 2	NEB	R0104S
Proteinase K	-	Sigma	P-2308
*Sal*I	NEB 3	NEB	R0128S
Sp6 RNA polymerase	10x RNAPol Reaction Buffer	NEB	M0207S
T3 RNA polymerase	Transcription Buffer	Roche	11 031 163 001

T7 RNA polymerase	10x RNAPol Reaction Buffer	NEB	M0251S
*Xba*I	NEB 2	NEB	R0145S
*Xho*I	NEB 2	NEB	R0146S
*Not*I	NEB 3	NEB	R0189S
*Bam*HI	NEB BamHI buffer	NEB	R0136S
*Kpn*I	NEB 1	NEB	R0142S

2.2.7. PCR primers

mRNA	Forward Primer sequence	Reverse primer sequence	Reference
cAdam10	CCAAACTCACAGTGGGACCT	TGCATTCCATTCCAGAATCA	*
cMMP10	GCCCTTCAGAAAAATGGTCA	CACTTCTGGAGCAAATGCAA	*
cMT1-MMP	GAAGTGTCGACCCGGAAAC	GGTTCTGAAGGCAGAAGGTG	*
cTimp2	GAACCCCATCAAGCGAATCC	GGCGTGGACCAGTCTAACAT	[83]
GAPDH	TGGGTGTCAACCATGAGAAA	CATCCACCGTCTTCTGTGTG	[99]

* Primers were designed using Primer-Blast (Pubmed)

2.2.8. Equipment

Equipment	Company	Catalogue / Model number
Electrode holder (single)	Intracel	01-927-09 and 01-926-09
Borosilicate capillary glass	Clark electromedical instruments	GC100F-10
Footswitch	Intracel	01-920-09
Silver electrode (offset pole)	Intracel	01-929-06
TSS20 Ovodyne electroporator	Intracel	01-916-02
Tungsten electrode (5mm tip)	Intracel	01-935-06
Hybaid shake 'n' stack hybridisation oven	Thermo Electron Corporation	
Dissecting microscope	Motic	SMZ168
Fluorescent dissecting microscope	Nikon	DS-L2, SMZ1000, P-FLA2, C-HGFI
Vibratome		
Time-lapse microscope		
Twist shaker	Finemould Precision Ind. Co.	TW3

2.3. Reagent preparation

2.3.1. Transformation and plasmid preparation

Transformation of XL1-Blue competent cells (Stratagene) was carried out following the manufacturer's instructions. Transformed cells were grown overnight before plasmids were extracted and purified (Qiagen QIAfilter Plasmid Maxi kit). For use in electroporations, plasmids were further concentrated (Bioline Sure Clean system) to 10µg/µl.

2.3.1.1. Creating a PP2Ac expression construct

A PP2A expression construct was made by excising the PP2Ac DNA from a pCMV plasmid [100] and inserting it into the pCAB - IRES eGFP empty vector [96]. This was achieved using the SalI restriction enzyme to remove the PP2Ac fragment from the pCMV vector, the fragment was then isolated by running the digest on a 2% agarose gel with ethidium bromide. The PP2Ac was then cut from the gel following visualisation on a low energy UV lightbox and purified using a Quiagen Gel Extraction Kit. The pCAB vector was then linearised using a BamHI-ClaI double digest. The linear pCAB vector and PP2Ac fragment were then blunt ended using Klenow DNA polymerase. The pCAB vector was then incubated in Shrimp alkaline phosphatase (SAP) to dephosphorylate the ends and prevent recircularisation. Following this the mix was then heated to 65°C to inactivate the SAP. The pCAB vector and PP2Ac fragment were then ligated together using T4 DNA ligase. The resulting plasmid was then used to transform XL1 Blue competent cells. Transformed cells were grown overnight before colonies were picked and the DNA extracted and purified (Qiagen QIAfilter Plasmid Maxi kit). The isolated plasmids were then checked for correct orientation of the PP2Ac insert using a SalI-KpnI sequential digests. One plasmid with a correctly orientated PP2A fragment was selected and prepared for electroporations as in 2.3.1.

2.4. Solutions

2.4.1. Paraformaldehyde (PAF) fixative

To make a 4% PAF / 4% DMSO solution16g of paraformaldehyde and 2 PBS tablets were dissolved in 360ml of ddH_2O by heating on a magnetic stirrer. Once warm a little concentrated NaOH was added to the solution until the paraformaldehyde had dissolved. After the solution had cooled 40ml of DMSO was added and the pH was adjusted to pH7 and then stored at -20℃.

2.4.2. DEPC treatment of water

1ml of DEPC was added to a litre of sterile ddH_2O, thoroughly mixed and then incubated overnight in a water-bath at 37℃, the H_2O was then autoclaved before use.

2.4.3. Composition of various solutions

Solution	Ingredients	Application*
Blocking buffer	2.5g Marvel, 50ml TTBS	Western Blot
Dent's fix	20% DMSO, 80% MeOH	IF
ISH Detergent Solution	1% IPEGAL, 1% SDS, 0.5% Sodium Deoxycholate, 50mM Tris-HCL (pH 8), 1mM EDTA (pH8), 150mM NaCl	ISH
ISH Wash solution	50% Formamide, 2x SSC, 1% SDS	ISH
Luria Bertani (LB) agar	10g Tryptone, 5g yeast extract, 5g NaCl, 15g agar, made up to 1 litre dH2O (pH7.5) +ampicillin (100ng/ul)	Transformations
Luria Bertani (LB) media	10g Tryptone, 5g yeast extract, 5g NaCl, made up to 1 litre dH2O (pH7.5) +	Transformations

ampicillin (100ng/ul)

Lysis buffer	1xTNE buffer, 1% Triton X100, inhibitor cocktail (Aprotinin, Leupeptin, Pepstatin) at 1/100 dilution	Western Blot
NTMT	100mM NaCl, 100mM Tris-HCL (pH 9.5), 50mM MgCl2, 1% Tween 20	ISH
PAF fixative	4% PAF, 4% DMSO, pH7	IF, ISH
PBST	PBS, 0.1% Tween 20	IF
Pre-Hybridisation Solution	50% Formamide, 5x SSC, 2% SDS, 200ug/ml RNA, 2% Boehringer Blocking Reagent, 50ug/ml heparin	ISH
PTW	PBS, 1% Tween 20	ISH
Running buffer	30.3g Tris base, 144g Glycine, 10ml 10x SDS in 1 litre dH_2O	Western Blot
Sample Buffer	2% SDS, 10% Glycerol, 2.5% Mercaptoethanol, 125mM Tris pH 6.8, Bromophenol blue crystals	Western Blot
SOB	20g Tryptone, 5g yeast extract, 0.5g NaCL, 10ml filter sterile 1M $MgCl_2$, 10ml filter sterile $MgSO_4$ in 1 litre dH_2O	Transformations
TAE 50x	50mM EDTA, 5.71% acetic acis, 2M Tris-HCl	Electrophoresis

TBS	250mM Tris-HCL (pH 7.5), 1.36M NaCl, 26.8mM KCl	ISH
TBST	TBS, 1% Tween 20	ISH
Transfer buffer	3.03g Tris base, 14.4g Glycine, 200ml methanol in 1litre dH_2O	Western Blot
TTBS	500µl Tween in 1litre TBS	Western Blot

*IF – Immunofluorescence, ISH – In-situ hybridisation

2.5. In ovo manipulations

2.5.1. Egg preparation

White leghorn fertilised eggs (Joice and Hill, Norfolk) were placed horizontally in egg trays and sprayed with 70% ethanol before incubating in a humidified incubator at 38°C (±1°C) until the embryos reached the appropriate Hamburger Hamilton (HH) stage. A small hole was made in the wide end of the horizontal egg and 2ml of albumin removed using a needle and syringe. A window was then cut in the side of the egg (~2cm in diameter), and contrast to the embryo provided by injecting a solution of Sugarflair Colours paste (Liquorice) in PBS (1% v/v) underneath the embryo through the blastodisk. After experimental manipulations (detailed in 2.2.2) the eggs were resealed using sellotape and placed back into the incubator for the required incubation period.

2.5.2. Labelling with cell tracker dyes

Cell tracker dyes are lipophilic fluorescent dyes that intercalate into the cell membrane and allows the labelled cells to be tracked, labelling is also passed onto daughter cells allowing cells to be tracked through several cell divisions. Two spectrally distinct cell

trackers were used: one red (CM-DiI, excitation at 553nm and emission at 570nm) and one green (CM-FDA, absorption at 492 nM and emission at 517 nm). CM-DiI is still present after fixation and permeabilization as it is a DiI derivative that binds covalently to thiols in the cell membrane. For use *in ovo* the cell tracker was prepared by dissolving 1 vial of cell tracker (50µg) in 10µl of DMSO, then 90µl of 20% sucrose was added and the vial vortexed. Prepared dyes were stored at 4°C for up to 4 months.

2.5.2.1. Surface ectoderm labelling

To label cells of the surface ectoderm, the vitelline membrane was removed and 2µl of the cell tracker solution was pipetted over the head of the embryo. This was done 10 mins after electroporations to allow the neural tube to close up a little and bubbles to dissipate, or 10 mins before bead placement to allow labelling of the SE without the bead obstructing any tissues.

2.5.2.2. Neural crest labelling

Cranial neural crest cells were labelled by flooding CM-DiI into the lumen of the neural tube. First a small puncture was made in the neural tube using a glass needle at the anterior forebrain to relieve pressure, and then the CM-DiI was injected into the neural tube at the level of the first/second somite. The embryos were given at least 30 mins to allow the dye to label the cells. The excess dye was then flushed out of the neural tube with PBS to prevent spreading of the dye during further manipulation of the embryo.

2.5.3. Bead implantation/placement

Beads were used to provide a localised, sustained exposure of the compound to the targeted tissue [101]. Three different types of implant/placement were employed

- Implantation of a bead into the cranial mesenchyme adjacent to r2, r3 or r5.

- Insertion of a bead into the lumen of the neural tube at the level of r2, r3 or r4.
- Placement of a bead over the surface ectoderm.

Three different types of bead were used to deliver compounds to the tissues, hydroxide and formamide ion-exchange beads and affi-gel blue beads. The hydroxide and formamide beads were used to deliver the retinoic acids due to the ability of the beads to adsorb charged molecules. The Affi-gel blue beads have the ability to bind neutral molecules and so were used to deliver the Cyp26 inhibitors and Okadaic Acid.

The hydroxide beads were prepared by washing in PBS (1 x 5 mins), spinning down the beads and removing the supernatant, then washing the beads in DMSO (1 x 10 mins), before spinning down, removing the supernatant and finally resuspending the beads in RA diluted in DMSO. Formide beads were prepared by washing the Hydroxide beads in dH_2O (1 x 5 mins), then incubated in 1M formic acid for 10 mins, before washes in dH_2O (2 x 5 mins). The beads were placed in DMSO (1 x 5 mins) before adding the retinoic acid of the appropriate concentration. Both formamide and hydroxide beads were left to incubate in the dark for 30 mins before a wash in PBS just before use. To prepare the affi-gel blue beads the beads were washed in PBS (1 x 5 mins, then 2 x 10 mins) before incubating the beads in a solution at the correct concentration of the required compound for at least 30 mins. Beads were washed briefly in PBS immediately before use.

Individual beads were maneuvered into place using a glass needle, for implants incisions were made where the bead was to be placed and the tip of a glass needle used to push the bead into the incision. The eggs could then be sealed and returned to the incubator.

When beads were placed over the r4 surface ectoderm, before removal it was always checked that the bead had stayed on the correct side of the embryo, as the beads are not fixed in place, and as the embryos turn as they grow the beads could move out of

position. Most of the time beads settled in the developing otic vesicle, which means that the r4 mesenchyme should still be receiving an effective dose of OA.

2.5.3.1. Retinoic acid (RA)

9-cis retinoic acid and all-trans retinoic acid were dissolved in DMSO to a stock concentration of 0.1M (stored at -20°C), working concentrations were made by diluting the stock further in DMSO. The retinoic acid was kept in the dark and only used under a safe light. The light exposed RA was made by exposing 50mM all trans RA to direct sunlight (in summer) for a day.

2.5.3.2. Okadaic acid (OA)

Okadaic Acid salt was dissolved in ddH_2O to a stock concentration of 30.2µM and kept at -20°C in a dark container. Concentrations used were 10nM for beads (2.2.3.2) and 1nM for the cell cultures (2.4.4). The OA was always stored in the dark and only used under a safe light due to the light sensitivity of OA.

2.5.4. Retinoic acid injections

Injections were also used as an alternative delivery method for RA to beads as used in previous studies [45]. Various concentrations of RA (all-trans, 9-cis and light exposed) in CM-DiI (2.5µg/µl) were used to target one side of a single rhombomere by injection. The CM-DiI allowed the injection site to be confirmed and also labelled the neural crest allowing quick identification of embryos with a phenotype. Glass needles were used to deliver the solution into the rhombomere, a mouthpiece was used to fill the needle and subsequently inject the targeted tissue.

2.5.5. Electroporations

Electroporations were carried out using an Intracel system (2.1.7) with a flat positive silver electrode and pointed negative tungsten electrode. The lumen of the neural tube was flooded with the desired plasmid by puncturing the front of the forebrain and then injecting the plasmid at the level of the second somite. The negative tungsten electrode was placed inside the neural tube while the positive silver electrode was placed on the surface of the embryo. Two parameters for electroporations were used, one for targeting single rhombomeres, which is localised to the middle of the dorsal-ventral axis of the rhombomere. The second gives good electroporation results throughout the whole dorsal-ventral axis of the neural tube on the targeted side with a spread of around 6 rhombomeres.

Very localised single unilateral rhombomere targeting - 7V, 2 pulses, 20ms pulse width, 200ms space. This technique was most commonly used for *in ovo* electroporation.

Widespread unilateral rhombomere targeting - 20V, 2 pulses, 50ms pulse width, 200ms space. This second technique causes substantial damage to the rhombomeres immediately targeted, therefore tissue 3 rhombomeres up or down from the targeted area was electroporated. Due to the wide spread targeting of the technique the intended rhombomere was well electroporated without any tissue damage. This technique was used for electroporation of tissue for western blotting.

2.5.6. Rhombomere transplantations

To label all the cells in an explant, rhombomeres were removed from donor embryos of the appropriate age and incubated at 37°C for 4 hours in complete DMEM (2.4.1.1) containing RA and CM-FDA (1:1000). The explants were then washed in fresh warm media (1 x 5 mins, then 2 x 30 mins). The NCC's in host embryos were labelled by flooding the neural tube with CM-DiI (2.2.2.1) for 30 mins, the neural tube was then

washed by injecting PBS to flush out the unbound CM-DiI. The host rhombomere could then be removed and replaced with the labelled donor tissue.

2.6. Embryo tissue processing

2.6.1. In-situ hybridisation

2.6.1.1. Riboprobe synthesis

Insitu-hybridisation riboprobes were synthesised by first linearization of the plasmid DNA using a restriction enzyme (RE) with a cut site at the beginning of the gene. The antisense probe is then synthesised using a DNA polymerase with a primer site at the end of the gene and dNTP's labelled with either a digoxigenein (DIG) or fluorescine (FITC) tag (2.1.1.4).

The template DNA is first linearised using the following recipe. This ensures that the riboprobe is only as long as the gene by preventing the DNA polymerase from continuing further around the plasmid past the beginning of the gene.

Ingredient	Volume
plasmid DNA (10µg/µl) *	1µl
restriction enzyme *	5µl (100units)
10x buffer *	5µl
dH_2O	39µl (or 34µl dH_2O and 5µl 10x BSA if required)

* see table 2.1.4 for exact combinations of plasmid, restriction enzyme and buffer

Incubation was at 37°C for 1 hour, then heat inactivated by incubating at 65°C for 15 mins.

The linear plasmid DNA product of this RE digest was then used as a template for riboprobe synthesis using the following protocol.

Ingredient	Volume
linear DNA (0.2µg/µl) from 2.3.2.2 *	3µl
10x DIG or FITC labelling mix	2µl
10x transcription buffer	2µl
RNase Inhibitor	0.5µl
Polymerase *	2µl
dH_2O	8.5µl

* see table 2.1.4 for exact combinations of polymerase and plasmid

Samples were incubated at 37°C for 2hours. The riboprobe was then precipitated by addition of the following to each sample.

Ingredient	Volume
0.2M EDTA pH8	2µl
7.5M NH_4Ac	3.3µl
dH_2O	30µl

The samples were vortexed and then 160µl of ice cold ethanol was added to the mixture and incubated at -20°C for 1 hour. The samples were spun at 4°C at 23,000 xg for 30 mins and the supernatant discarded, the precipitated riboprobes were then washed in 300µl of 70% ethanol, and spun at 4°C for 15 mins, the supernatant was removed. The

remaining pellet was air dried for 5 mins to remove residual ethanol then resuspend in 25µl TE / 25µl formamide. This method generates a huge excess of riboprobe to template therefore the template is not removed. Riboprobes were maintained at -20°C (or -80°C for long term storage).

2.6.1.2. Gel electrophoresis

DNA digests, plasmids preps and probes were run on 0.8% agarose gels, made with 2 x TAE and 0.5µg/ml of ethidium bromide. Gels were run in 2 x TAE at 50V for 40 mins and then visualised using a FirstLight UV transilluminator and the VisionWorks LS image capture software.

2.6.2. In-situ hybridisation on wholemount embryos

Embryos were dissected to remove excess tissues and membranes, and left in PAF fixative overnight at 4°C. The embryos were then washed (3 x 5 mins) in PTW before being dehydrated in increasing concentrations of methanol (25%, 50%, 75%, 100%) in PTW with a 5 min incubation in each concentration. Embryos could then be stored at -80°C until needed.

Embryos were rehydrated in decreasing concentrations of methanol (75%, 50%, 25%) in PTW, before 2 washes in PTW only, each incubation and wash was 5 mins. Tissues were then bleached in 6% H_2O_2/ PTW for 1 hour and washed again in PTW (3 x 5 mins).

The embryos were placed in ISH detergent solution for 1 hour with 3 changes of wash, before refixing in 4% PAF / 0.2% Glutaraldehyde. The fixatives were washed out of the tissue with PTW (3 x 5 mins).

Embryos were then incubated in pre-heated pre-hybridisation solution for 1 hour at 70°C. The pre-hybridisation solution was then replaced with hybridisation solution containing the RNA probe/s and incubated at 70°C overnight.

The probe and hybridisation solution were removed and the embryos washed in pre-heated (70°C) ISH wash solution (first 2 x 5 min, then 6 x 30 mins). The ISH wash solution was then washed out of the tissues using TBST (3 x 5 mins) before blocking in 10% sheep serum / TBST for 2 hours. The embryos were then incubated in the AP-conjugated antibodies (α-DIG or α-Fitc, see 2.1.2.1) overnight in 2% sheep serum / TBST at 4°C.

The embryos were washed in TBST (first 2 x 5 mins, then 5 x 1 hour and finally overnight) before incubating in NTMT (3 x 10 mins). The chromogenic AP substrate (BM purple or fast red) was then added to the embryos and incubated in the dark at 4°C to allow the colour to develop.

Once the colour had developed sufficiently, the reaction with the substrate was stopped by addition of 0.1% Tween 20 / 1mM EDTA / PBS (3 x 10 mins).

For a double insitu the activity of the first antibody was eliminated by dehydrating the embryos in 100% methanol for 15 mins. The tissues were then rehydrated into TBST (2 x 5 mins) and re-blocked for 1 hour in 10% sheep serum / TBST. The embryos are then incubated with the second antibody overnight in 2% sheep serum / TBST. The steps following were the same as for the first antibody only a different substrate is used. The weakest probe is stained for first, as the message can degrade with time and processing.

All steps were carried out on a rocking platform, at room temperature unless otherwise stated. All solutions were made using DEPC treated dH_2O to prevent contamination by RNases.

2.6.3. Immunostaining wholemount embryos

2.6.3.1. PAF fixative protocol

Embryos were dissected, removing all excess membranes and the caudal end of the embryo from about the 3rd somite. Embryos were then fixed in PAF fixative overnight at 4°C.

Embryos were washed in PBS 3 times for 5 mins, and then permeabilised and blocked in 0.3% TX100 / 20% sheep serum in PBS. The primary antibodies (2.1.2.1) were added in 0.1% TX100 and incubated on a rotating platform at 4°C for 2 days. Embryos were then washed for 8 hours on a rotating platform at room temperature in 0.1%TX100/PBS with regular changes of solution.

The only exception was the HNK1 primary antibody, as it is a IgM antibody it is around 5 times larger than an IgG antibody and required higher concentrations of detergent and longer incubations to achieve adequate tissue penetration. The embryos were permeabilised and blocked in 1% TX100 / 20% sheep serum in PBS and the HNK antibody was diluted in 0.3% TX100 / PBS. The embryos were incubated in the primary antibody for 3 days. Embryos were then washed for 8 hours on a rotating platform at room temperature in 0.1%TX100/PBS with regular changes of solution.

Secondary antibodies (2.1.2.2) were added overnight in 0.3% TX100/PBS on a rotating platform at 4°C. The embryos were washed several times in 0.1%TX100 / PBS before viewing.

2.6.4. In-situ apoptosis detection

Cell death by apoptosis was detecting using the ApopTag red *In Situ* apoptosis detection kit, which identifies degraded nuclear DNA in the late stages of apoptosis. Embryos were fixed in PAF fixative for 8 hours or O/N at 4°C before being washed in increasing gradients of ethanol (75%, 95% 100%) for 15 mins each.

Embryos were then rehydrated in decreasing gradients of ethanol (75%, 50%) in PBST for 15 mins each, and then washed in PBST (2 x 5 mins). Samples were Proteinase K digested (1 min per HH stage) at room temperature without agitation. The digestion was stopped by washes in dH_2O (4 x 5 mins).

Embryos were then incubated in equilibration buffer for 30 mins before incubation in the reaction buffer with TdT enzyme (1hour at 4°C, followed by 1hour at 37°C). The Tdt enzyme adds a fluorescein nucleotide to the 3' OH end of the DNA. The reaction was stopped by addition of stop wash buffer / 0.1%TX100 (1hour at 4°C) to the embryos. The samples were washed in PBST (3 x 5 mins) and then blocked for 1hour in 10% sheep serum / 0.1% TX100 / PBS.

The fluorescein antibody was added for 2 days at 4°C in 0.1% TX100 / PBS and then the embryos washed thoroughly in 0.1% TX100 / PBS (2 x 5 mins, then 4 x 1hour) before viewing.

2.6.5. Sectioning embryos

Embryos were dissected to retain the hindbrain area and a couple of somites, and placed in 20% gelatine / PBS at 37°C. The embryos were incubated for 1hour inverting occasionally. The embryos were then transferred into some fresh molten 20% gelatine / PBS in the lid of a 1.5ml eppendorf tube and arranged to an appropriate angle for sectioning. Once the gelatine had set, the lids were incubated in 4% PAF at 4°C

overnight. After a brief wash in PBS, the gelatine blocks containing the embryos were removed from the lids and pared down to an appropriate size for sectioning. The blocks were attached to a cutting platform with a drop of superglue and sections were cut at 70 microns using a vibratome. Sections were placed on slides and mounted using DakoCytomation fluorescent mounting media and glass coverslips. Slides were sealed using nail varnish for long term storage and kept at 4°C.

2.7. In vitro cell cultures and processing

2.7.1. Cell culture of neural crest

Cell culture plates were coated using fibronectin (1/1000) diluted in DMEM and incubated at room temperature for 1hour. The fibronectin media was removed and the plates allowed to air dry for a few minutes before adding complete DMEM (2.4.1.1) or CO_2 Independent media (2.4.1.2) to the wells. Tissue explants were added to the plates and manoeuvred until spread out and separate in the centre of the dish, and allowed to sit undisturbed for 10 mins to allow the tissue to adhere. Cultures were incubated overnight at 37°C / 5% CO_2 to allow NCC's to migrate out of the tissue. The tissue explants were then removed the next day. For standard cell culture cells and explants were incubated in complete 10% FCS/Pen/Strep/L-glut DMEM, along with the supplements N2 and B27 at 37°C / 5% CO_2. To allow incubation of the cells without CO_2, cells were incubated at 37°C in a humidified chamber in complete CO_2 Independent media containing 10% FCS / Pen/Strep / L-Glut. This method was used for time-lapse of the cells, it was found to be more effective than gassing the time-lapse chamber with CO_2.

2.7.2. Cell tracker labelling of rhombomere specific NCC populations

Tissue explants were placed in uncoated non-tissue culture plastic dishes, to prevent adherence, in complete media with 1/1000 dilution of a concentrated cell tracker (5µg/µl) and incubated at 37°C for 30 mins. The explants were then washed in 37°C media 4 x 20 mins to remove excess dye. The labelled explants were then transferred to coated plates to culture the neural crest as in 2.4.1.

2.7.3. Immunostaining cells in vitro

Live cells were fixed in PAF fixative for 30 mins at room temperature, washed twice with PBS and then permeabilised in 0.1%TX100 / PBS (1 x 10 mins). Cells were then washed in PBS (2 x 5 mins) before blocking in 20% sheep serum / 0.25%TWEEN / PBS for 30 mins.

Primary antibodies were added to the cells in 0.25% TWEEN / PBS and incubated overnight at 4°C. Cells were washed in PBS (5 x 5 mins) and then the secondary antibodies added in 0.25% TWEEN / PBS for 1 hour. The cells were viewed after washes in PBS (3 x 10 mins).

All steps were carried out on a rotating platform (once the cells were fixed) at room temperature unless otherwise stated.

2.7.4. Time-lapse studies

Neural crest was cultured from explants as in 2.4.1 using the CO_2 Independent media. Time-lapse pictures were taken of the cells every 2 mins using a 20x objective using the MediaCybernetics In-Vivo software package. For cultures on fibronectin where OA (2.2.3.4) was added to the cells, the cultures were first filmed without OA for 2-4 hours, before adding the OA, the same field of view was then filmed for another 10 hours.

The average speed of each cell within 2 hour bins was calculated using the ImageJ software package using the plugin mtrackj [102].

2.7.5. Adherence assay

Tissue from dorsal r4 were removed from embryos at 10ss and incubated in CO_2 independent media overnight at 37°C either with or without 1nM OA added to the media. The rhombomere tissue was then removed with the end of a pipette tip, before photographing the remaining cNCC's. The tissue culture plates were then placed on a horizontal shaker at full speed for 1 hour. The cells in the same frame were rephotographed and the cells before and after shaking were counted using the 'cell counter' plugin in ImageJ [102]. The percentage loss in cell numbers was calculated to make it easier to compare counts due to the high difference in cell numbers in different photo frames.

2.7.6. Western blot

Tissue samples were placed in lysis buffer and then broken down by freeze-thawing, repeated pipetting and finally sonication. The protein concentration was then determined using a DC assay (BioRad) and the absorbance read using a plate reader at 650nM. Tissue homogenates were then diluted in sample buffer to 1µg and then boiled for 4 mins. Diluted samples were then loaded onto a 10% SDS gel and ran at 180V until the dye front reached the bottom of the gel. The gel and nitrocellulose membrane were soaked in transfer buffer before mounting in a cassette in more transfer buffer and the proteins blotted onto the membrane at 80V for 2 hours at 4°C. The gel was mounted he following order in the transfer cassette, cathode, filter pad, 2x3mm filter paper, gel, nitrocellulose membrane, 2x3mm filter paper, filter pad, anode. The membrane was removed from the cassette and washed in TTBS (1x10 mins) before blocking in blocking buffer (1hour RT).

The primary antibody was diluted in blocking buffer and the membrane incubated in the solution (2 hours RT). The membrane was washed in TTBS (3x10 mins) before incubation in the secondary antibody diluted in blocking buffer (1 hour RT). The membrane was washed again (3x10 mins) before draining the membrane and then incubating it in 1:1 ECL solution for 1 min. The membrane was then dried between two pieces of 3mm filter paper before exposing it to the film. The film was then processed using an X-Omat developer. The membranes were then taken and washed in TTBS (2x5 mins), before incubation in actin antibody diluted in blocking buffer overnight at 4°C, the membrane was washed in TTBS (3x10mins) before incubation in the secondary antibody diluted in blocking buffer (1hour RT). The membrane was dried and developed as before.

All washes and incubations took place on a horizontal rotational shaker.

2.7.7. PCR

Rhombomere 4 tissue was dissected from chick embryos at HH10 (10ss), and incubated in complete DMEM (2.4.1.1) either with or without the presence of 1nM OA for 5 hours. The tissue was washed in fresh media before addition of 1ml trizol to the tissue (10xr4 for each condition) before being placed at -20°C overnight. The tissue was then homogenised by passing it through a 30 gauge syringe tip. The RNA was extracted through addition of chloroform (200µl), mixing the solution before incubation (3mins RT), the solution was then spun (15mins 4°C 12000xg). The supernatant was discarded and the pellet washed with 75% ethanol (1ml) before another spin (5mins 4°C 12000xg). The supernatant was discarded and the RNA was air dried to remove residual ethanol (5 mins). The RNA was then resuspended (10µl DEPC dH_2O).

The RNA was DNase treated through the following steps

Ingredient	Volume
RNA	8µl
DNase1 buffer x10	1µl
DNase1 (1u/µl)	1µl

The mix was then incubated (15mins RT) before addition of 1µl 25mM EDTA. The solution was then incubated again at 65°C (10 mins). From this mix 4µl was taken for first strand synthesis as follows.

Ingredient	Volume
RNA (DNase treated)	4µl
Oligo (dT) 12-18 500µg/ml	2µl
dNTP mix (10mM each dNTP)	2µl
dH_2O	16µl

This mix was then incubated at 65°C (5 mins) before being cooled on ice, the following was then added to the above mix.

Ingredient	Volume
First strand buffer x5	8µl
DTT 0.1M	4µl
RNase Out	2µl

The solution was then incubated at 42℃ (2 mins) before being split into two 19µl aliquots. One was used for the positive RT-PCR to which 1µl of superscript II reverse transcriptase was added and the other aliquot for the negative control RT-PCR (-reverse transcriptase) to which 1µl of dH_2) was added. Both tubes were then incubated at 42℃ for 50 mins, before incubation at 70℃ for 15 mins. The PCR reaction was then set up as follows.

Ingredient	Volume
cDNA (from last step)	1µl
PCR buffer x10	2.5µl
$MgCl_2$ 50mM	0.75µl
dNTP mix (10mM each dNTP)	0.5µl
Forward primer (1;10 of 10µM stock)	0.5µl
Reverse primer (1;10 of 10µM stock)	0.5µl
Taq polymerase	0.2µl
dH_2O – DEPC treated	14.05µl

The mixes were then run on the following PRC program

Temperature	Time
Start 95℃	5 mins
40 cycles of:	
95℃	30 secs
60℃	30 secs
72℃	30 secs
End Cycles	
Finish 72℃	5 mins

Each of the reactions were then loaded onto a 2% agarose TBE gel, using molecular weight ladders (Low molecular weight ladder, 1kb ladder both NEB) and run at 40V for 45 mins before being visualised using a FirstLight UV transilluminator and VisionWorks LS image capture software.

3. The role of Midline1 (Mid1) in cranial development

3.1. X-linked Opitz BBB/G Syndrome and Mid1

3.1.1. X-linked Opitz BBB/G Syndrome

X-linked Opitz BBB/G syndrome (XLOS) is a very rare condition characterised by midline developmental abnormalities. Patients present with a range of abnormalities that involve the ventral midline, these include ocular hypertelorism and/or telecanthus (100% of patients), hypospadias (90%), laryngo-tracheo-esophageal deformities (70%), mental retardation and developmental delay (>50%), cleft lip/palate (>50%), congenital heart defects (>50%) and ectopic or imperforate anus (>50%) [10].

3.1.2. The Mid1 Gene

Mutations in the gene *Midline1* (*Mid1*), located on the X chromosome, are responsible for XLOS (OMIM 300000) [103]. *Mid1* is around 300kb in size, 9 exons have been shown to be constitutively expressed leading to an open reading frame of around 2kb [104]. Fourteen other exons have been discovered, which may contribute to alternative *Mid1* transcripts, the Mid1 mRNA transcripts found to date are 3.5kb, 4.5kb and two at around 7kb [105]. The *Mid1* gene in affected patients shows a variety of mutations, including nonsense and frameshift mutations (68%), missense mutations (18%), in frame deletions (14%) and in frame insertions (3.6%) [104]. In XLOS patients most of the mutations found in the *Mid1* gene are at the 3' end of the ORF (68%), which encodes the C-terminus of the Mid1 protein [104].

3.1.3. Protein Structure of Mid1

The Mid1 protein belongs to the RBCC family of proteins. These consist of a RING-finger domain, either one or two B boxes, and a Coiled Coil domain [106]. The Mid 1 protein itself is 667 amino acids in length and has a molecular weight of 72kDa, it has the RING-finger domain, as well as 2 Bboxes, and the coiled coil domain (**Figure 3-1**).

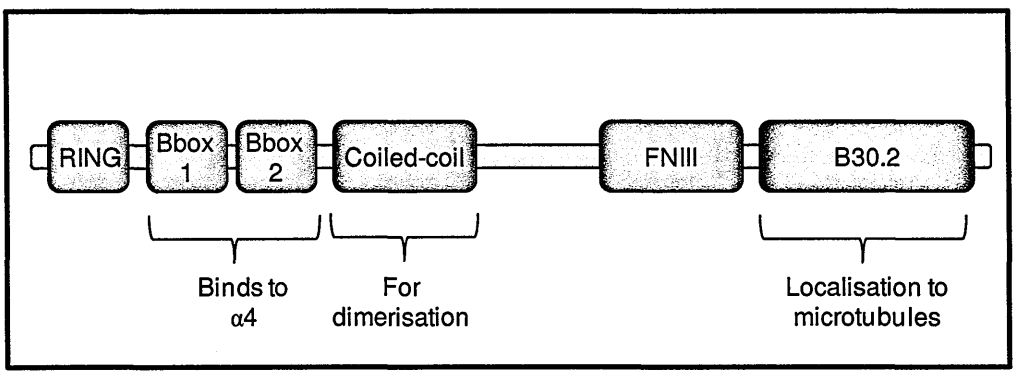

Figure 3-1. Mid1 – the X-linked Opitz Syndrome protein
Schematic diagram portraying the protein structure of Mid1 and its domains, including known domain functions.

Many of the various domains identified in the Mid1 protein have had their function elucidated. The coiled-coil domain involved in dimerisation, Mid1 functions most efficiently in dimers, either as a homodimer or as a heterodimer with the homologue Mid2 (introduced later) [97, 107]. The Bbox domains and the B30.2 domain are required for the two known functions of Mid1, firstly the B-Box domains are responsible for binding to the α4 protein [108], secondly the B30.2 domain is responsible for the localization of Mid1 to the microtubules [109]. Both of these functions are described in more detail in section 3.1.5.

Deletion of the RING-finger or B-Box domains leads to a loss-of-function mutation, furthermore the defective Mid1 protein then acts as a dominant negative, preventing the

regular function of any normal Mid1 protein that it binds to [97]. It has also been found that deletion of the C-terminus leads to a loss of function; therefore as many XLOS patients have mutations in the C-terminus, it is possible that XLOS is caused by a loss-of-function mutation [97].

3.1.4. Expression Pattern of the Mid1 Gene

Mid1 has been found to be expressed from a very early stage of development, indeed in chick cMid1 has been found to be expressed as early as stage 4 (primitive streak). At this point cMid1 is expressed in the ectoderm and bilaterally at the node, by stage 5 cMid1 is limited to the right side of the node, where it has been shown to stabilise asymmetric gene expression of BMP4 and Shh [96]. As the embryo develops cMid1 can be seen to be expressed in the neural folds and in the somites at 4ss [96], by 10ss Mid1 is found in the mesenchyme adjacent to the hindbrain and mesencephalon and is also strongly expressed in r2/r3 [110]. Later in development cMid1 is expressed in the developing trigeminal ganglia and also in the second branchial arch (37ss), by 40ss and into HH28 cMid1 is in the central frontal mass mesenchyme, and is also from HH24 strongly expressed in the limb bud, muscle tissue and cardiac muscle [110].

The expression pattern of Mid1 has also been examined in mice at a later stage of embryo development. Expression in the head region at E12.5-E12.5 mMid1 is found rostrally in the CNS and highly expressed in proliferating neuroepithelium of telencephalic vesicles and is down-regulated where post-mitotic neurons are located. By E16.5 mMid1 can be found in the outer layer of the neural retina where proliferating neuroblasts are located [111]. With regards to mMid1 expression in the rest of the body at E14.5 mMid1 is highly expressed in the developing kidneys, by E16.5 expression can also be found in the stomach, hindgut and small intestine, where mMid1 is restricted to crypts where regenerating cells develop [111].

3.1.5. Functions of Mid1

As the craniofacial structure develops abnormally in XLOS, this implies that Mid1 is involved in correct craniofacial development. Indeed the expression patterns of Mid1 observed during development are in tissues which are involved in the correct development of craniofacial structures, such as the mesenchyme such as the mesenchyme, which contains cNCCs, making it of interest in my studies of cNCC development. To date two specific functions have been identified for the Mid1 protein. Firstly the Mid1 protein exhibits an ubiquitin ligase function on PP2A, thus targeting it for degradation (Section 3.1.5.1). Secondly Mid1 has been shown to bind microtubules and provide stabilization from depolymerisation (3.1.5.2).

More generally, a particular role of Mid1 in early development has been proposed, as a regulator of Snail [96]. Snail is involved in regulating EMT through changes in gene expression patterns, therefore increases in signalling upstream, such as through Mid1, may lead to increased EMT.

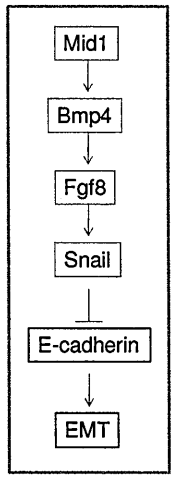

Figure 3-2. Mid1 signalling cascade and induction of EMT

The Mid1 signalling cascade as outlined by Granata [96] (shown here in pink boxes). The diagram depicts how Snail is known to repress E-cadherin transcription and thus induce EMT.

3.1.5.1. Mid1 Mediated Ubiquitination of PP2A

Protein Phosphatase 2A is a serine/threonine phosphatase involved in many cellular processes. It has been demonstrated that PP2A is involved in cell migration; since siRNA knockdown of PP2A leads to accelerated wound healing, migration and invasion by cancer cells [112]. Okadaic acid (OA) is a well known and extensively used inhibitor of PP2A, and the observation that OA acts as a tumour promoter has led to the suggestion that its PP2A target may act as a tumour suppressor [113]. This has also led to the suggestion that Mid1, because it targets PP2A for degradation, may also act as a tumour promoter [114].

PP2A is bound by the cytosolic α4 protein, which negatively regulates the catalytic subunit of PP2A [115] (**Figure 3-3**). The α4 protein associates with Mid, specifically the B-Box1 domain [108], as shown through colocalisation, co-immunoprecipitation and yeast two-hybrid screening [116]. Upon binding to Mid1, α4 is recruited to the microtubules. Through the binding of Mid1 to the α4 protein, Mid1 is able to execute its ubiquitin ligase activity upon PP2A [116]. Ubiquitin ligase (E2 enzyme) binds to Mid1 at the RING finger domain, therby facilitating the PP2A ubiquitin ligase activity of Mid1, although more evidence to prove this is needed [104, 117].

In the event that Mid1 is truncated and missing its C-terminus, it cannot associate with microtubules and therefore is not able to bind to PP2Ac via the α4 protein. Thus, PP2A remains intact and active, resulting in hypophosphorylation of microtubule associated proteins [104].

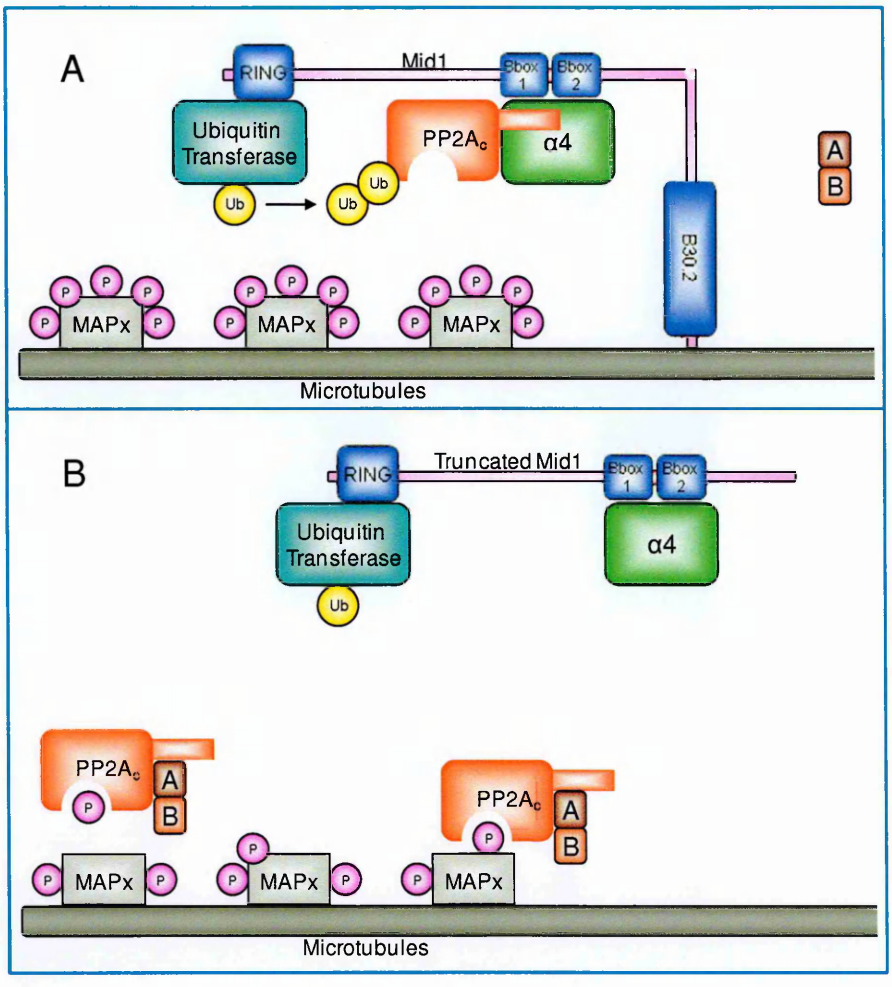

Figure 3-3. Mechanism of the ubiquitination of PP2A by Mid1

A – Schematic diagram demonstrating the binding of functional Mid1 protein to the microtubules, mediating polyubiquitination of the PP2Ac protein. B – Schematic diagram depicting loss of Mid1 binding to the microtubules due to truncation and the subsequent hypophosphorylation of microtubules due to a lack of PP2Ac ubiquitination. P – phosporylated protein, Ub – ubiquitin, AB – A and B subunit of PP2A, MAPx - microtubule associated proteins (unidentified as of yet)

Consistent with its proposed role in tumour metastasis, studies on PP2A have shown that it negatively regulates cell motility. PP2A colocalises and interacts with μ and m-calpains, when PP2A activity is disrupted there is an increase in the phosphorylation of these calpains, which then leads to an increase in wound healing, migration and invasion [112].

This evidence suggests that PP2A is a suppressor of cell motility. Furthermore PP2A has been observed colocalized with E-cadherin and β-catenin in cell-cell adhesion sites between adjacent cells *in vitro* and when OA is used to inhibit PP2A, there is a loss of cell-cell adhesion [118]. It is thought that the B56 subunit of PP2A specifically is involved in the control of cell motility as truncation of the B56 subunit leads to increased cell motility through paxillin phosphorylation [119].

3.1.5.2. Mid1 Binding to Microtubules

Another well documented action of Mid1 is the binding to and stabilization of microtubules. At a subcellular level Mid1 has been shown to colocalise with microtubules through Mid1-GFP fusion constructs and filamental staining [109]. It has also been shown that Mid1 extracts from XLOS fibroblasts cannot bind to microtubules, due to XLOS mutations being in the C-terminal end of the protein this was the candidate area for the binding domain. Indeed the C-terminus of Mid1 was found to be responsible for microtubule binding, as deletion of the domain leads to clumping of Mid1 protein in the cytoplasm instead of microtubule association [109]. Furthermore work has shown that monomers of Mid1 are unable to bind to the microtubules; Mid1 homodimers and Mid1-Mid2 heterodimers are required in order for Mid1 to bind to microtubules and also recruitment of the α-subunit of PP2A to microtubules [107].

Mid1 binding to the microtubules acts to stabilize them, incubation of cells in colcemid leads to depolymerisation of microtubules, *in vitro* cells expressing Mid1 show a resistance to colcemid treatment [109]. Another protein Mig12 is also recruited to the microtubules by Mid1, and is thought to also aid in microtubule stabilization [120].

3.1.6. Regulation of Mid1 function

There are several ways that the activity of Mid1 may be regulated, these include alternative splicing, protein interactions and phosphorylation of the Mid1 protein. Firstly, alternative splicing may regulate Mid1 activity, to date, 4 different Mid1 mRNA transcripts (3.5kB, 4.5kB and 2 at around 7kB) have been identified from both fetal and adult human tissue [105, 121, 122]. Some of these transcripts lead to production of a truncated Mid1 protein, which lacks the c-terminus and binds to the α4 protein in a dominant negative fashion [105].

Secondly, it is also possible that Mid1 translation could be regulated by a Mid1 protein complex. This protein complex has been shown to exist by yeast-two hybrid screening, immunofluorescence, affinity purification of the protein complex and immunoprecipitation. The components of this Mid1 protein complex have been shown to include elongation factor-1 (EF-1), Rack1, Annexin A2, Nucleophosmin and proteins of the small ribosomal subunits [123]. This protein complex has been postulated to have a translation-related function. Several proteins involved in translation have been found to associate with the complex, EF-1 is a protein translation regulatory factor and as the Mid1 mRNA has been found associated with the complex [123], it is possible that the Mid1 protein regulates its own translation through its protein complex.

Thirdly control of Mid1 function may also be through its protein interactions. As Mid1 interacts with α4 enabling it to bind to PP2A and target it for degradation, an absence of α4 would imply that Mid1 could not perform this function. As the α4 protein is not ubiquitously expressed but is instead expressed in a tissue specific manner [124], although its expression pattern in early development has not yet been characterised, this may be one way that Mid1 ubiquitination of PP2A is controlled. Furthermore the

expression of Mig12 is also tissue specific [120], although its expression pattern in early head development has not been characterised to date. Because Mid1 recruits Mig12 to microtubules to aid in stabilization [120], it could be that when Mig12 is absent Mid1 may not be able to stabilize microtubules to the same degree.

Finally proteins are often activated by phosphorylation; Mid1 is a phosphoprotein, therefore the phosphorylation status of Mid1 may affect its activity. One finding which supports this theory is that the serine-threonine protein kinase, MAPK, has been shown to be required in order to sustain binding of Mid1 to the microtubules [108]. Overall, the mechanisms behind how Mid1 activity is controlled are still poorly understood.

3.1.7. Mid2

Mid2 is a homologue of Mid1, indeed both *Mid* genes are located on the X chromosome and furthermore show a 92% similarity and a 77% identity [107]. Mid2 has been shown to exhibit some of the same functions as Mid1 and indeed the two proteins do show functional redundancy (See 3.1.8). In the case of XLOS, it is possible that Mid2 could make up for the loss of Mid1 functional protein, as long as the XLOS Mid1 protein does not exert any dominant negative effect over Mid2. However during craniofacial development the expression patterns reported do not overlap between Mid1 and Mid2. Thus Mid2 is unlikely to be able to sufficiently compensate for Mid1 loss of function and therefore is probably why XLOS patients still exhibit craniofacial abnormalities.

The expression pattern of Mid2 has been studied in chick, mouse and human tissue. The early expression pattern of cMid2 has been found in the node, much like cMid1, but mesodermal expression is absent. At HH4 cMid2 is found bilaterally at the node, by HH5 expression is restricted to the right side of the node and persists to 1ss when light expression at the neural plate can be seen, however by 4ss cMid2 is down-regulated in

the node but expression persists more strongly at the neural plate [97]. At a later stage of embryo development in mice at E10.5 Mid2 can be found expressed in the trigeminal ganglia and the DRG and also at low levels in the CNS and heart tissue. By E14.5 mMid2 is expressed strongly in the heart and kidney tissue, however when compared to stage matched embryos of ISH for mMid1 the expression is still weaker than that of mMid1 [125]. Mid2 is also expressed in adult human tissue, it can be found in prostate, ovary and small intestine tissue [125].

3.1.8. Functional redundancy between Mid1 and Mid2

The midline proteins, Mid1 and Mid2 have been shown to be functionally redundant, Mid2 studies to date have shown Mid2 functions in the same way as Mid1. Mid2 can be found at the same subcellular location as Mid1, bound to microtubules [125], and furthermore Mid2 can also bind α4 [107]. To further reinforce the theory that Mid1 and Mid2 are functionally redundant, in situations where Mid2 has been used to replace endogenous Mid1 knockdown, Mid2 can rescue defects normally caused by decreased Mid1 activity [97]. Moreover Mid1 and Mid2 can hetero or homo-dimerise to tether α4 to the microtubules [107], suggesting that they may act in the same fashion.

3.2. Aims

Studies have previously examined the expression pattern of Mid1 throughout development in both chick and mice and the function of Mid1 during early chick midline development [96, 97]. To date there has been little focus on the function of Mid1 at a stage of development where the cranial neural crest is delaminating from the neural tube and migrating within the cranial mesenchyme.

Richman and Fu [110] have shown that Mid1 is expressed in the hindbrain at the level of r1/r2 and also in the mesenchyme adjacent to r1/r2 at 10ss. The published expression pattern is consistent with Mid1 being expressed in r1/r2 cNCCs. Therefore it is possible that Mid1 plays a role in the correct formation, EMT or migration of r1/r2 cNCCs.

As already described, there are two known functions of Mid1, firstly it acts as an ubiquitin ligase targeting PP2Ac for degradation [116], secondly it has been shown to bind to and stabilise microtubules [107, 109, 120]. A lack of correctly-functioning Mid1 in XLOS patients could be due to either one or both of these functions of Mid1 being affected, or an as of yet unknown function of Mid1 being interrupted, which could lead to the XLOS characteristics.

As PP2A is widely expressed and involved in many cellular functions [114], it would be expected that any changes in PP2A activity would have significant effects on cell function/behaviour. Therefore it is possible that XLOS could be caused by interrupting the ubiquitin ligase activity of Mid1 and therefore altering the level of PP2A protein and so the activity level of PP2A.

However it is feasible that XLOS is caused, either completely or in part, by interrupting Mid1 microtubule binding activity. Mid1 also has been shown to not only bind to and

stabilise microtubules but it also forms multi-protein complexes at the microtubules and in the cytoplasm. These protein complexes are thought to possibly be the mechanism through which Mid1 can be regulated by other proteins and also how it can regulate its own transcription as Mid1 mRNA transcripts have been found to be associated with these protein complexes as well as proteins involved in translation. As these proteins are involved in translation they could also regulate the translation of other unidentified proteins. Without a correctly functioning Mid1 protein the microtubule associated protein complex may not form or function correctly, this could therefore be the mechanism through which XLOS occurs.

The aim of this study was to more accurately define the spatio-temporal expression of *MID* genes during chick craniofacial development and then to use various expression constructs to alter Mid1 and PP2A activity *in ovo*, in order to elucidate the roles of Mid1 in the cNCCs of chick embryos during the period when cNCCs are delaminating from the hindbrain and migrating within the cranial mesenchyme. This was achieved by use of dominant negative Mid1 (DN-Mid1), or full-length Mid1 expression constructs in order to study the effects of inhibiting Mid1 function in r2 cNCCs (DN-Mid1) or ectopic expression of Mid1 in r4 cNCCs. It was also investigated whether alterations in Mid1 and PP2A function in cNCCs had an effect at later stages of development once the cNCCs have migrated from the neural tube and begin to differentiate. In order to further elucidate the mechanism through which Mid1 is involved in cNCC delamination, migration and differentiation both a PP2A expression construct and a PP2A inhibitor were used to clarify if Mid1 is acting through its PP2A ubiquitin ligase function.

3.2.1. Chapter Overview

The findings in this chapter cover the following;

A. Mid1 and Mid2 expression pattern (3.3.1)

B. Knockdown of Mid1 activity in r2

   a. Validation of the dominant-negative Mid1 expression construct function (3.3.2)

   b. Abnormal cNCC migration pattern (3.3.3)

   c. Delayed trigeminal ganglion formation (3.3.4, 3.3.5)

C. Ectopic expression of Mid1 in r4

   a. Validation of the Mid1 expression construct and the PP2A inhibitor, OA (3.3.6)

   b. Faster cNCC migration of cNCCs from the neural tube (3.3.7)

   c. Premature epibranchial geniculate placode development (3.3.8, 3.3.10)

D. *In vitro* cNCCs treated with OA

   a. Increased cNCC migration speed (3.3.12, 3.3.16)

   b. Reduced cell adhesion (3.3.12.1)

   c. Increased differentiation into neurons (3.3.13)

E. Mechanism of premature ganglion development following ectopic Mid1 expression or OA exposure

   a. Not due to increased neuronal cell differentiation (3.3.13)

   b. Premature placodal cell migration to site of ganglion development (3.3.14,3.3.15)

F. Changes in protease expression in OA exposed r4 (3.3.17)

3.3. Results

3.3.1. Mid1 and Mid2 expression patterns during hindbrain development

In order to propose functions for Mid1 and Mid2 in craniofacial development, detailed analysis of their expression patterns were initially required. I used chick specific Mid1 and Mid2 antisense riboprobes [96] to study the expression patterns of the *MID* genes in embryos between 6-13ss, a time-window when cNCC are delaminating from the neural tube and migrating to their targets [126, 127]. This time point in development is important in terms of correct craniofacial development, as any errors in cNCC migration at this time could have repercussions later in development, possibly leading to characteristics such as cleft lip/palate that are frequently seen in XLOS patients. So if the *Mid* genes are found to be expressed during this stage of development, it would provide evidence for their involvement in cNCC development, migration and/or differentiation and thus would be one way in which they are involved in craniofacial development.

3.3.1.1. Expression pattern of Mid1 in chick embryos

Mid1 is expressed in r2 at 10ss [110], although the expression of Mid1 in the r2 cNCCs is unclear. Here the expression of Mid1 between 6-13ss was investigated as well as the possible cNCC expression. The results of ISH (n=6 for all stages) showed that at 6ss there is strong expression of Mid1 in the neural tube in the entire cranial region (**Figure 3-4** A). By 10ss expression has concentrated more in the r2-r3 neural tube and is also seen in the mesenchyme adjacent to the midbrain and r1-r2 (**Figure 3-4** B). At 13ss the expression was discrete within r2 and also in the cranial mesenchyme adjacent to r1-r2 and the midbrain in a pattern suggestive of the expression within the migrating cranial neural crest. Double ISH with Mid1 and Sox10 (expressed by migrating NCCs) confirmed that migrating r1/r2 cNCCs did express Mid1 (**Figure 3-4** D,E). At all somite stages investigated no expression was observed in r4. Transverse sections of these embryos

additionally revealed that although the cNCCs adjacent to r1 showed double staining close to the neural tube, Mid1 expression was not observed in cNCCs further laterally from the neural tube (**Figure 3-4** E,F), indicating that Mid1 becomes down-regulated as r2 cNCCs enter the first branchial arch.

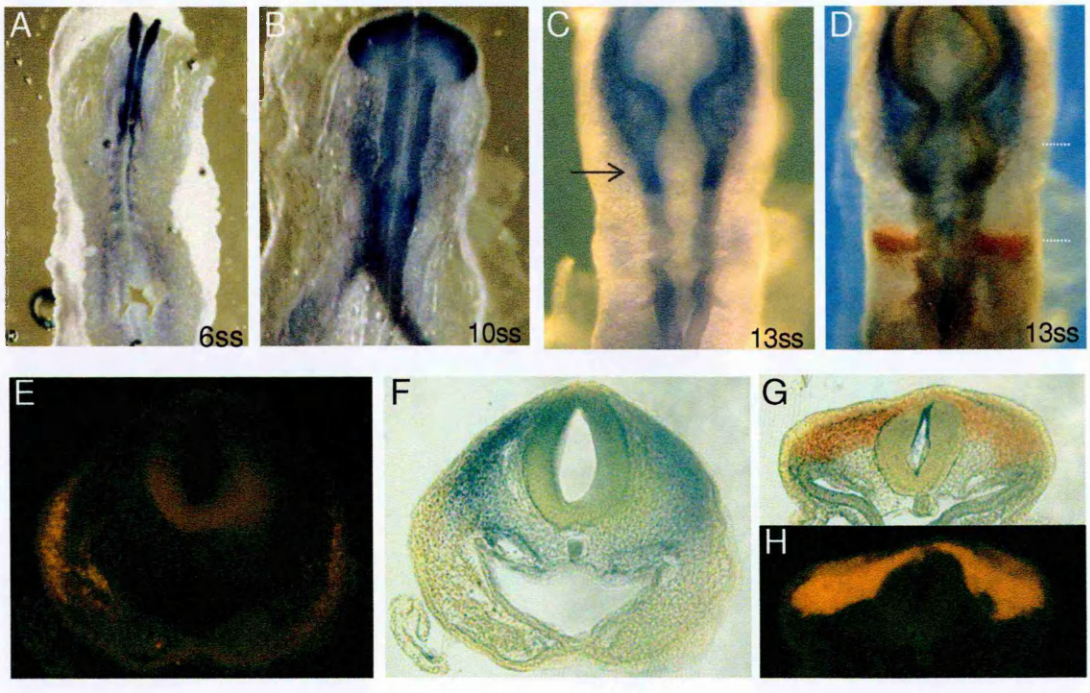

Figure 3-4. Expression pattern of Mid1.

In situ hybridisation for Mid1 (Blue) and Sox10 (Red/Orange) of embryos at 6ss (**A**), 10ss (**B**) and 13ss (**C, D**). Sections through a 13ss embryos at the level of rhombomere 1 (**E,F**) and rhombomere 4 (**G,H**). Dotted lines show level at which E-H were located. Arrow indicates expression in r2. All images are representative, n=6 embryos for all stages.

3.3.1.2. Expression pattern of Mid2 in chick embryos

Previous studies have shown that Mid2, a homologue of Mid1, can compensate for Mid1 in the event that there is a loss of the protein [97]. In order to assess the extent of possible compensation from Mid2 in subsequent experiments, the expression pattern of Mid2 was also examined by ISH. The expression of Mid2 at 3ss (n=5), is seen in the neural plate and in extraembryonic tissue, this is in agreement with that observed by Granata [97]. By 6ss (n=6), Mid2 is expressed in a similar distribution to Mid1, being strongest in the neural tube of the cranial region, but not the trunk (**Figure 3-5** B). By 10ss (n=6) Mid2 is strongest in the neural tube in the midbrain, but is weaker in the hindbrain neural tube (**Figure 3-5** C). There was no detectable expression in any of the migrating neural crest. At 13ss (n=6), the expression remains strong in the midbrain neural tube, but also shows a distinct area of expression in the caudal part of r5, and also some expression around the developing otic vesicle (**Figure 3-5** D). However it is possible that the expression of Mid2 is from the migrating r4 cNCCs, as the staining at this level and time point is similar to that of the NCC marker Sox10. If Mid2 is indeed being expressed by the r4 cNCCs the studies performed here are investigating the effect of high expression of Mid proteins on cNCC function, therefore a low expression level of Mid2 in these cells should not hinder the experiments.

Figure 3-5. Expression pattern of Mid2.

In situ hybridisation for Mid2 (Blue) of embryos at 3ss (**A**) n=5, 6ss (**B**) n=6, 10ss (**C**) n=6, and 13ss (**D,** same embryo in both views)n=6. Double insitu hybridisation for Mid2 (Blue) – Sox10 (Red/Orange) at 10ss and 13ss (**E**). OV – Otic vesicle, red lines indicate midbrain. All images are representative.

The expression pattern of Mid2 in conclusion should not have a significant effect in following experiments as the expression pattern does not overlap with those of Mid1 in the mesenchyme. Furthermore it is possible that the DN-Mid1 construct would reduce Mid2 function in r2 due to the known ability of Mid1 to heterodimerise with Mid2 [107], although

there is no published evidence to prove a dominant-negative effect of the DN-Mid1 construct on Mid2.

3.3.2. Knockdown of Mid1 activity in r2 leads to PP2A accumulation

In order to elucidate the function of Mid1 during the period of development when cNCCs are migrating, the next aim was to inhibit Mid1 function and study the effects on cNCCs. As I found that Mid1 is strongly expressed in r2, and r2 adjacent cNCCs, in all stages of development examined by ISH, r2 was selected to be the target of Mid1 function knockdown. This was achieved using a dominant-negative Mid1 (DN-Mid1) construct electroporated into r2 at the 8ss stage. This construct produces a truncated Mid1ΔR protein, where the RING finger domain of Mid1 is disrupted, therefore preventing binding of Mid1 to ubiquitin transferase. As shown by Short *et al.* [107] Mid1 dimerises in order to function, both in binding to microtubules and also for targeting PP2Ac for ubiquitination. The DN-Mid1 protein binds to both endogenous Mid1 proteins and other DN-Mid1 proteins, forming DN-Mid1 and endogenous Mid1 dimers, or DN-Mid1 homodimers. The ubiquitin ligase activity of the DN-Mid1 and endogenous Mid1 dimers is compromised, therefore leading to a knockdown in $PP2A_C$ ubiquitination. XLOS patients often have deletions in the C-terminus of the Mid1 protein (which includes the RING domain), preventing microtubule binding [103, 121, 128] (Section 3.1.3). Thus, the DN-Mid1 construct closely resembles the genetic defect in XLOS.

Although the DN-Mid1 construct has been shown to inhibit the function of Mid1 [96, 97], it has not been formally confirmed that this occurs through loss of PP2A ubiquitinylation and subsequent impairment of PP2A proteasomal degradation. Thus, to validate the inhibition of ubiquitin ligase function by the dominant-negative construct, r2 tissue was taken 6 hours post electroporation with the DN-Mid1 construct (n=30 r2s) and a homogenate of tissue was run on a western blot and probed with a $PP2A_C$ antibody which recognises the

catalytic subunit of PP2A. The blot was stripped and reprobed with a β-actin antibody to provide a protein loading control. The chemiluminescent signal intensities of both PP2Ac and β-actin were quantified for each sample and the ratio of PP2Ac:β-actin signal intensity was calculated. The Western blot data showed that the r2 tissue transfected with the DN-construct had around a third more $PP2A_C$ protein present than when r2 tissue was transfected with the control GFP construct (**Figure 3-6**).

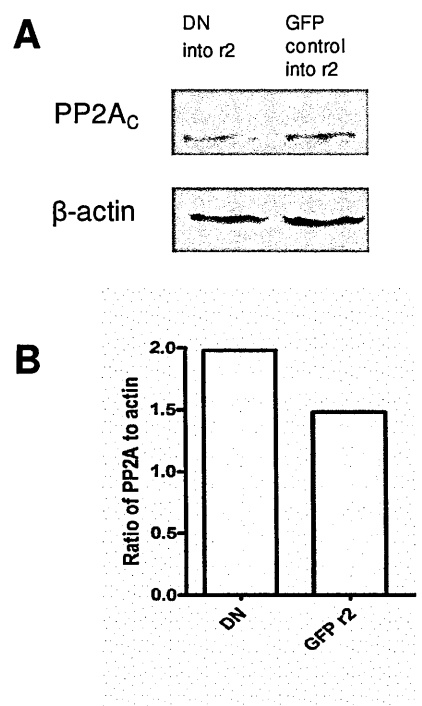

Figure 3-6. Analysis of PP2A catalytic subunit protein levels following electroporation. Western blot analysis of PP2A protein levels following DN-Mid1 or GFP control electroporations (**A**) and subsequent densitometry to compare ratios of PP2A (36kD) and β-actin (**B**) (43kD), showing more $PP2A_c$ in the DN electroporated tissue. Tissue was pooled from r2 from 30 embryos for each electroporation, n=1.

3.3.3. Mid1 plays a role in correct cNCC migration

Mid1 was found to be expressed in the migrating cranial cNCCs from the r1-r2 region, it is therefore possible that the Mid1 is involved in the migration or patterning of the cNCCs. In order to investigate this possibility, a DN-Mid1 construct was used to inhibit Mid1 activity

in r2 and therefore inhibit the PP2A-degradation function of Mid1. The DN-Mid1 was unilaterally electroporated into r2 at 8ss, the contralateral unelectroporated side was used as an internal control. After 9 hours of incubation, embryos were fixed and processed with HNK1 antibody, a marker for migrating cNCCs. These time points were chosen for the following reasons: At 8ss there are still cNCCs in neural tube at the level of r2, enabling electroporation of the cNCCs before migration. The migration pattern of the cNCCs adjacent to the neural tube at the level of r2 showed that there was a region of the mesenchyme that was in deficit of cNCCs in comparison to the unelectroporated control side. The GFP control electroporated embryos showed no such asymmetric NCC distribution (**Figure 3-7**).

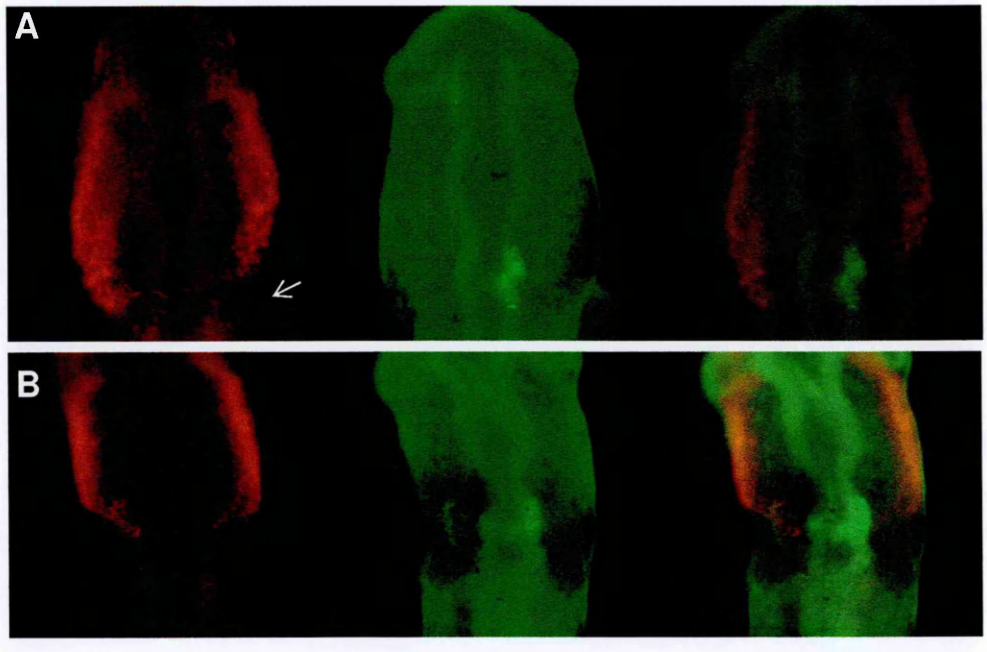

Figure 3-7. Neural crest staining following electroporation with the DN-Mid1 construct.

Embryos immunostained for HNK (red), a NCC marker, and GFP (green), following electroporation of the DN-Mid1 (**A,** n=3/8), or GFP (**B,** n=6/6), construct unilaterally into r2. Embryos were electroporated at 8ss and incubated for 9hours to 14ss. Embryos expressing the DN-Mid1 in r2 showed a lack of neural crest cells adjacent to r2 (arrow).

To determine if the migration pattern observed was partially due to cell death, DN-Mid1 electroporated embryos (+9hrs after electroporation) were processed with an Apoptag kit, which is based upon a TUNEL staining method to detect apoptotic cells. The stain was quite weak, and it is difficult to see at the wholemount level if there is a difference in cell death between the DN and GFP electroporated side and the contralateral unelectroporated side (**Figure 3-8**). The wholemounts do not show a detectable difference by eye, certainly not to the extent expected to cause the NCC migration phenotype observed. Therefore sections were taken of the embryos and scanned by confocal microscopy. As the staining was clearer in the sections and no obvious differences were observed, cell death was ruled out as a contributing factor to the NCC phenotype.

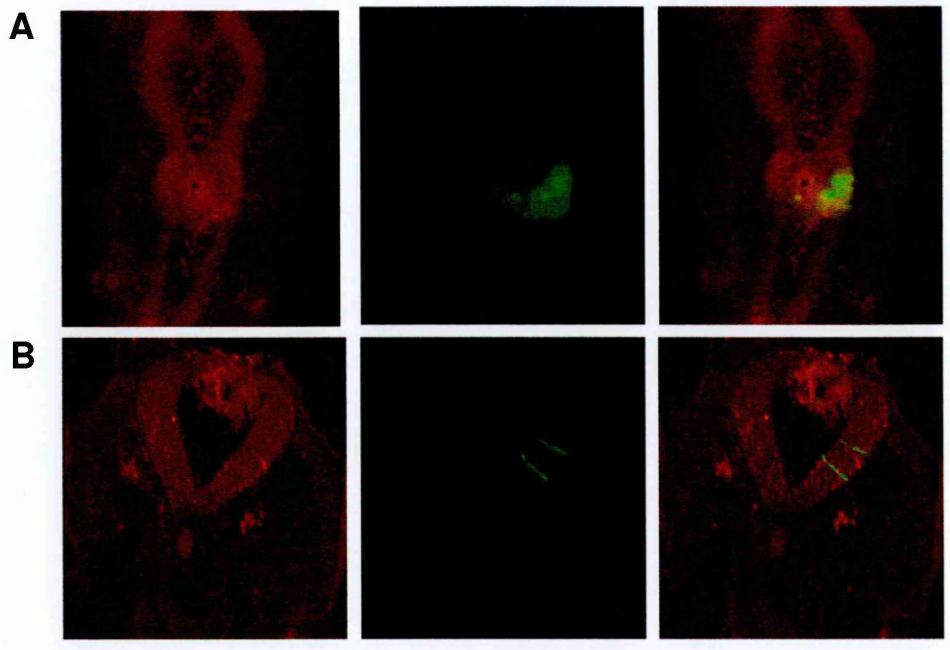

Figure 3-8. Apoptag staining following electroporation with the DN-Mid1 construct. Embryos stained using the Apoptag kit (red), to label cells undergoing apoptosis, and GFP (green) antibody staining, following electroporation of the DN-Mid1 construct unilaterally into r2 at 8ss and following incubation to 13-14ss (+9hrs, n=8). Embryos did not show an obvious left-right difference in the number of cells undergoing apoptosis. Panel **A** shows a wholemount embryo, Panel **B** shows confocal sections of the same embryo from **A**.

3.3.4. Inhibition of Mid1 function in r2 neural crest cells leads to delayed trigeminal ganglia formation

Cranial neural crest form much of the trigeminal ganglia (Figure 1-7), the rest of which is derived from placodal cells. In order to investigate if the deficit in cNCCs observed in the DN-Mid1 electroporated embryos was affecting ganglion development, embryos were unilaterally electroporated with DN-Mid1 at 8ss and incubated for 22 hours, to 22/23ss, a stage in development where early ganglia development should be well underway. As ganglia development occurs quite discretely and is well documented, any differences should be easily detectable by eye. Staining with a phosphorylation independent NF

antibody, a marker for neurons, showed a decrease in the trigeminal ganglia, specifically the mandibular processes of the ganglia, which r1 and r2 cNCCs contribute to, when electroporated with the DN-Mid1 construct (**Figure 3-9**) in 3/6 embryos (50%). These embryos also appear to have a thinner ophthalmic branch of the trigeminal ganglia, which is also contributed to by the cNCCs (Figure 1-7). Embryos unilaterally electroporated with control GFP construct showed no difference in NF staining (6/6). A possible explanation of this observation is that the DN-Mid1 cNCCs are not migrating as quickly as normal and are therefore not reaching their destination and differentiating on a normal timescale, therefore development of the ganglia is delayed. If this is the case, then ganglion development following DN-Mid1 electroporation should eventually catch up with the contralateral control sides. To test this, embryos were incubated for longer, for 48 hours, to ~40ss. Consistent with the idea that NCC emigration is delayed in DN-Mid1 r2 NCCs, the cranial ganglia were now the same size on both electroporated and non-electroporated sides in DN-Mid1 (4/4 100%) embryos, as was the case for control GFP electroporated (3/3 100%) embryos (**Figure 3-9** C).

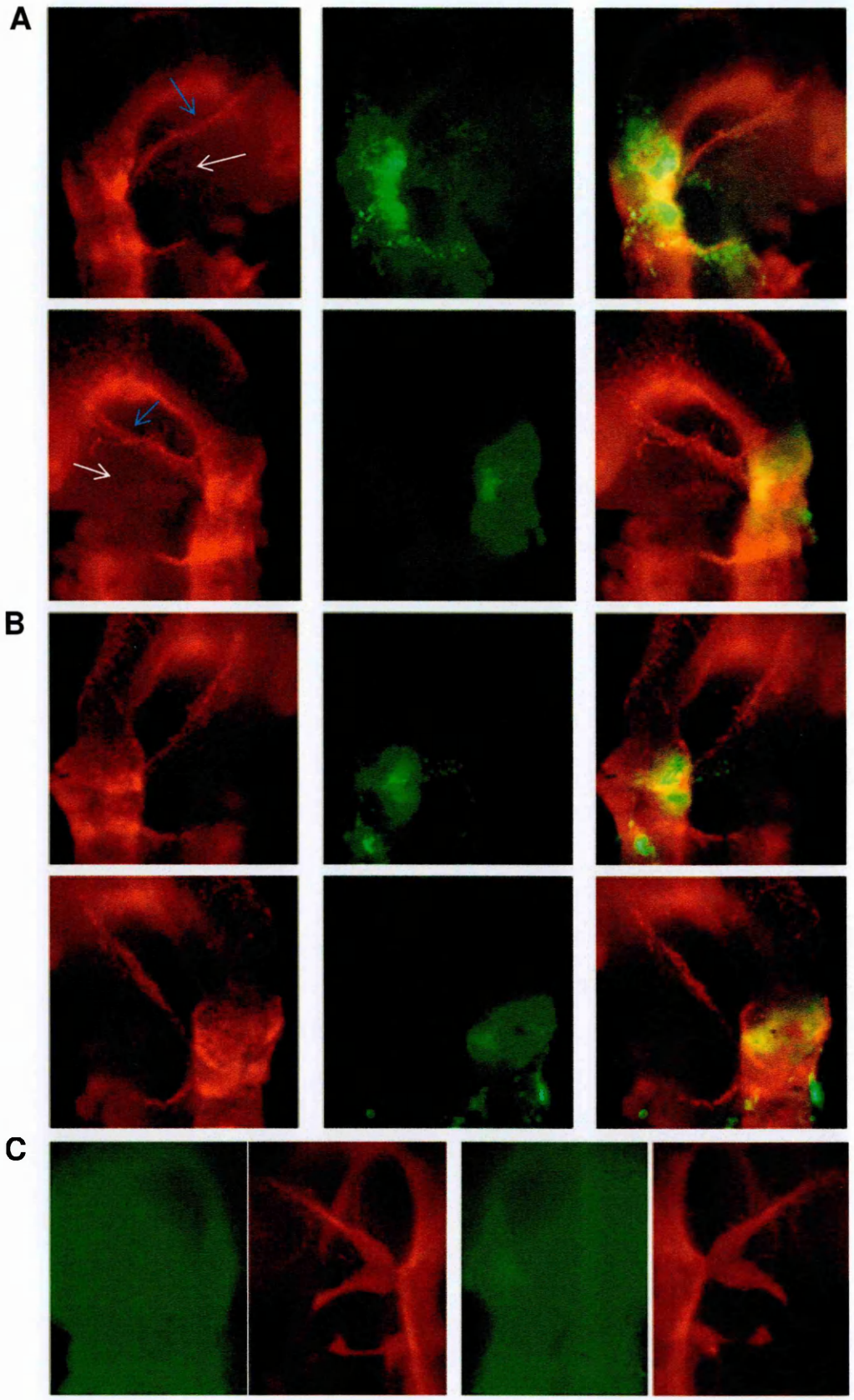
A
B
C

Figure 3-9.Cranial ganglion development in embryos electroporated with the DN-Mid1 expression construct.

Embryos were unilaterally electroporated into r2 at 8ss and incubated to 23ss before being immunostained for the neuronal marker neurofilament (Red) and GFP (Green). Left and right views of DN-Mid1 embryos (Panel **A**, n=3/6) depicting less neuronal staining of the maxillo-mandibular branch (white arrows) and a thinner ophthalmic branch (blue arrows) of the trigeminal ganglion on the electroporated side. The GFP control embryos (Panel **B**, n=6/6) show no left-right differences. Panel **C** shows DN-Mid1 embryos after a 48 hour incubation showing left-right symmetrical ganglia development by this stage (n=3/3).

3.3.5. Increased PP2A activity in r2 leads to delayed trigeminal ganglion formation

PP2A is ubiquitinated by Mid1 [116], and targeted for degradation. Therefore it could be that because the DN-Mid1 prevents function of the endogenous Mid1 protein and therefore the active PP2A protein levels increase, the increased PP2A activity is responsible for the phenotype observed above. Therefore in order to increase the protein levels of PP2A without directly affecting Mid1 activity, a construct expressing PP2Ac was built, pCAB-PP2Ac-IRES-GFP (see materials and methods [100]). The original construct although published in several previous studies and shown to be functional [100, 129], was not optimal for expression in chick tissue and lacked an IRES-GFP cassette; therefore the PP2Ac was cut out of the original vector and placed into an empty pCAB-IRES-GFP. As this is the same vector used for DN-Mid1 expression it alleviates the problem of differences in expression from the DN-Mid1 expression construct due to varying vectors.

The neural tube of embryos were electroporated unilaterally at the level of r2 with the PP2Ac expression construct at 8ss, incubated for 22hours to 22-23ss and then stained with a NF antibody. By 22-23ss the development of the trigeminal ganglia is well

underway, allowing any abnormalities in its development to be seen. The electroporated embryos showed the same underdevelopment of the trigeminal ganglia, particularly the maxillary processes (5/9 55.6%) as the DN-Mid1 embryos (**Figure 3-10**). Therefore this reinforces the hypothesis that Mid1 is acting through its PP2Ac ubiquitination function in this instance.

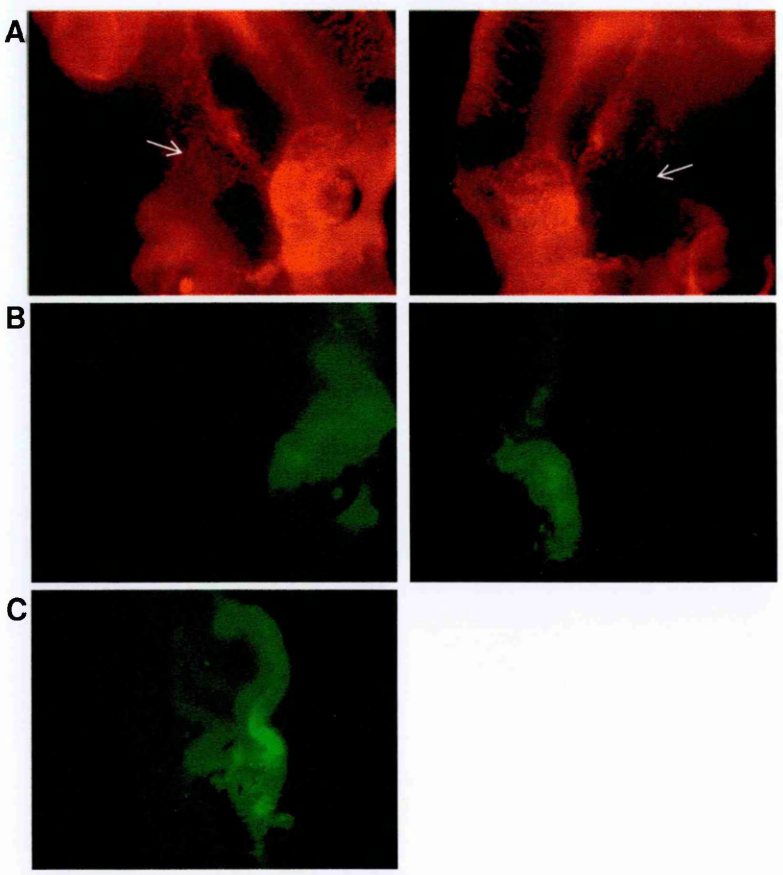

Figure 3-10. Cranial ganglion development in PP2A expression construct electroporated embryos.

Embryos were electroporated at 8ss unilaterally into r2 using the PP2A expression construct and incubated to 23ss. Embryos were then stained for neurofilament (**A**), to show neurons, and a GFP (**B**) antibody for electroporated cells. Each panel shows the right and left sides of the same embryo, showing the same DN-Mid1 phenotype of fewer neurons on the electroporated right side (arrows, n=5/9), and a dorsal view (**C**) showing the unilateral electroporation into the right side of the neural tube.

3.3.6. PP2Ac protein levels decrease following Mid1 overexpression or pharmacological inhibition of PP2Ac

If the migration of the cranial neural crest that normally expresses Mid1 is impaired upon transfection with the DN-Mid1, thereby affecting development of the ganglia, then it is possible that ectopic expression of Mid1 in cNCCs that do not normally express Mid1 would lead to enhanced migration. Therefore the second approach for further investigation into the function of Mid1 involves the ectopic expression of Mid1 in r4 and its cNCCs.

Rhombomere 4 was selected as a target since it is the next caudal rhombomere to r2 that outputs cNCCs directly into the adjacent mesenchyme, but I found it does not express Mid1 mRNA to a level detectable with ISH, either in the neuroepithelium or in the cNCCs. It is therefore an appropriate target for studying the effects of Mid1 ectopic expression. In order to check the effectiveness of the Mid1 expression construct, a western blot was performed on r3-r5 neuroepithelium that had been electroporated with the Mid1 construct at 10ss and then incubated for 6 hours. The blots were probed for PP2Ac and β-actin. The Mid1 electroporated neuroepithelia showed around half as much PP2Ac protein in comparison to GFP control electroporated neuroepithelia (**Figure 3-11**), confirming Mid1-mediated PP2Ac destruction.

Evidence from the PP2A-expression construct results suggests that PP2A is the effector through which Mid1 is acting, OA, an inhibitor of PP2Ac, was used to mimic the ectopic expression of Mid1. OA is a well characterised inhibitor of PP2A that binds the PP2Ac active site [130], although at higher concentrations it does have an inhibitory effect on other protein phosphatases. The IC_{50} value for PP2A is 0.1-1nM, whereas it is 20-50nM for PP1 and >5000nM for PP2B [114].

Western blot analysis was performed on tissue exposed to 10nM OA at 10ss and incubated for 6 hours (n=30 r4s pooled). The results surprisingly showed a decrease in the protein level of PP2Ac (**Figure 3-11**). This was not expected and suggests that inactivated PP2Ac is targeted for degradation.

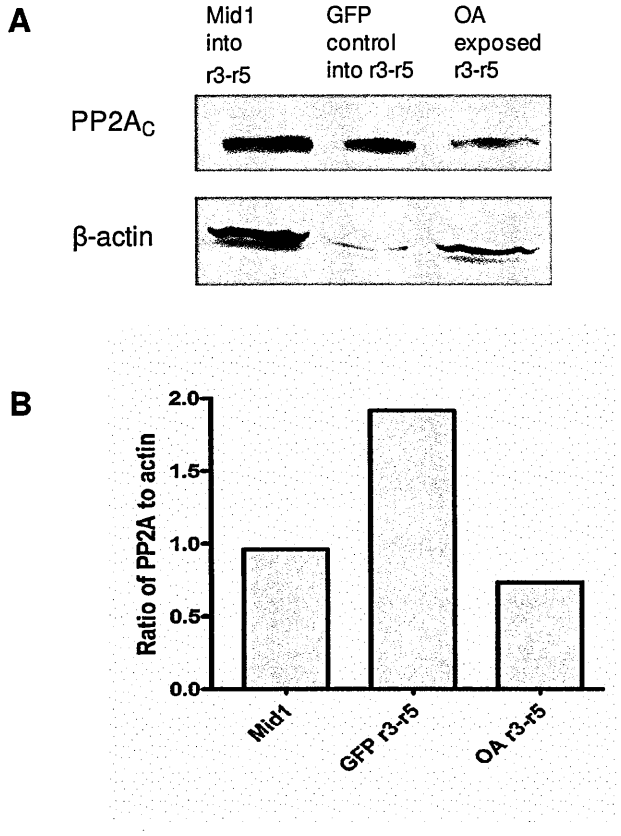

Figure 3-11. Analysis of $PP2A_C$ protein levels following Mid1 electroporation or Okadaic acid exposure.

Western blot analysis of PP2Ac protein levels following Mid1 or GFP control electroporations and OA exposure (**A**) and subsequent densitometry to compare ratios of $PP2A_C$ (36kD) and β-actin (43kD) (**B**). These results show less $PP2A_C$ present in the presence of Okadaic acid and following electroporation with the Mid1 construct in comparison to the GFP control electroporated tissue. Tissue for western blotting was pooled r2 from 30 embryos for each condition (n=1).

3.3.7. Ectopic expression of Mid1 promotes faster migration of r4 cNCCs from the neural tube

As we know that the migration pattern of cNCCs that endogenously express Mid1 was altered by DN-Mid1 expression, the next step was to determine if Mid1 had any affects on the migration pattern of r4 cNCCs that do not normally express Mid1. Embryos were unilaterally electroporated with the Mid1 expression construct at 10ss and then processed at various times with a HNK1 antibody to determine if the cNCC migration pattern was affected. In the wholemount embryos, there was no evidence that the electroporation of Mid1 into cNCCs affected their migration pattern, as determined by HNK1 immunostaining 9 hours following electroporation (8/8 100%) (**Figure 3-12**). However, at the whole-mount level, it appears that there may be an increase in the number of cells migrating in the r4 stream of cNCCs, as it does seem to look wider than on the contralateral control side (6/8 75%) (**Figure 3-12**). Thus, although the pattern appears not to be affected, cell migration speed could be altered; cells may be migrating faster and/or leaving the neural tube earlier.

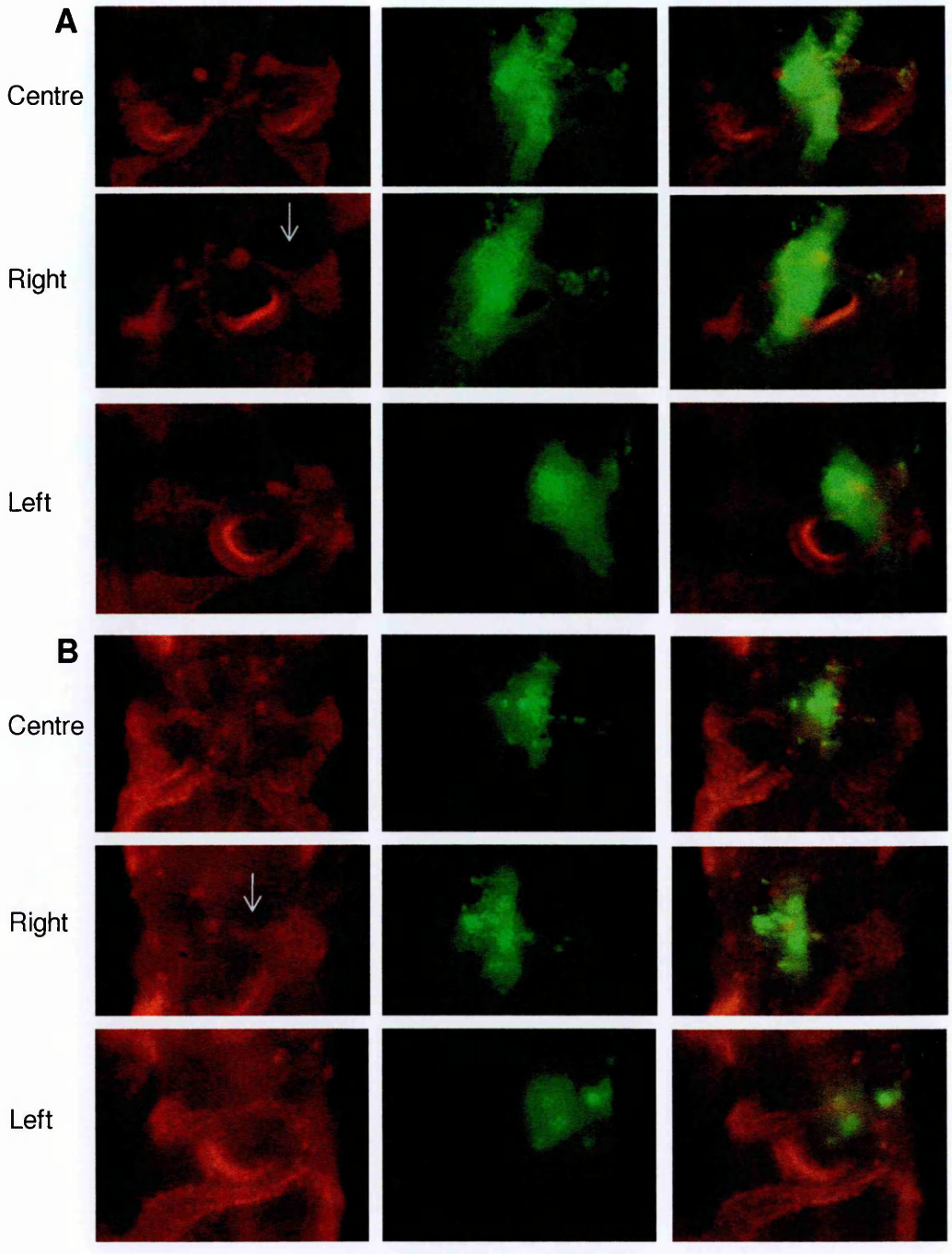

Figure 3-12. Neural crest cell pattern following Mid1 electroporation.

Embryos were electroporated with Mid1 (**A,** n=6/8) or GFP control (**B,** n=6/6) constructs at 10ss and incubated for 9 hours to 16ss. Embryos were subsequently stained with anti-HNK (red) and anti-GFP (green). Panels show left, right and centre views of the same embryo for each electroporation. Arrows indicate r4 cNCC streams on electroporated side of the embryo.

In order to see if cNCCs were undergoing EMT prematurely and therefore contributing to the r4 cNCC migrating stream earlier therefore leading to a slightly thicker stream of cells, embryos unilaterally electroporated with Mid1 were immunostained with a Pax3 antibody (labels premigratory and migratory cNCCs) to check if there were fewer cNCCs in the neural tube due to early delamination. Upon confocal analysis of sections, it was clear that the Pax3 staining was less on the Mid1 electroporated side of r4, but was unaffected in GFP electroporated embryos (**Figure 3-13**). This, along with the possibly thicker cNCC stream (**Figure 3-12**), supports the theory that Mid1 over-expression does promote early delamination of cNCCs from the neural tube.

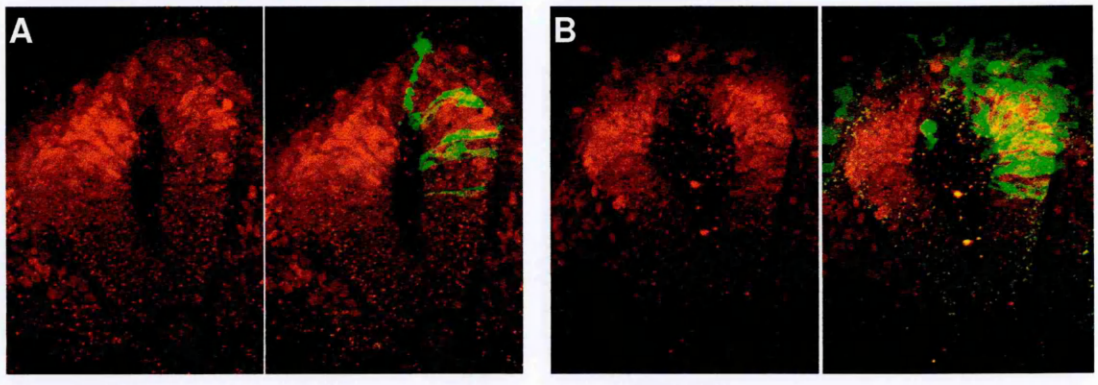

Figure 3-13. Pax3 staining of Neural Crest cells in the neural tube following electroporation.

Embryos were electroporated with Mid1 (**A**) or GFP control (**B**) constructs at 10ss and incubated for 6 hours to 14ss. Embryos were subsequently stained for Pax3 (red) and GFP (green). Sections showed a decrease in the number of Pax3 stained cells within the neural tube on the electroporated side in the Mid1 expressing embryos. Sections were cut at 70 microns and scanned using a confocal microscope, n=2/4.

3.3.8. Ectopic expression of Mid1 in r4 neural crest causes premature geniculate ganglia development

At the level of r4, the cNCCs contribute to the acoustic ganglia, while the placodal cells from the epibranchial geniculate placode contribute to both the geniculate and acoustic ganglia ([72, 131], Figure 1-7). As demonstrated in **Figure 3-9** and **Figure 3-10**, development of the peripheral nervous system was affected by an increase in PP2A activity, leading to delayed gangliogenesis, either by down regulating the activity of Mid1 through the DN-Mid1 construct or by using the PP2Ac expression construct. If regulation of PP2A activity via Mid1 is important for cNCC migration and gangliogenesis, then it could be predicted that inhibiting PP2A in r4, either by electroporating a Mid1 expressing construct or by pharmacological inhibition of PP2A, should have the opposite effect, leading to precocious ganglia formation. The geniculate ganglion begins to form at around 13ss, and by 20ss the development of the geniculate and acoustic ganglia is well underway [132]. Therefore viewing the peripheral nervous system at 20+ somites would be an appropriate time point to study if Mid1 has any affect on the development of the geniculate-acoustic ganglia. Embryos electroporated with the Mid1 construct were fixed at different time points in order to ensure there was a better chance of covering the correct period of development to observe any changes in nerve growth. Embryos were electroporated unilaterally into the neuroepithelium at the level of r4 at 10ss and incubated for 22hours to early 24-25ss and also 24 hours to late 26-27ss, before being stained for NF (a neuronal marker). Interestingly the embryos did show a distinct difference in the development of the geniculate ganglia, there was much more NF positive staining covering a larger area, in the Mid1 electroporated embryos (**Figure 3-14**), 9/14 (64%) at 22 hours and 9/21 (43%) at 24 hours. As previous results showed that the ganglia development phenotype was transient, the experiment was repeated using the Mid1 construct electroporated into r4 at 10ss and incubated for 48 hours (~40ss). The embryos were then stained using the NF and GFP antibodies and the ganglia were found to be of

the same size (3/3) (**Figure 3-15**), therefore the effect is transient, as was seen in longer-term DN-Mid1 electroporated embryos. At all experimental times, no obvious differences were observed in neuronal staining within the neural tube, therefore the Mid1-induced changes are specific to the cNCC.

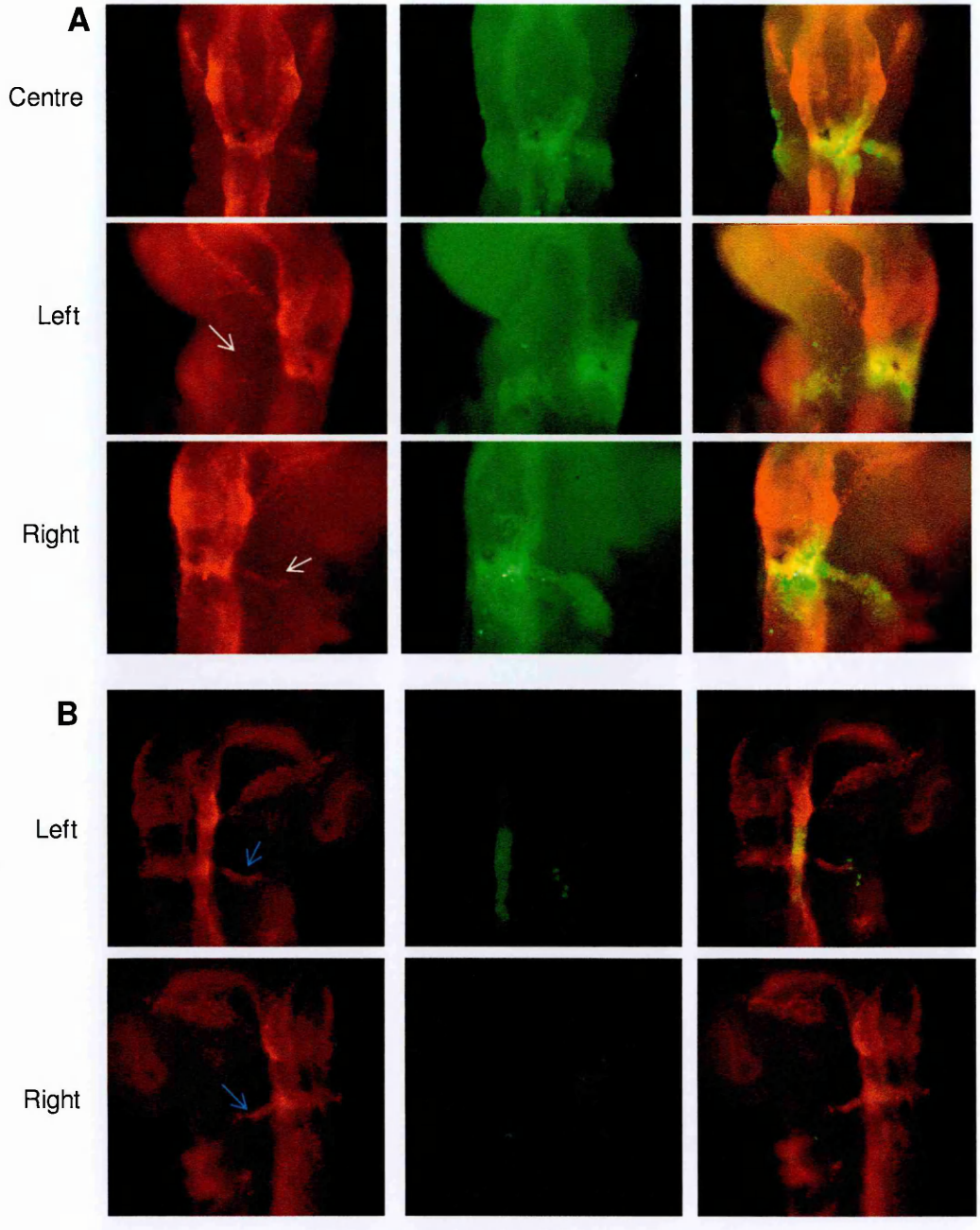

Figure 3-14. Ganglia development following Mid1 electroporation.

Embryos were electroporated with Mid1 (**A**) or GFP control (**B**) constructs at 10ss and incubated for 22 hours to 25ss. Embryos were subsequently stained for NF (red) and GFP (green). Panels show left and right views of the same embryo for each electroporation. The figures show that there is increased neuronal staining (compare white arrows) on the right side of the embryo, which has Mid1 positive neural crest (n=9/14). In comparison the GFP control embryos do not show a left-right difference in neuronal staining (compare blue arrows, n=8/8).

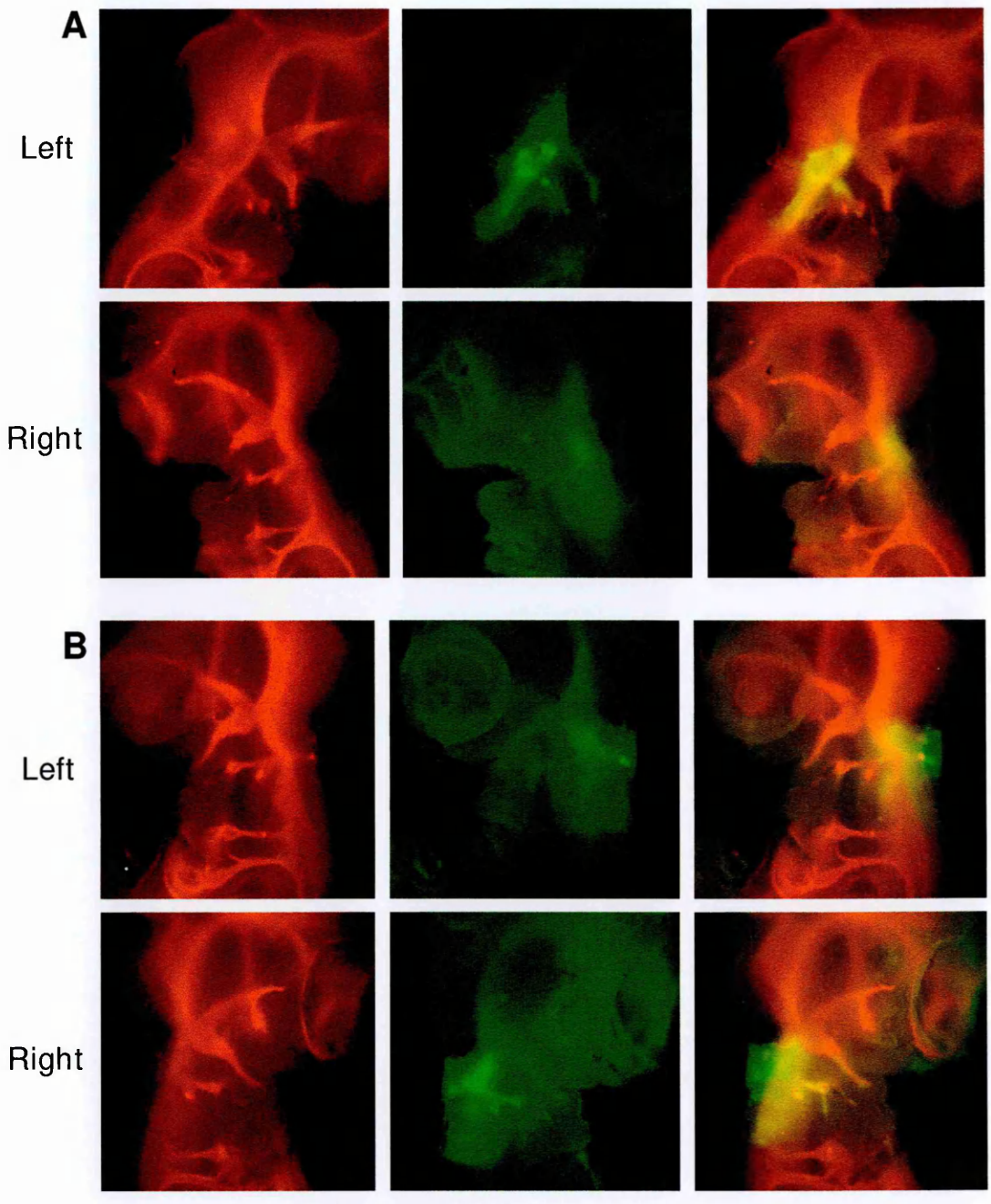

Figure 3-15. Ganglia development following Mid1 electroporation.

Embryos were electroporated with Mid1 (**A**) or GFP control (**B**) constructs at 10ss and incubated for 48 hours. Embryos were subsequently stained for NF (red) and GFP (green). Panels show left and right views of the same embryo for each electroporation and illustrate how the development of the ganglia is now left-right symmetrical by this stage, n=3/3 for both Mid1 and GFP embryos.

3.3.9. Premature ganglion formation is not contributed to by cell death

The observations of changes in cNCC migration patterning, ganglion development and Pax3 staining are consistent with the hypothesis that alteration of active PP2A protein levels is affects the migration of NCCs and also the subsequent development of the peripheral nervous system. However it is possible that other mechanisms could be involved, cell death could be being altered, the NCCs expressing Mid1 may be being protected from dying therefore there are more available to affect development of the geniculate placode. The possible involvement of altered cell death in the observed ganglia phenotype was investigated in both Mid1 and GFP control unilaterally electroporated embryos. To test this, embryos were electroporated as usual at 10ss and incubated for 9hours to 16ss before being processed with an Apoptag kit, which labels all strands of DNA with breaks, in cells, thus labelling cells undergoing apoptosis with red fluorescence. The Apoptag staining of the embryos was not very strong, however some positively stained cells could be observed (**Figure 3-16**). It appears as though there was little difference in apoptosis at the placode region or in the r4 cNCC stream in all embryos (Mid1 6/6, GFP 4/4). It is difficult to tell if there is a change in the rate of cell death in the neural tube as the GFP masks the red staining, although some increased cell death would be expected on the electroporated side in any case, as a result of the electroporation technique. Overall it does not appear as though the amount of apoptosis has been greatly affected by expression of either the Mid1 or GFP construct, as a reasonably large difference would need to be seen in order to lead to the changes in ganglia development, which should be identifiable, even with weak staining. Therefore apoptosis has been ruled out as the main cause of the premature ganglia phenotype.

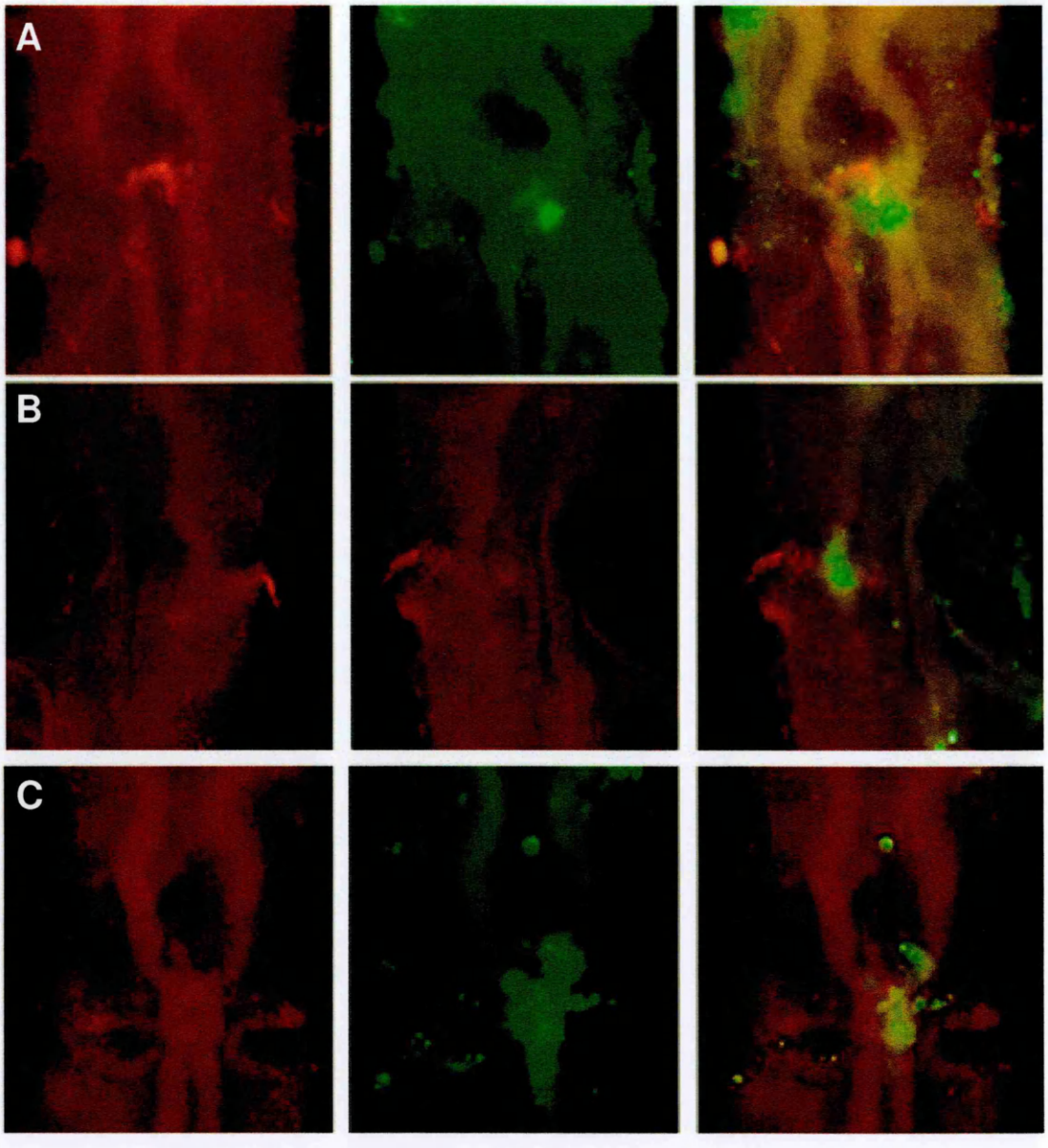

Figure 3-16. Cell death following electroporation.

Embryos were electroporated with Mid1 (**A,B**) or GFP control (**C**) constructs at 10ss and incubated for 9 hours to 16ss. Embryos were then processed using an Apoptag kit (red) for cell death and GFP (green). Panel **A** shows a dorsal view of a Mid1 electroporated embryo, Panel **B** shows the same embryo as in A, left and right views showing no visible change in apoptosis following Mid1 electroporation. (n=9 Mid1 electroporated, n=6 GFP electroporated).

3.3.10. Okadaic Acid delivery to r4 mesenchyme mimics the effects of ectopic Mid1 expression in r4 on premature ganglia development

Mid1 expression or OA treatment, both lower PP2Ac levels in r4. In order to determine whether premature geniculate ganglia formation in Mid1-electroporated embryos was due to reduced PP2A, I used the pharmacological PP2A inhibitor, Okadaic acid (OA). Affi-blue resin beads soaked in OA, were applied to the surface of embryos at the level of the r4 mesenchyme. The beads should allow a focal, slow release of OA to the surrounding tissue, therefore mimicking the constant presence of Mid1 in electroporated cells.

The OA concentration used to soak the affi-blue beads was 10nM. This is in line with previous studies using OA on NCCs or chick embryo tissue, which range from 0.1-20nM [113, 133-135]. Embryos were exposed to OA beads at 10ss for 22hrs to 24ss, as in the electroporation experiments. After staining with anti-NF, the OA-treated geniculate ganglia could clearly be seen to have the same premature development as in the Mid1 electroporated embryos (**Figure 3-17**). The general neuronal patterning within the neural tube did not appear to be affected, as was the case with the Mid1 electroporated embryos. Overall these results support the theory that a decrease in PP2A activity is the cause of the premature development of the ganglion.

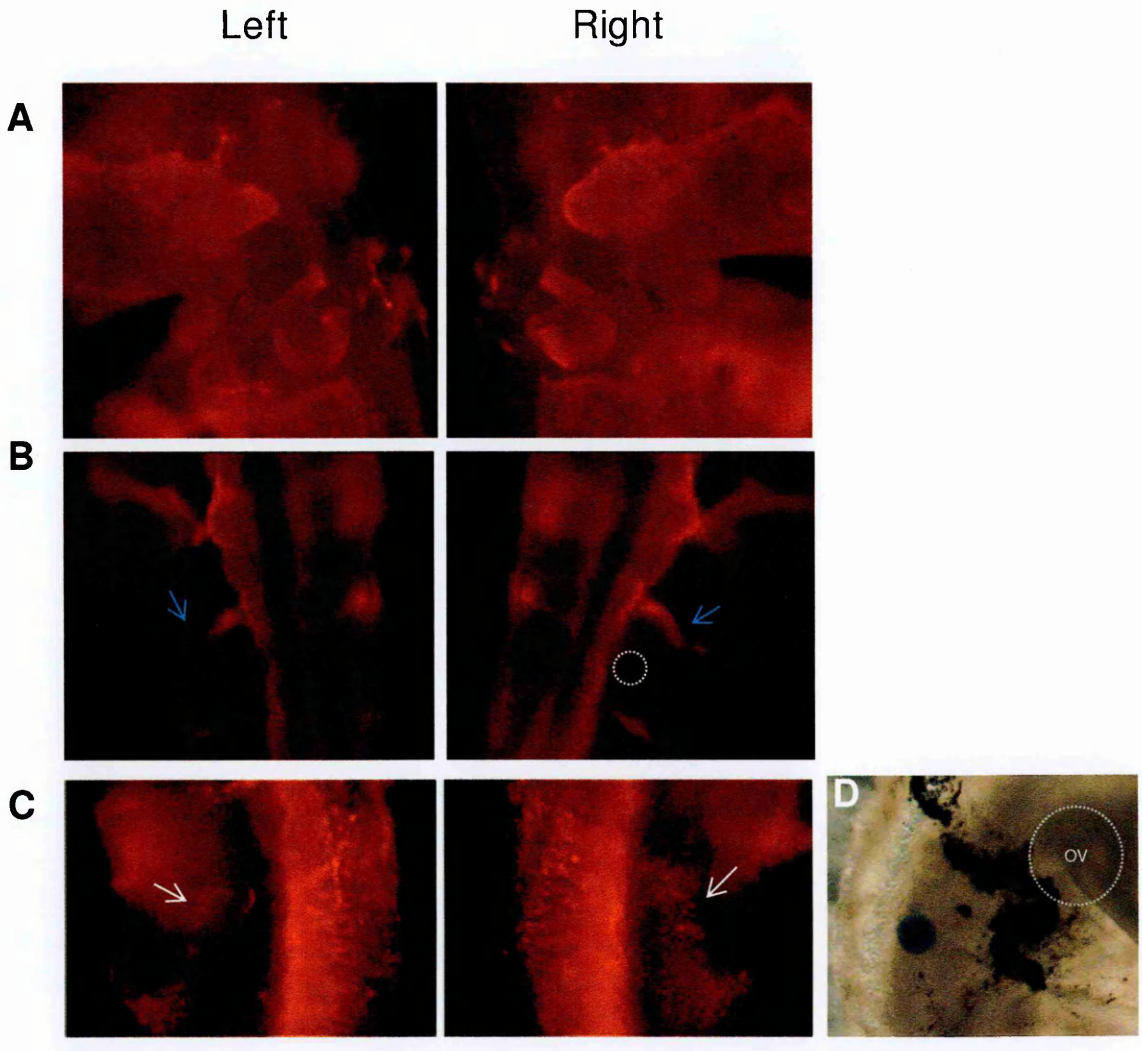

Figure 3-17. Okadaic Acid application to r4 mesenchyme mimics Mid1 over-expression in r4 NCC.

Embryos were incubated with a 10nM bead of OA over the r4 mesenchyme at 10ss and incubated to 25ss. Panel **A** shows left and right views of an embryo processed for the neural crest marker, HNK (red, n=9/9). Panel **B** shows an embryo stained for the neuronal marker, NF (red, n=9/17), the dotted circle depicts the placement of the OA bead, blue arrows show the geniculate ganglia. In **C** an embryo was also stained for NF (red), but had the OA bead placed over r6 mesenchyme, instead of r4 mesenchyme, the dotted circle shows the otic vesicle and bead placement, white arrows show the location of the developing ganglion for comparison (n=4/6).

In order to check that the changes in ganglion development are not exclusive to the geniculate ganglia following OA exposure, beads of OA were placed over the r6 mesenchyme at 10ss and incubated for 22 hours, before immunostaining with anti-NF. Interestingly the neuronal staining adjacent to r6 showed the same phenotype of more neurons on the OA exposed side (**Figure 3-17** C, white arrows n=4/6 embryos). Therefore it can be concluded that the effect of decreasing PP2A activity leading to premature ganglion formation is not exclusive to the r4 mesenchyme and geniculate ganglia.

3.3.11. Premature gangliogenesis is not due to diffusible cues from the neural tube

Because the neural tube is the target of the electroporations performed here, and the OA bead will most likely also be affecting the neural tube, the phenotypes I report could be due to altered secretion of molecules from the neural tube which could indirectly affect the cNCCs, in addition to the direct effect of Mid1 and OA on cNCCs. To test this, embryos were electroporated in r4 with pCAB.Mid1 or pCAB.GFP, as usual, or treated with OA beads, and allowed 6 hours incubation in order to allow GFP positive cells to migrate out of the neural tube and into the surrounding mesenchyme. After the 6 hour incubation, the neural tube and notochord of rhombomere 4 were removed and the embryos reincubated to 25ss before fixation. All embryos were stained for NF, and the electroporated embryos additionally for GFP. Mid1 (3/9 33%) and OA (4/9 44%) treated embryos showed the premature ganglia development phenotype (**Figure 3-18**), although this was not as pronounced as in unoperated embryos. This could be due to fewer Mid1 positive cells delaminating from the neural tube before its removal, and fewer cNCCs for the OA to have an effect on. However, if the phenotype were exclusively due to neural tube secretions,

then far fewer embryos with phenotypes would be expected. For these reasons, the data suggest that the phenotype is due to cNCC-intrinsic changes.

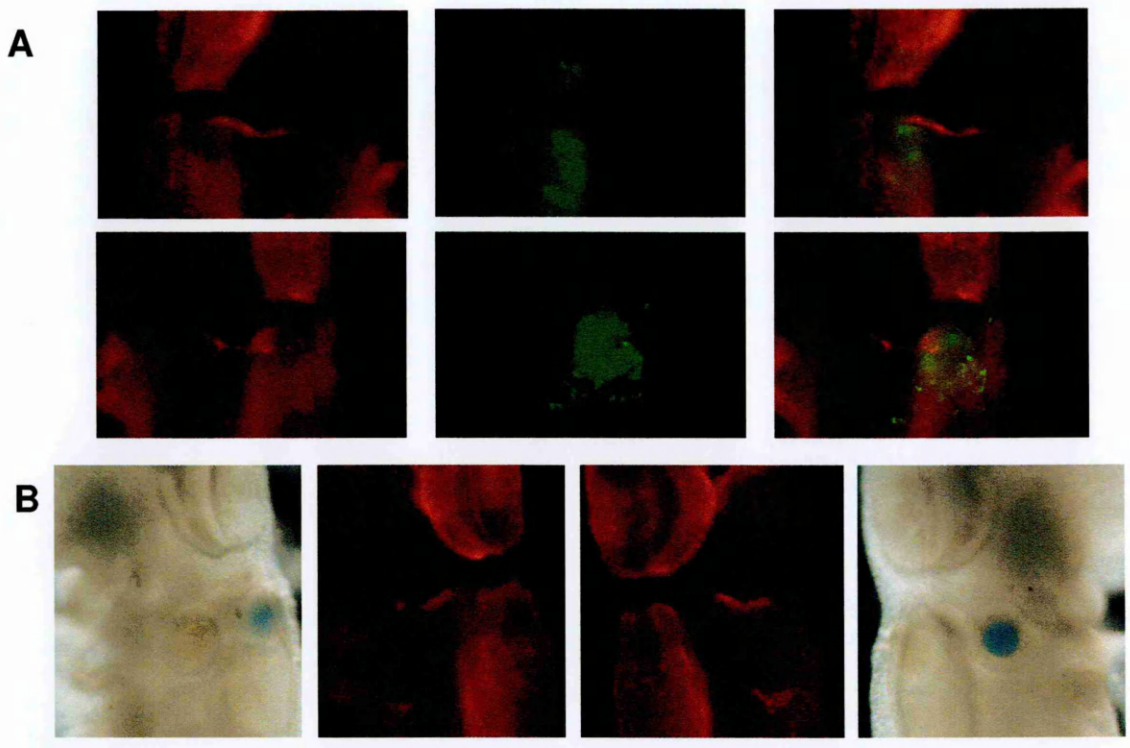

Figure 3-18. Removal of the neural tube partway through incubation following Mid1 electroporation or OA exposure leads to premature ganglia development.
Embryos were electroporated with the Mid1 (**A,** n=3/9) construct or had a 10nM OA bead placed over r4 mesenchyme (**B,** n=4/9) at 10ss and incubated for 6 hours before whole removal of rhombomere4 and re-incubation to 25ss. Embryos were then immunostained for Neurofilament (Red) and for the electroporated embryos GFP (Green) in addition.

3.3.12. Decreased PP2A activity in cNCCs *in vitro* leads to increased cell speed and reduced substrate adhesion

To further investigate the theory that PP2A causes premature ganglia development by promoting cell migration, studies were conducted on cNCCs *in vitro* in the presence of the PP2Ac inhibitor OA. Okadaic Acid has been shown to be toxic to cells at high concentrations [136-138], so a range of concentrations (100pM, 1nM, 5nM, 10nM) were tested on cNCCs grown on fibronectin. 1nM was found to be a workable concentration that did not induce a significant level of cell death (data not shown), cell morphology was also more similar to that of cells incubated without OA at this concentration.

Neural crest cells were obtained by explanting r4 from 10ss embryos or r2 from 8ss embryos, allowing cNCC to emigrate onto the culture substrate for 4hr and then removing the neural tube (to exclude any neural tube effects). The speed of the cells was then measured over successive 2 hour periods using time-lapse video microscopy. Cells in the r4 cultures increased in speed very significantly ($p<0.001$) when compared to before OA addition, and migrated around a quarter faster than before the OA was added to the culture media. After 2 hours, the r4 cNCCs with OA were still increasing their speed of migration in comparison to the r4 cNCCs without OA, at every time point the difference in speed from that before OA addition was highly significant ($p<0.001$). The r2 cNCCs showed no significant difference in cell speed with OA (**Figure 3-19**), which is expected as they already express Mid1 and therefore should have little PP2A to inhibit, in comparison to the r4 cNCCs, in order to affect cell speed. One observation made during these *in vitro* experiments was that untreated r2 cNCCs migrated significantly slower than the r4 cNCCs. Furthermore the speed of the r2 cNCCs was unaffected by OA, implying that the r2 cNCCs were already migrating at their maximum speed, possibly due to their constitutive expression of Mid1. This could explain why Mid1 is needed in the r2 cNCCs, if they are slow cells to migrate in the absence of Mid1, the activity of Mid1 may be

needed to speed them up in order for them to migrate to their correct destination in time for correct development. Therefore inhibiting Mid1 activity, through the DN-Mid1 expression construct, should slow them down.

To test this and also reinforce the OA data, cells were transfected with the DN-Mid1 (r2 cNCCs) or Mid1 (r4 cNCCs), by electroporating the appropriate construct into the correct rhombomere and then removing the tissue as in the OA experiments to allow the electroporated cNCCs to migrate into the dish for culture and subsequent time-lapse. This was not as successful as the OA time-lapse culture as many of the cNCCs that migrated out subsequently died, leaving very few cells to track. This was a problem with the technique and not due to the expression of Mid1, as the same was observed with the control GFP construct. Another problem was that in order to track the electroporated cells, they needed to be immunostained for GFP at the end of the filming period, in order to identify the construct expressing cells, because the endogenous fluorescence of the GFP was too weak to be seen on a single cell level. As the electroporation method was unsuccessful, a lipofection approach was tried. However, once again the NCCs mostly died and there was still the same problem of needing to immunostain the cells after filming to identify GFP positive cells.

The behaviour and morphology of cells migrating in the presence of OA was quite different to that of the cNCCs in the absence of OA. Cells exposed to OA were more likely to round up, to be more spherical, and move quickly over the surface of the culture dish, compared to the more flat, slow moving cNCCs without OA.

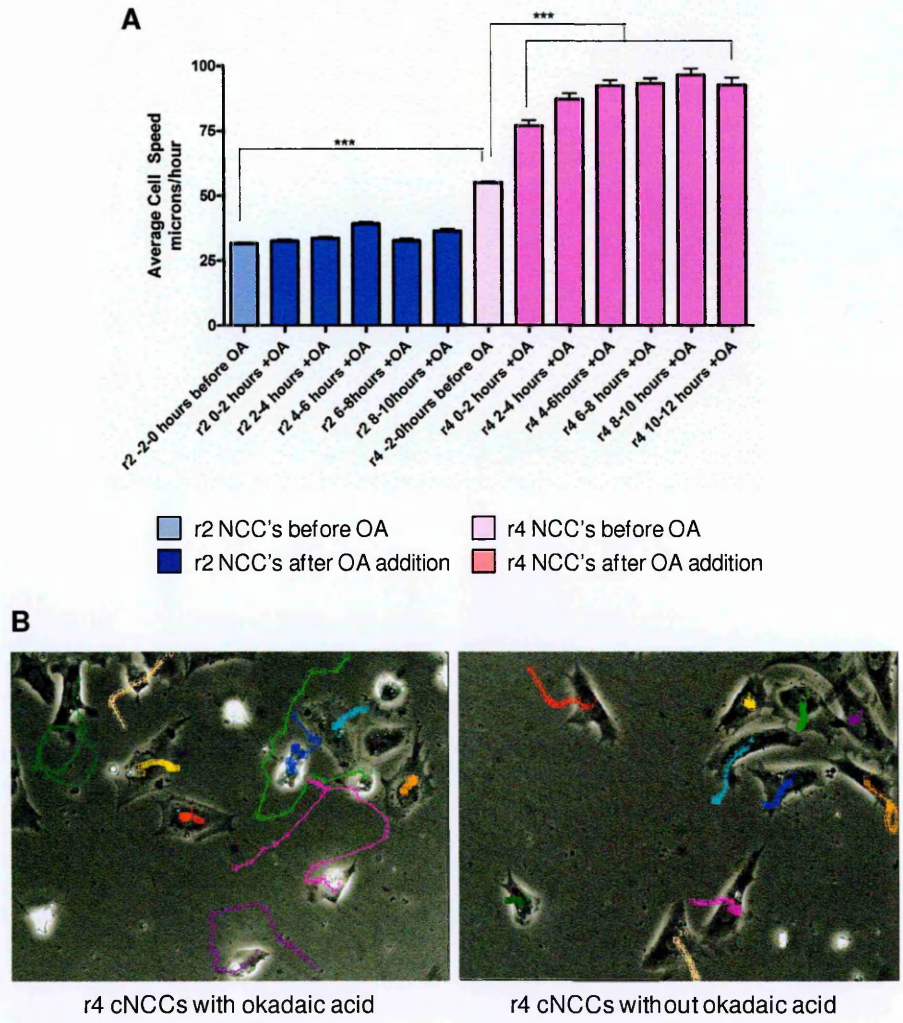

Figure 3-19. Time-lapse analysis of r2 and r4 cNCCs *in vitro*, with and without the presence of Okadaic Acid.

Cranial neural crest cells were grown *in vitro* on fibronectin coated tissue culture plates, with or without the presence of 1nM OA in the culture media. The first two hours of filming were done without OA in both experimental and control cultures. **A** shows a graph of the average cell speed μm/hour, **B** shows a representative photo of tracked cNCC movements both with and without OA over the 10 hour period. $P<0.001$ (***), $P<0.05$(*). Numbers of cells tracked n=111 r2 prior to OA, n=16-48 r2+OA, n=93 r4 prior to OA, n=17-26 r4 +OA. The time lapses were performed on 4 separate occasions.

3.3.12.1. OA reduces cNCC cell adhesion on fibronectin

A possible explanation of the observed motility behaviour is that it was caused by a lack of adhesion to the substrate, therefore allowing the cells to move more quickly. In order to test this hypothesis, cNCCs were incubated in the presence of OA overnight and then agitated for 1 hour on a shaker. The number of cells before and after agitation was counted. OA significantly increased the number of cells that could be detached from a fibronectin substrate. However when the cNCCs were grown on PLL, there was no significant difference in the loss of cells following agitation between the OA and non OA incubated cells (**Figure 3-20**). As no significant change in the number of cells is observed on PLL, it can be concluded that the changes in adherent cell numbers on other substrates is due to a loss of adhesion and not due to an increase in cell death, which would then lead to cell detachment.

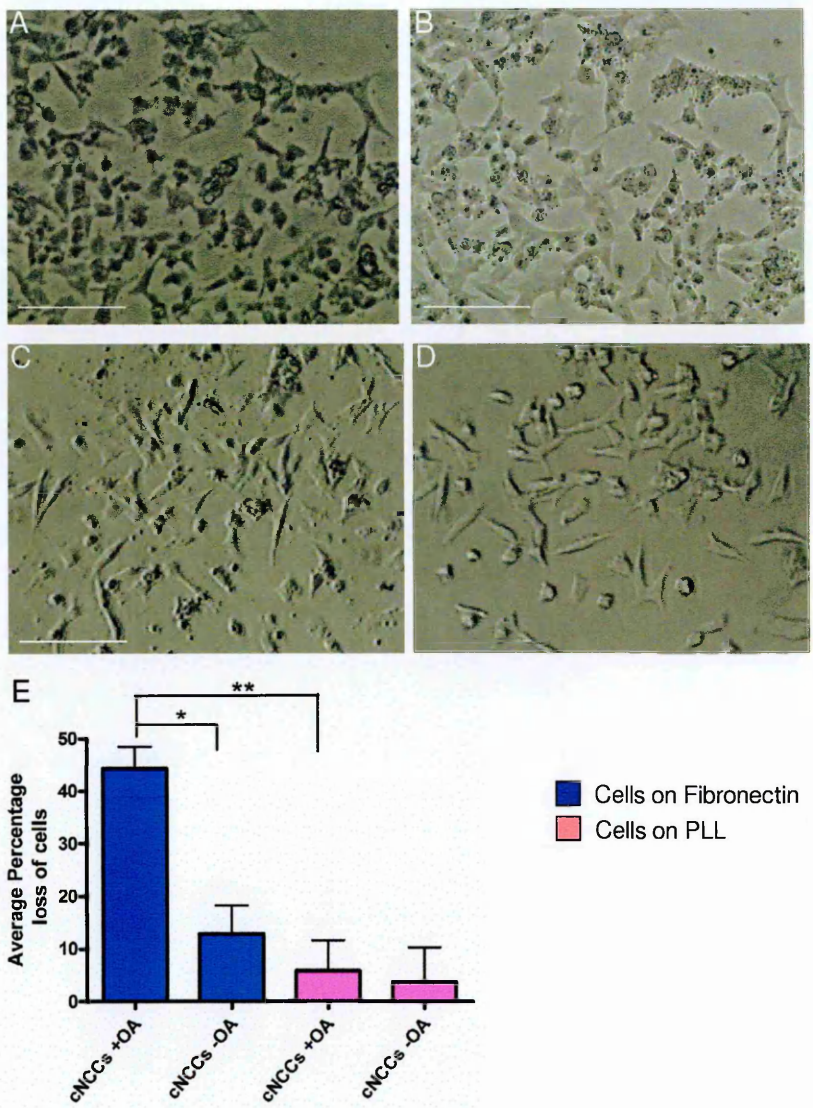

Figure 3-20. Okadaic Acid reduces cell adhesion to fibronectin, but not to PLL

Rhombomere 4 explants were cultured overnight before the addition of 1nM OA to the culture media, the cells were photographed then placed on a shaker for 1 hour before being photographed again. **A** – cNCCs on fibronectin before agitation, **B** – cNCCs on fibronectin after agitation, **C** – cNCCs on PLL before agitation, **D** – cNCCs on PLL after agitation. **E** - Cell counts were taken and the percentage loss of cells during the agitation period were calculated. The average percentage loss was taken from 3 separate rhombomere explants in the same culture dish for cell counts for each condition. $P<0.01$ (**), $P>0.05$ (*), one-way ANOVA. Numbers of cells counted per frame before agitation, 3 frames per condition, 1 frame of view from each rhombomere, n=20-85 cells fibronectin –OA, n=21-223 cells fibronectin +OA, n=35-60 cells PLL –OA, n=41-96 PLL+OA. Scale bar – 50μm. This experiment was performed once.

3.3.13. Decreased PP2Ac in r4cNCCs encourages a neuronal cell fate in vitro

In order to investigate if Mid1 has a role in cell fate decisions of cNCCs Mid1 electroporated r4 cNCCs, or normal r4 cNCCs we cultured in the presence of OA, and then stained for NF. (**Figure 3-21**). Pilot experiments in which cNCCs were cultured for 24hours before fixation and subsequent immunostaining for NF showed no NF positive cells. However by day 5 in culture several NF positive cells had developed, therefore a 5 day culture of cNCCs was used as the endpoint in this experiment. The counts demonstrated that the cells treated with OA or electroporated with Mid1 more readily differentiated into neurons than those electroporated with the GFP control construct. The conclusion here is that decreased PP2A activity could have a small effect on cell fate, but is probably not significantly contributing to the *in ovo* phenotype, unless environmental factors have a significant effect. If so, then sections through the ganglia should show more NF-GFP double positive cells in Mid1 electroporated embryos, than in GFP electroporated controls. Therefore sections were taken transversely through embryos showing the phenotype at wholemount level, the sections (4/4) mainly showed no NF-GFP double staining (**Figure 3-22**), with only 1 section showing 2 double stained cells. In conclusion Mid1 expression does not appear to be driving a cell-autonomous neuronal cell fate at this stage of development and so is not the mechanism behind the observed ganglion phenotype.

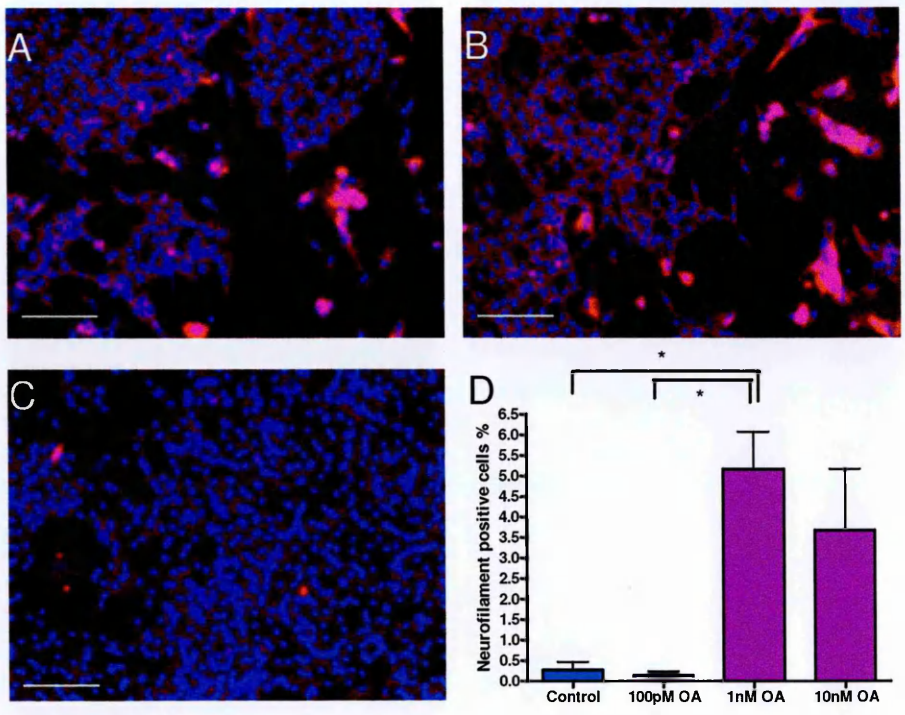

Figure 3-21. Long-term exposure to Okadaic acid promotes neuronal differentiation in r4 NCCs.

Neural crest cell culture from r4, incubated with OA for 5 days and stained for Neurofilament (red) and Hoechst (Blue). Figure shows cells incubated at 1nM OA (**A**), 10nM OA (**B**), Control (**C**) and a graph showing percentage Neurofilament positive cells in each condition (**D**). $P<0.05$ (*). Numbers of cells counted per frame, 3 frames per condition, n=1544-1983 cells at 100pM, n=185-409 cells at 1nM, n=426-698 cells at 10nM, n= 901-1862 cells for controls. Results representative of 3 repeats of the experiment. Scale bars – 100μm.

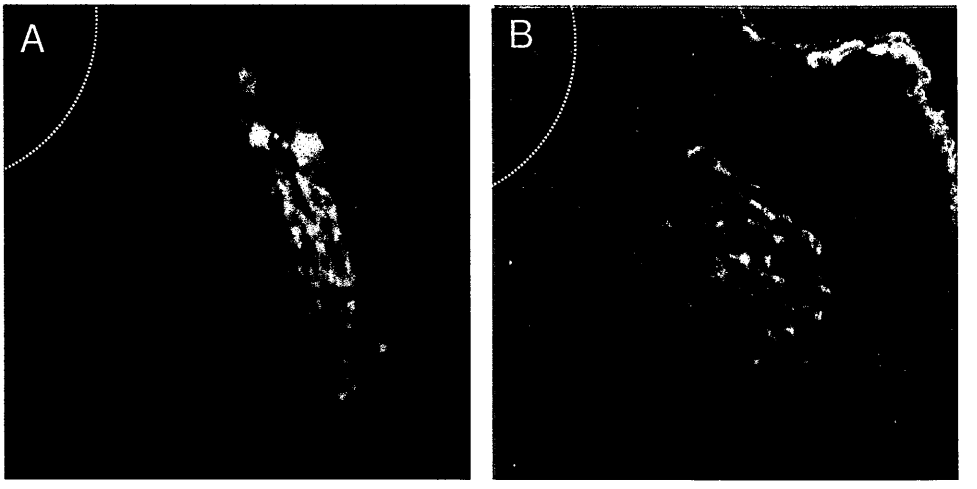

Figure 3-22. Confocal sections though the geniculate ganglia following Mid1 electroporation.

Embryos were electroporated with Mid1 (**A**, n=4/4) or GFP control (**B**, n=4/4) constructs at 10ss and incubated for 22 hours to 25ss. Embryos were subsequently stained for NF (red) and GFP (green) then sectioned at 70 microns. Staining revealed a lack of double stained cells, implying that the Mid1 transfection is not encouraging cells to differentiate into neurons. Dotted white line shows location of neural tube.

3.3.14. Premature placode cell migration following Mid1 r4 cNCC expression

Cells of the epibranchial geniculate placode differentiate into the neurons of the developing geniculate ganglion; the acoustic ganglion is populated by neurons derived from neural crest cells from the r4 cNCC stream and also placode cells from the epibranchial geniculate placode [72] (see Figure 1-7). The epibranchial placode cells do not enter the mesenchyme and begin to migrate towards the site of ganglion development until the cNCCs migrate to them first [80]. The neural crest cells are required for the placodal cells to migrate, in the absence of cNCCs the cells of the placode remain there [80]. However, neural crest cells reach the placode well before placode cells enter the mesenchyme, suggesting that, whilst NCC are necessary, additional factors or

maturational changes in NCC are also required before placode cell migration can occur. Breakdown of the basal lamina that separates the ectodermal placodes from the mesenchyme coincides with placode cell migration [70]. Thus it is possible that the premature ganglion formation observed in the Mid1 electroporated embryos is due to premature basal lamina breakdown, allowing release of placodal cells into the mesenchyme to form the geniculate ganglia sooner than normal. This could be caused by the OA exposed or Mid1 expressing r4 cNCCs secreting something that affects the rate at which placodal cells are able to leave the placode, such as proteases that break down the basal lamina.

In order to investigate the possibility that placodal cell migration was affected when PP2A activity is decreased, a cell tracker dye (CM-DiI) was used to label the placodal cells. This was achieved by covering the entire surface ectoderm of an embryo at 10ss which had been either electroporated with the Mid1 construct or an OA bead was placed over the r4 mesenchyme. Embryos were incubated to 25ss, then removed and processed with a NF antibody, with or without a GFP antibody as appropriate, and sectioned. This end point was selected because the embryos are at a stage when the geniculate ganglia formation would be well underway, allowing any changes in their development to be more easily observed.

The sections showed that the placodal cells had indeed migrated further into the embryo with OA treatment or Mid1 electroporation (**Figure 3-23**). Sections through the Mid1 electroporated embryos show clearly that there is increased migration of the DiI (red) labelled placodal cells into the mesenchyme towards the neural tube on the electroporated side compared to the contralateral side. Moreover the Mid1 r4 electroporated embryos and the OA treated embryos clearly show that the placodal cells are the cells contributing to the premature geniculate ganglia.

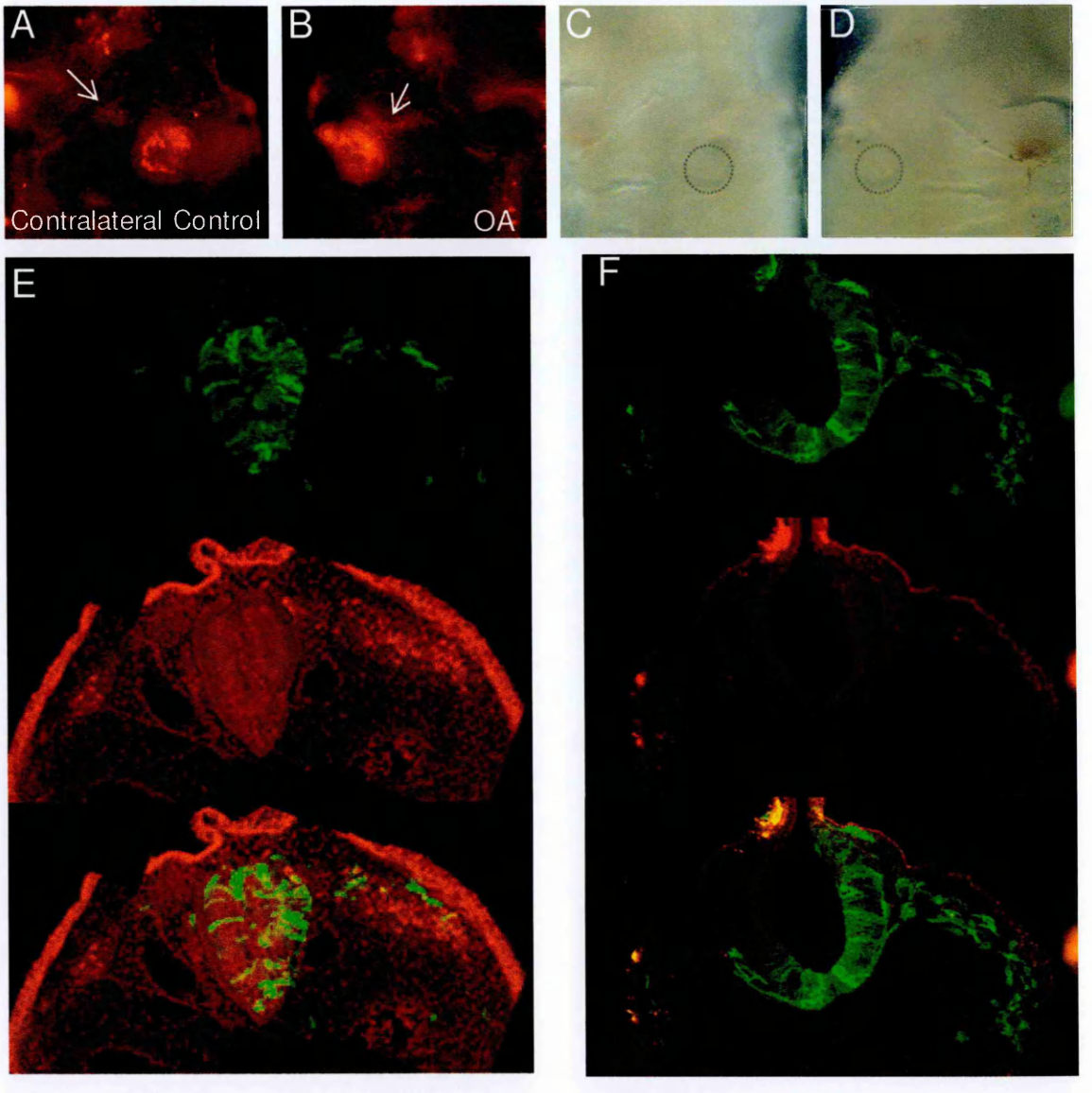

Figure 3-23. Migration of placodal cells following electroporation

Embryos were electroporated with the Mid1 construct, 30 mins later the embryos were covered in CM-DiI (red) and then incubated from 10ss to 25ss, before fixing and staining with GFP antibody (green). A,B – wholemount view of embryos before antibody staining, arrows show position of placode and labelled placodal cells that can be seen migrating inwards (n=5/9), same embryo is shown in C,D the otic vesicles are outlined by the grey dotted line. Panel E shows sections through an r4 Mid1 electroporated embryo at the level of the placode, Panel F shows an embryo electroporated with the GFP construct at the level of r4 (n=6/6).

3.3.15. Increased breakdown of basal lamina at the placode following OA treatment

The question at this point is how does Mid1 in r4 cNCCs cause placodal cells to prematurely form the geniculate ganglia? A few possible explanations are that the placodal cells could migrate earlier, they could be more motile or they could have a higher rate of proliferation. After electroporation, the number of cNCCs with detectable levels of GFP is small. However this small number of cNCCs could secrete molecules that promote placodal cell migration or increase cell proliferation rates. As placodal cell migration only occurs once the basal lamina has broken down enough for the cells of the placode to pass [70], it is possible that there may be an increase in protease activity caused by the presence of Mid1 electroporated cNCCs or exposure of the cells to OA. It is well-known that cranial neural crest cells secrete metalloproteases [83, 85, 86] that can break down the basal lamina around the placode, thus allowing the cells of the placode to migrate away. OA treatment or Mid1 expression could cause a change in the secretion of MMPS or other proteases by cNCCs, if this is the case, then it would be expected that the protease secretion would increase in order to break down the basal lamina faster. In order to test if there is a premature or more extensive basal lamina breakdown following Mid1 or OA exposure, embryos were treated with OA as before, incubated to 16ss and stained with a laminin antibody, to show the basal lamina, and Pax2, to stain the cells of the placode. The sections through these embryos showed that the OA-treated embryos have increased sub-placodal basal lamina breakdown on the treated side, in comparison to the contralateral side (**Figure 3-24**).

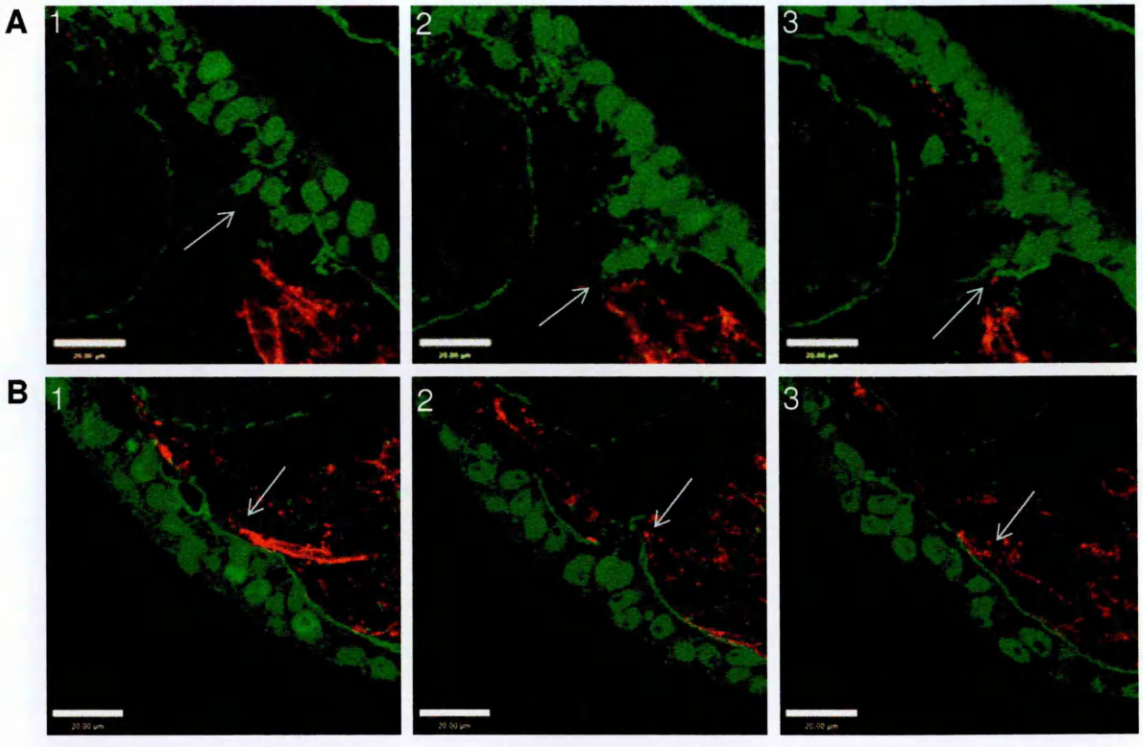

Figure 3-24. Confocal sections though the geniculate placodal region following Okadaic Acid exposure.

Embryos were treated with Okadaic Acid beads over r4 mesenchyme (**A,B**) at 10ss and incubated for 9 hours to 16ss. Embryos were then stained for NF (red) and Pax2-Lam(green) and sectioned at 70 microns. Panels show successive confocal images through the same section for both the OA bead treated side (**A**), and the contralateral untreated side (**B**). The sections illustrate an increased migration of the placodal cells inwards and an increased breakdown of the basal lamina (arrows) on the embryos treated with OA, but not the corresponding untreated side of the same embryo (n=2/4). Sections were taken 14µm apart from a confocal stack.

Okadaic Acid is likely to have a much faster effect on PP2A activity in comparison to electroporation with Mid1, as the cells take a few hours to begin expressing the protein. Therefore one question is whether the OA bead could be applied at a later stage to the placode and still have the same effect. To test this possibility beads were placed over the r4 adjacent mesenchyme at 15-16ss and incubated to 25ss. After staining with NF it was clear that there was no difference in development of the ganglia in experimental OA (9/9)

and control (8/8) embryos. Therefore late inhibition of PP2A at the placode level was not effective. This result shows that it is the exposure of the cNCCs to OA, at an earlier stage of development, which causes the ganglion phenotype and not exposure of the placodal cells to OA before they migrate away from the placode. Therefore a change in PP2A activity levels in the placodal cells does not affect their normal migration or development.

3.3.16. Changes in the observed speed of cNCCs in vitro on different substrates following OA exposure

Proteases have different substrates (see Figure 1-9), so it is possible that the proteases involved here are targeting other matrix proteins, either in addition to or instead of laminin. Although the analysis of basal lamina breakdown *in vivo* described above focused on laminin, it is possible that disruption of other matrix proteins could lead to the breakdown of the basal lamina. To further test the hypothesis that the OA treated cNCCs are secreting additional proteases that break down the basal lamina, by degrading matrix proteins, the cNCCs were analysed by time-lapse microscopy in culture with and without OA addition on different substrates. As fibronectin was used in the previous time-lapse studies, these time-lapses were performed with laminin, collagen and PLL coated tissue culture plates. Collagen and laminin were chosen as both are components of basement membranes. The *in vivo* data showed that laminin was increasingly degraded in the presence of Mid1 electroporated cNCCs, therefore it is possible that there is increased degradation of laminin by the proteases, which may affect cell motility. PLL was used as a substrate as proteases should not have an effect, and therefore acts as a control for cell motility. Depending on which combination of substrates show differences in cell speed, if any, it should help to narrow down possible candidates of proteases with elevated secretion/activity.

Overall the results showed that cells on collagen and PLL increased cell speed following OA exposure, however untreated cells moved faster on both PLL and laminin, but not on collagen. The collagen results show that there is a significant increase in the speed of the r4 cNCCs on collagen at every time-point after the first 2 hours in the presence of OA (**Figure 3-25** A). There is a large increase in cell speed between 0-2 and 2-4 hours in the presence of OA and then the cell speed remains relatively constant until the end of the observed period. This mirrors the observations of the cells on fibronectin the closest.

When the cells are on grown on laminin the opposite occurs; the speed of the cNCCs in the presence of OA is slower than without; there is a significant difference in the cell speed at all time periods except 0-2 hours (**Figure 3-25** B). In the absence of OA the cNCCs show a gradual increase their cell speed; however with OA the cell speed remains relatively constant with no significant differences in cell speed between the time periods observed. This could be indicative of a change in protease action in the presence of OA, perhaps there is an increase in laminin degradation which leads to the cells moving more slowly, possibly due to the action of membrane bound proteases.

When the cells are grown on PLL, there is no significant difference in cell speed at the 0-2 hour and 4-6 hour time periods, but at the 2-4 and 6-8 time periods there is a significant difference (**Figure 3-25** C). Overall the cells show a gradual increase in cell speed over time in both cell sets with and without OA, which is by the last time period, significantly faster than at the 0-2 hour time period ($P<0.001$ for both with and without OA cell groups).

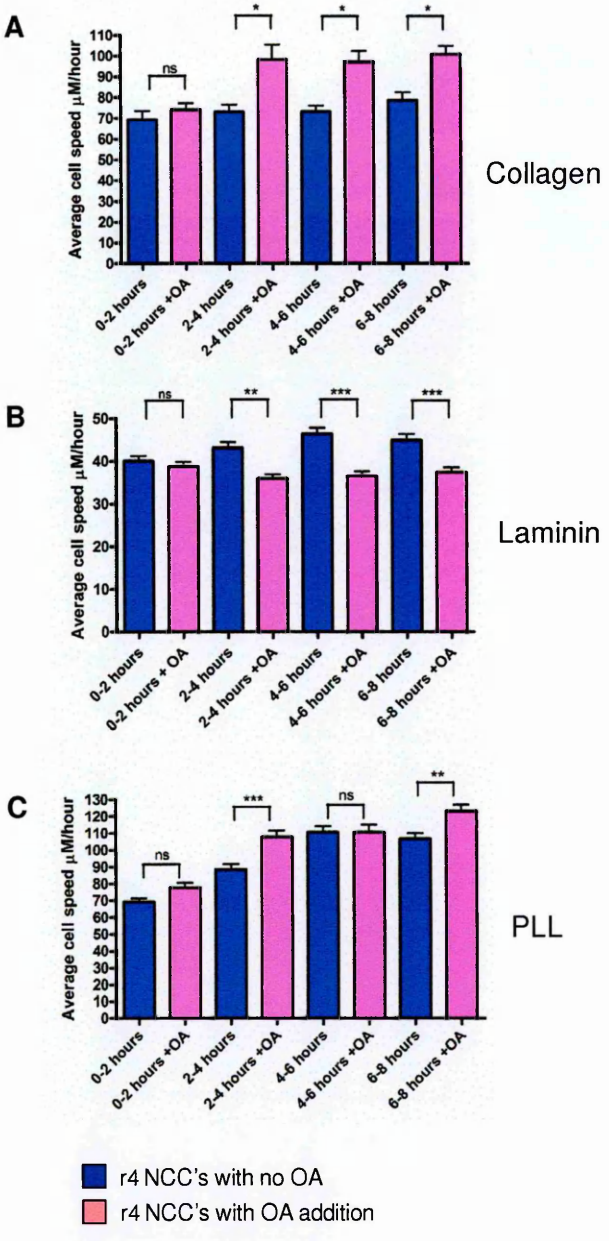

Figure 3-25. Time-lapse analysis of r4 cNCCs *in vitro* on different substrates, with and without the presence of Okadaic Acid.

Cranial neural crest cells from rhombomere 4 were grown *in vitro* on PLL (**A**), Laminin (**B**) or Collagen (**C**) covered tissue culture plates, with or without the presence of 1nM OA in the culture media. P<0.001 (***), P<0.01 (**), P>0.05 (*). Numbers of cells tracked per condition, n=17-19 Laminin +OA, n=18-21 Laminin –OA, n=21-26 PLL +OA, n= 27-34 PLL –OA, n=37-52 collagen +OA, n=34-44 collagen -OA. Each experiment was repeated twice and had 3 separate rhombomeres for each condition. At least 3 different fields of view for each condition from different rhombomeres were analysed.

3.3.17. RT-PCR analysis of OA treated r4 tissue

In order to determine more specifically which, if any, proteases were up-regulated in response to OA exposure, RT-PCR's were performed on tissue exposed to OA (RT-PCR was performed by Jon Golding, **Figure 3-26**). We chose to analyse the expression of proteases known to be expressed by neural crest and/or with substrate specificities for fibronectin, collagen and laminin, which had demonstrated OA-dependent changes in time-lapse analyses. Rhombomere 4 was dissected from embryos at 10ss and then incubated in media for 5 hours, with or without the presence of 1nM OA. RT-PCR's were performed using primers for cMMP10, cMT1-MMP, cTIMP-2, cADAM10 and cGAPDH. Interestingly cMMP10, is down-regulated following OA incubation, while cADAM10 is up-regulated. There also appears to be a reduction in the expression of cTIMP2, however not as marked as the others. GAPDH was used here as a control as it is a constitutively expressed housekeeping gene, the similar quantities of cMMP2, cADAM10 and the high level of cTIMP-2 to GAPDH implies that there is a high level of expression of these proteases in r4 tissue. Other RT-PCR's performed that did not show any changes include, MMP1, MMP2, MMP13 and ADAM13. These results show that changes in the expression of the MMP's and related proteins may well be responsible for the phenotypes observed.

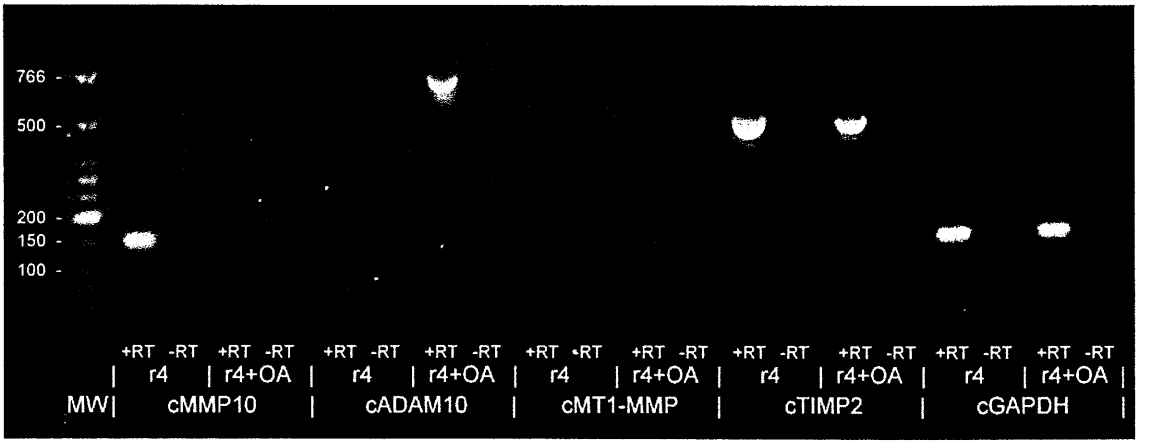

Figure 3-26. RT-PCR of r4 tissue following OA exposure

Rhombomere 4 was dissected out of 10 embryos for each condition. The tissue was then incubated in complete DMEM, either with or without the presence of 1nM OA in the culture media, for 5 hours. The tissue was then used for RT-PCR analysis, using primers for chick MMP10, MT1-MMP, ADAM10, Timp2 and GAPDH. Control PCR's were executed for each different probe in the absence of reverse transcriptase (**-RT**). n=1, RT-reverse transcriptase. MW – molecular weight marker.

3.4. Discussion

Because of its potential role in regulating very many cellular processes (i.e. via its effects on microtubules and PP2A), the precise roles of Mid1 in cranial development have remained unclear. The work shown here demonstrates for the first time how defects in Mid1 could affect cranial morphogenesis. Changes in cell migration and protease activity of the cranial neural crest affect the development of the cranial ganglia as shown here. Although the effects on ganglia formation appear temporary, they may have longer-term consequences, especially considering that I made only transient transfections into individual rhomomeres. Furthermore, since Mid1 is re-expressed in the frontonasal processes at the time of midline fusion, these findings could provide a basis for the understanding of how Mid1-regulated protease activities remodel the cranial mesenchyme during face formation.

The gene expression pattern of Mid1 as described here is in agreement with the findings of Richman (2002) that Mid1 is expressed in rhombomere 2 at 10ss [110]. Furthermore my results show that Mid1 is also expressed by the cNCCs migrating into the mesenchyme adjacent to r1/r2, but Mid1 expression is then down-regulated as cNCCs migrate further away from the neural tube. PP2A is ubiquitously expressed throughout development [139], therefore where there is no Mid1 activity, it could be expected that PP2Ac activity would increase. For example as Mid1 is down regulated in cNCCs the branchial arches, it is reasonable to believe that the level of PP2Ac activity would be high in these cells compared to the cNCCs closer to the neural tube, leading to hypophosphrylation of the microtubules. Down-regulation of genes in neural crest cells as they enter the branchial arches has been observed before; expression of both *Slug* and *RhoB* have been found to be down-regulated as cNCCs migrate further away from the neural tube [140]. Moreover *RhoB* and *Slug* have been implicated to be involved in delamination of the cNCCs from the neural tube [141, 142]. Interestingly a protein

interaction survey has shown that RhoB interacts with PP2Ac [143]. This possible RhoB/PP2A interaction, along with the decreased number of Pax3 positive stained cells in the neural tube and down regulation of Mid1 as cNCCs migrate further from the neural tube, implies an involvement of Mid1 in EMT.

The Mid1 homologue, Mid2, can compensate for the loss of Mid1 in early embryo development [97], therefore to check that Mid2 was not being expressed in r4 cNCCs and that its expression was not in the r1/r2 migrating cNCCs or in r2 ISH were performed for Mid2. The results showed a low expression of Mid2 throughout the neuroepithelium and slightly stronger expression in the midbrain at 10ss. No expression was observed in the r4 cNCCs at 10ss, however there is some expression of Mid2 at 13ss in the r4 adjacent mesenchyme, although this appears to be possibly from the developing otic vesicle from the curved pattern of expression.

Western blots were carried out using total cell lysates from rhombomeres 2 or 4 that had been electroporated with either the experimental or control constructs as well as rhombomere 4s that had been exposed to OA. Although these constructs have been used in previous studies, no verification of the effect of these constructs on PP2A protein levels has been published. The changes in PP2A protein levels following electroporations were as expected, with reduction in PP2A protein following Mid1 construct electroporation and an increase in PP2A protein following DN-Mid1 electroporation in comparison to the control GFP electroporated tissues. Interestingly there was a reduction in the level of PP2A protein following treatment of rhombomere 4 tissue with OA, even more so than that of the Mid1 electroporated tissue. As OA is an inhibitor of PP2A it was unexpected that it would affect the level of protein and not just the protein activity. However as the OA appears to have reduced the level of PP2A and hence mimics the effect of Mid1 over-expression it is therefore serving its intended purpose.

Although PP2A has been shown to autoregulate in the presence of OA [144], this activity was not observed in the western blots presented here. This difference from previously published work could be attributed to the difference in the methods used, Baharians and Schonthal [144] maintained the cells in culture for 24-48 hours in the presence of OA, whereas in the present study the tissue was only exposed for 6 hours to OA before removal. The concentration of OA used here was also significantly lower, only 10nM in comparison to the 50nM used in the Baharians and Schonthal study. The autoregulation of PP2A may be a dose dependent response, therefore at the lower concentration shown here, PP2A autoregulation may not be triggered.

3.4.1. Neural crest and changes in Mid1 activity

Less Pax3 staining, and therefore less cNCCs, were observed within the neural tube following Mid1 construct electroporation. Furthermore a wider r4 cNCC stream was observed on the Mid1 electroporated side than the contralateral control side of the neural tube. These results imply that the Mid1 positive cNCCs are delaminating sooner than the control unelectroporated cells. This is backed up by the observations made when DN-Mid1 is expressed in r2 and its cNCCs, the cNCCs on the DN-MID1 electroporated side failed to migrate into the r2 adjacent mesenchyme. A likely explanation is that cells are not delaminating from the neural tube and expression of the DN-Mid1 is affecting delamination, migration or EMT of the cNCCs. Together with the DN-Mid1 results, it can therefore be concluded that Mid1 is likely to be involved in the delamination, migration or EMT of the cNCCs from the neural tube.

The mechanism by which Mid1 affects the delamination, migration or EMT of cNCCs, could either be by PP2A ubiquitination or microtubule stabilization, but it is most likely due to the PP2A function. This is because it has been found in previous studies that when

microtubules are destabilised there is an increase in EMT [145], however Mid1 has been shown to be responsible for the stabilisation of microtubules [109]. Therefore if this was the mechanism through which Mid1 affects EMT it should be expected that reduction in Mid1 activity would increase EMT as the microtubules would be less stable.

Cell death was considered as a possible reason for the decrease in cNCCs in the neural tube observed. The transcription factor Foxo1 has been found to be, expressed in migrating cNCCs of mice embryos; it has also been shown to be inhibited by phosphorylation upon inhibition of PP2A, which leads to a decrease in Foxo1 mediated cell-death [146]. Therefore Mid1 activity would be expected to increase cell survival, which would not explain the lack of cNCCs in the neural tube, and in addition no obvious differences were observed with the Apoptag staining following Mid1 electroporation of r4.

One possible mechanism through which changes in PP2A activity, by Mid1, could lead to alterations in EMT is the BMP4 pathway as proposed by Granata [96]. As summarised in **Figure 3-27**, BMP4 has been shown to induce EMT *in vitro* [147] and further down the signalling pathway, Snail has long been known to induce EMT by repressing transcription of E-cadherin [148]. As Mid1 acts upstream of both BMP4 and Snail, an increase in Mid1 activity could therefore lead to an increase in BMP4 and Snail activity, which would then increase EMT, which is in line with the observations made here. During the course of this thesis several attempts were made to prove that changes in Mid1 activity were affecting EMT, through immunostaining wholemounts and sections for E-cadherin, Occludin and Claudin, however no working protocol could be found for these antibodies. Therefore no changes in tight junctions between the cNCCs in the neural tube could be studied. In conclusion Mid1 probably affects cNCC delamination or EMT through its PP2A ubiquitination function.

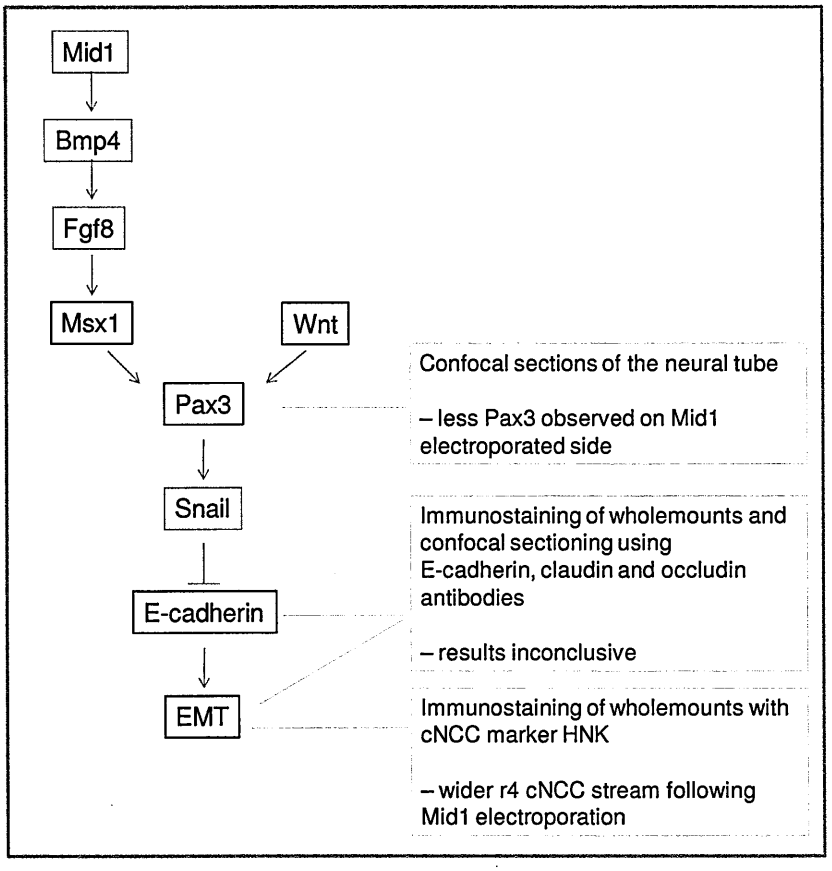

Figure 3-27. Mid1 signalling cascade and induction of EMT

The Mid1 signalling cascade as outlined by Granata [96] (shown here in pink boxes) and Monsoro-Burg [149] (shown in blue boxes). The experiments tried over the course of this PhD, and their outcomes, to address points of the cascade are shown in yellow boxes.

3.4.2. PP2A and its affect on ganglia development

The results shown here provide evidence that PP2Ac activity plays a role in cranial ganglion development. Increases in the level of active PP2Ac by decreased Mid1 leads to delayed trigeminal ganglion development, while an increase in Mid1 activity or OA exposure, and therefore a decrease in PP2Ac, leads to premature development of the geniculate ganglia. In order to test the path through which Mid1 is acting OA was used to treat cNCCs at the same stage of development as the Mid1 construct was electroporated into cNCCs of r4. Okadaic acid is an inhibitor of PP2A [150], therefore if Mid1 is acting

through its PP2A ubiquitination function, application of OA would be expected to mimic the premature ganglia formation observations. Indeed the OA did mimic Mid1 electroporation, confirming that Mid1 is most likely acting through its PP2A ubiquitination function.

As cells of the placode form much of the geniculate ganglia [72], and cNCCs are required for the correct migration of the placodal cells from the geniculate placode to the point of ganglia formation [80], it was hypothesised that the PP2Ac inhibited/decreased r4 cNCCs may have changed their behaviour somehow, perhaps through a change in secretions, and therefore initiating placode migration prematurely. Using a method similar to that of Begbie and Graham 2001 [80], the placodal cells were labelled with a lipophilic fluorescent dye, the results showed that more cells of the placode were prematurely migrating towards the ganglia site on the Mid1 electroporated/OA treated side compared to the contralateral control side. Therefore it can be deduced that the cells of the placode are in fact the cells forming the premature ganglia.

3.4.3. Regulation of protease activity by Mid1

There are a few ways that the increased Mid1 in r4 cNCCs may initiate placodal cell migration. First the cNCCs may be migrating faster and the increased numbers of cNCCs in the vicinity of the placode may be enough to initiate migration. Secondly as MMPs are required for cNCC detachment from the neural tube [88], it is possible that changes in MMP activity by altering Mid1 expression could be leading to the increased migration of the cNCCs and also the premature breakdown of the sub-placodal basement membrane and subsequent detachment of the cells of the Placode. The increased protease activity could also be the reason for the increased EMT from the neural tube, as observed with the Pax3 staining, possibly by breaking down the cell-cell contacts, between premigratory NCCs. Therefore if there is an increase in MMP activity the basal lamina of the placode may be broken down sooner, which means the placodal cells would be able to migrate

away from the placode earlier. It was observed that there was an increased breakdown of the basal lamina at the placode and the following premature influx of placodal cells from the placode confirmed that changes in MMP activity may well be involved in the premature migration of the cells of the placode.

Furthermore the time-lapse results on different substrates gave indication that both cell speed and changes in MMP activity may well be involved in the premature ganglion development. As different MMPs have different substrate specificities the multiple time-lapse observations on collagen, fibronectin, laminin and PLL were used to try to narrow down possible candidates. PLL was used as a control as protease activity will not affect it, and although no real changes in cell speed were expected, there were some significant increases in cell speed following OA exposure. This suggests that there are also changes in cell motility following PP2A inhibition, which has been observed before [112]. A possible explanation for this finding is that BMP4 is up-regulated by OA, as has been observed in *Xenopus* [151], which leads to an increase in cell motility [147]. Although this mechanism could be involved here, the changes in cell motility are not as striking on PLL as on the other substrates or on r2 cNCCs. Therefore changes in MMP activity could be the main change in cNCC properties upon OA exposure, leading to premature ganglia development, rather than cell motility.

Of the known MMPs and their substrates, one is known to digest all 3 of collagen, fibronectin and laminin, this is MMP10 in chick, and its orthologue in human and rodents, MMP3 [152]. Interestingly MMP3 has been shown to be upregulated in the presence of OA in fibrosarcoma cells [153]. It is viable that the observations in the time-lapse studies may not be due to one MMP alone but a combination of several proteases or related proteins. Therefore RT-PCRs were performed to look at the expression levels of different

MMPs and related proteins that were candidates for changed expression, which were chosen due to known expression at this stage of development.

Adam10 has been found to be expressed in avian neural crest cells [85] and has been shown to be involved in the breakdown of N-cadherin, which in turn stimulates neural crest delamination from the neural tube [154]. Therefore an upregulation of Adam10, as observed in the RT-PCR results, would be expected to increase cNCC emigration from the neural tube, such as that observed following Pax3 staining of the neural tube following Mid1 expression.

MT1-MMP is expressed in the cranial neural crest tissues in *Xenopus* [86] and in cardiac neural crest cells in chick [83] and its substrates are both laminin and collagen. Timp2 is expressed in migrating cardiac neural crest cells, but not the cNCCs from r2 or r4, it is also expressed in the neural tube in rhombomeres 5 and 6 [83]. MT1-MMP, along with low levels of Timp2, is responsible for the cleavage and subsequent activation of MMP2, which in turn promotes migration of the cNCCs [83, 92], an absence of Timp2 action with MT1-MMP leads to decreased NCC migration [83]. A high level of Timp2 inhibits the action of MT1-MMP [155] and therefore reduces the amount of active MMP2 which would then decrease migration. Therefore there must be a delicate balance between having a low level of TImp2 required for MMP2 activation and then too low or too high a level of Timp2 leading to a lack of NCC migration. There was little change observed in the expression of MT1-MMP in the RT-PCR, however there was a decrease in the expression level of Timp2, therefore predicting an increase in MMP2 activity which would increase migration. This is in line with the observations made by the time-lapse studies *in vitro*. Although it has been observed that a low level of Timp2 prevents cardiac NCC delamination [83], an increase in Adam10 may be able to compensate for the TImp2 action. Furthermore the level of Timp2 may have to be extremely low for it to have a

delamination inhibiting effect, as the previously recorded data was seen using a morpholino to knockdown expression, and there is still a reasonably detectable level of Timp2 detected using RT-PCR.

MMP10 was an obvious candidate due to its ability to digest all 3 substrates used in the time-lapse experiments. The transcription factor Mef2 is expressed in the neural tube of mice embryos at E9.5 (21-29ss) [156] and appears to be in chick cranial mesenchyme at the level of r2 and r4 at 16ss [157], as Mef2 is able to directly activate expression of MMP10 [158], it is possible that MMP10 is also expressed at this stage in the neural tube. This was confirmed by the RT-PCR results, showing MMP10 expression without OA, and undetected MMP10 following OA exposure. MMP10 has been shown previously to enhance migration in keratinocytes in mice, therefore it would be expected that an increase in MMP10 would be observed following OA exposure to increase cell migration. However MMP10 does not have to be the effective MMP in this case, other MMPs may be the responsible proteins for the observations made *in vitro*.

The results of the *in vitro* time-lapse analysis in the presence of OA and the subsequent RT-PCR results give strong evidence that Mid1 has a role in regulating MMP expression and this may be related to the observed changes in NCC speed *in ovo* and *in vitro*. These observations raise the possibility that PP2Ac plays a similar role in other cell type migration, cell fate, invasiveness and protease activity [159]. In other tissues or stages of development, PP2Ac activity could be regulated in other ways, such as by growth factors. Previous work has shown that growth factors are able to phosphorylate PP2A leading to transient loss of activity [160]. Overall these changes in protease activity levels could be the mechanism by which Mid1 controls the development of craniofacial structures as it is present at the stage of craniofacial tissue remodelling.

3.5. Conclusions

The spatio-temporal expression and functions of Mid1 in the hindbrain during development have until now been unclear. The data shown here provides evidence that Mid1 is not only expressed in the hindbrain but also in the migrating cranial neural crest cells in the r1/r2 adjacent mesenchyme. Mid1 appears to be responsible for maintaining the correct cell speed of the cNCCs and also is involved in the secretion of MMPs, which may be important in both EMT from the neural tube and also in breakdown of the basal lamina at the placodes. The results also show that the function through which Mid1 is having these effects is probably by its PP2A ubiquitination function and not through stabilisation of the microtubules. This work provides evidence that PP2Ac activity regulation is important for correct cNCC migration and cNCC developmental cell biology. Overall these data provides evidence for an important role in the correct migration of the cranial neural crest and also in the development of the peripheral nervous system at the very first stages of its initiation.

3.6. Future work

The data provided here depicts many novel findings; however there are several lines of research that remain open for further investigation. Firstly it would be interesting to perform some real-time RT-PCRs on the proteases; this approach would allow further insight into the levels of increases or decreases in the expression level of these proteins necessary to provide a phenotype caused by OA exposure or Mid1 construct electroporation. Following this, further artificial mimicking of the MMP changes observed here, by RNAi or expression constructs, in order to see if this would also produce the same observed changes in peripheral nerve development, would further elucidate the involvement of each individual MMP or combinations of the MMP proteins.

In order to further understand the possible effect of OA or Mid1 expression level changes on EMT or emigration of cNCCs from the neural tube and also sub-placodal basal lamina breakdown it would be beneficial to perform time-lapse confocal microscopy on sections of embryos in culture. A method has been developed by Wilcock and Swedlow [161] allowing slices of embryos to be cultured and studies by time-lapse, which would allow tracking of neural crest cells as they go through EMT or would allow interactions between cNCCs and the placode to be monitored. Therefore any changes in how the cells behave, such as morphology or cell-cell interactions would be able to be clarified.

It would also be beneficial to confirm the breakdown of the basal lamina in Mid1 electroporated embryos at a later time point. At 16ss no obvious differences were observed in the breakdown of the basal lamina, especially when compared to the OA treated embryos. This could be due to the possibility that OA can act immediately, whereas Mid1 needs more time to be expressed before it can be active

Use of a Mid2 construct to express Mid2 in r4 cNCCs would also be interesting, other studies have demonstrated the functional redundancy between the Mid proteins in other situations, it would be interesting to see if Mid2 can also mimic Mid1 in these circumstances.

4. Elucidation of the tissues responsible for retinoic acid-mediated defects in the migration pattern of cranial neural crest cells

4.1. Introduction and aims

It has been well documented that the hindbrain neural tube, the cranial mesenchyme and the surface ectoderm, each provide essential patterning information to direct the migration of cranial neural crest cells (cNCCs) (See **Figure 1-2**, section 1.3). When any of these patterning cues are disrupted, normal cNCC development, survival, migration and cell fate can be affected, resulting in craniofacial deformities [1]. An example of environmental effects which can lead to cNCC patterning disruption is retinoic acid embryopathy, pregnant ladies given a retinoid containing treatment for acne gave birth to babies with a range of congenital defects, such as cleft lip/palate, which can be caused by underlying cNCC defects [44].

Exposure of a developing embryo to retinoic acid (RA) can cause cranial neural crest cells to mismigrate (see section 1.6). When chick embryos are globally exposed to RA, crest begins to mismigrate into r3 mesenchyme and in 65% of embryos the r4 crest stream and the r2 crest stream are joined in a Type1 phenotype (Figure 1.5). A localised injection of RA into only r4 also induces a Type1 phenotype (in 54% of embryos) and causes the ectopic expression of Krox20 in r4, thus causing r4 to take on a more r3-like identity [45]. Injections of RA into r3 have no detected effect on crest patterning. Although the neural tube was the target of RA application, in the experiments quoted above, but it is by no means clear which tissue(s) are involved in responding to RA, to cause cNCC mismigration and, for this reason, I chose to focus on elucidating the tissues responsible for RA-induced cNCC migration defects.

Previous work has described tissues that are required for maintenance of a correct cNCC migration pattern (Figure 1.5). Removal of r3 or removal of the r3 surface ectoderm before cNCC migration leads to cNCCs incorrectly migrating through the mesenchyme adjacent to r3 in a Type1 phenotype [7]. Moreover several molecules, which are expressed within r3, have been identified as being essential for correct cNCC patterning, including ErbB4 [17, 24] and Cyp26s [68, 162]. However, although ErbB4 and Cyp26s have been identified as being involved in cNCC migration patterning, little more is known about how r3 is involved in cNCC migration patterning or the specific effectors.

ErbB4, a member of the EGF family of receptor tyrosine kinases, is required during development for axon and neural crest guidance and, in the hindbrain, is expressed in r3 and r5 [22, 23]. Furthermore previous work has shown that RA exposure can alter the expression levels of ErbB4 in breast carcinoma cells *in vitro* [163]. An ErbB4 ligand, neuregulin (NRG), is expressed in the developing chick hindbrain in r4 [22, 23]. This spatial arrangement of ligand and receptor suggests it is highly likely that interactions occurring between these rhombomeres activate the ErbB4 receptor. Loss of ErbB4 receptor activation leads to Type1 crest mismigration, with r4 cNCCmigrating through r3 mesenchyme to join the r2 cNCC stream as demonstrated by, a) the dominant negative loss of ErbB4 signalling in chick r3 [17], and b) absence of *ErbB4* in knockout mice (Box1) [24]. ErbB4 is not expressed by cNCCs and the absence of ErbB4 or ErbB4 signalling alters the environmental signals to which migrating NCCs respond. Thus when wild-type r4 NCCs are transplanted into ErbB4 knockout mice, they still mismigrate. Conversely, when ErbB4 knockout cNCCs are implanted into a WT mouse r4, they migrate normally [24].

When the RA catabolizing enzyme, Cyp26C, is knocked out in mice, the NCCs show a Type1 phenotype, similar to that seen in the absence of ErbB4 [164], suggesting that ErbB4 and Cyp26C may be in the same pathway. Although r4 does not express

detectable Cyp26C, it is produced in a segmented pattern within the r3 and r5 mesenchyme [67], and could therefore have a role in the maintenance of these crest-free zones. RA is also able to regulate the expression of the Cyp26 genes, down-regulating Cyp26C [165]. If Cyp26C is involved in preventing crest from entering r3 mesenchyme then its downregulation could make r3 mesenchyme less inhibitory to NCCs.

Because the observed cNCC mismigration patterns fit into two types (categorised in this thesis as Type1 or Type 2 defects (Figure 1.5), the work presented in this chapter aims to investigate the tissues involved in responding to RA which then leads to a Type1 phenotype. Furthermore this work aims to further elucidate if there is a common mechanism involved in Type1 phenotypes.

4.2. Results

4.2.1. Effects of retinoic acid on the neural tube and patterning neural crest cell migration

All-trans retinoic acid (at-RA), a well known teratogen [43], has been previously shown to cause cNCC mismigration, depicting a Type1 phenotype [45, 166]. The aim of this study was to better define which tissues respond to RA to give the Type1 mismigration phenotype and whether identifying these tissues could provide further information about common signalling pathways underlying this phenotype.

4.2.1.1. Optimising retinoic acid delivery and dose

Initially the method employed by Gale and Prince [45] was used, at-RA and DiI were co-injected unilaterally into the dorsal part of r4, where the premigratory cNCCs reside, at 10ss and the eggs were incubated for a further 24 hours. DiI is a lipophilic fluorescent dye that incorporates into the cell membrane allowing cNCCs to be tracked as they migrate away from the neural tube into the mesenchyme. The use of DiI allowed single cells that had mismigrated to be visualised, however the DiI labelling was variable and did not consistently label the entire cNCC population, as confirmed by subsequent Sox10 ISH processing of the embryos. The Sox10 ISH allowed the majority of the cNCC population to seen and allowed robust aberrant migration to be seen, but it was not possible to see individual ectopic cNCCs. Sox10 ISH was used as the basis for determining whether NCC mismigration had occurred, with DiI being used as an indication of correct injection site targeting and providing a backup for the Sox10 data. The concentrations of at-RA initially used were 10mM and 20mM, chosen because 16mM at-RA was used by Gale and Prince. However, neither concentration used replicated their findings of 55-65% NCC mismigration. Instead a very infrequent 4.2% (n=24) partial Type1 at 20mM and no phenotypes at 10mM (n=9) (**Figure 4-1**) were observed. The mismigration phenotypes

observed were either catagorised into either partial or full Tpe1 phenotypes, the partial Type1 shows cNCCs migrating into r3 adjacent mesenchyme from the r4 cNCC stream, but not all the way to the r2 cNCC stream. A full Type1 phenotype was recorded when the cNCCs were seen to have joined the r2 and r4 cNCC streams in a thin band through r3 mesenchyme. Therefore the concentration of injected at-RA was increased to 50mM, although this is a very high concentration of at-RA to be using in comparison to other studies, it was a test to see if this method of injection could work. Even at this high concentration the rate of incidence of a Type1 phenotype was only 22.5% (n=27). There are a number of reasons why this method may not have been effective. Firstly the RA may kill the cNCCs in the surrounding area or reduce their ability to delaminate [167, 168]. Secondly, the at-RA could be leaking out of the injection site, and so not be present for long enough to have an effect. Finally it is likely that variable volumes of the at-RA were injected into each embryo, this most likely the case for other published RA injection data too, as the same method is used and no indication of volume is given.

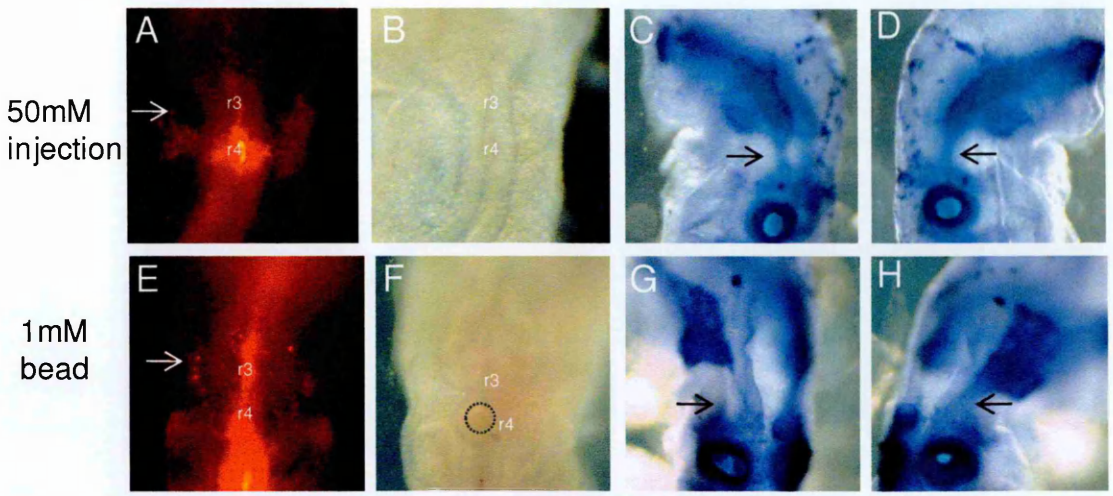

I

RA delivery method	Concentration of RA	Total number of sides with a phenotype %	Embryo sides with a partial type 1 phenotype (%)	G-test Significance
Injection	50mM	6/27 (22.2)	5/27 (18.5)	Yes
Injection	20mM	1/24 (4.2)	1/24 (4.2)	Yes
Injection	10mM	0/9 (0.0)	0/9 (0.0)	Yes
Bead – F	16mM	4/12 (33.3)	4/12 (33.3)	No
Bead –H	10nM	6/16 (37.5)	5/16 (31.3)	No
Bead – F	1mM	3/8 (37.5)	3/8 (37.5)	No

Figure 4-1 Neural Crest Cell Migration patterning defects following all-trans retinoic acid exposure.

Exposure of r4 to RA by either injection (50mM RA, **A-D** same embryo) or RA soaked beads (1mM RA formide bead, **E-H** same embryo) at the 10ss. The migration pattern of the NCCs were tracked by both DiI labelling of the cells at 10ss (**A,B,E,F**), and by subsequent processing by ISH for the NCC marker Sox10 (Blue, **C,D,G,H**). Table **I** shows the percentage occurrences of a Type1 mismigration phenotype, G-test of association was used to determine significance. ($G=3.8$, $p<0.05$, d.f.=1). Dotted grey line – bead placement. Arrows indicate mismigrating cNCCs. Bead types, F-formamide, H-hydroxide.

As there was a poor rate of cNCC mismigration phenotypes observed with the injection method, an alternative method of RA delivery to the neural tube was used, by an ion-exchange resin bead soaked in RA. The method of utilising a bead soaked in RA for hindbrain implantation has been used previously [169], but not to study the migration

pattern of cNCCs. It has been shown that this delivery method gives a slow release of the different RA isoforms [101]; it would be anticipated to give prolonged and focussed exposure of the tissue to the RA as opposed to the injection of RA, which might have been able to more rapidly diffuse away from the injection site. As this method was likely to give a more prolonged exposure, lower concentrations of at-RA were tested, from 16mM down to 1mM. Two types of bead were also used, a formamide and a hydroxide ion-exchange resin bead. The hydroxide form of the bead has been used in previous studies where RA bead implants have been utilised [101, 170-172]. The formamide form of the bead more readily releases the negatively charged compounds it is loaded with (e.g. RA) in comparison to the hydroxide form of the bead [173]. As beads are placed centrally in the neural tube, both sides of the embryo should receive the same dose of RA, therefore each side of the embryo was treated as an individual experiment. It was found that hydroxide beads loaded with 10mM at-RA (n=16 sides, 8 embryos) or the formamide beads loaded with 1mM at-RA (n= n=16 sides, 8 embryos) both gave 37.5% of embryo sides showing a partial or full Type1 phenotype (**Figure 4-1**). Some embryos showed a bilateral response to the RA beads, this could have been due to beads moving towards one side of the rhombomere as the neural tube expands during growth. Increasing the concentration of at-RA to 16mM gave only 33.3% (n=12 sides, 6 embryos) of embryos showing a Type1 phenotype, suggesting that there could be a threshold above which a higher RA concentration does not necessarily result in a higher proportion of embryos with a Type1 cNCC migration defect. Previous work has also shown that high concentrations of RA can inhibit cNCC migration [174]. This could be a factor here too, if the highest levels of RA prevented the cNCCs from emigrating from the neural tube and therefore prevent them from showing a Type1 phenotype even though they are affected by the RA.

These results show that the two administration routes lead to different results even when the same concentration of RA is used. The injections show a dose-response to the RA and are likely to give a high immediate dose, but then the effective dose decreases as the

RA leaches away from the injection site, which could mean the RA is free to affect tissues other than that targeted. The beads however give a better frequency of a Type1 phenotype at a lower concentration, presumably due to a longer, more constant release of RA to the targeted area than the injections.

4.2.1.2. Multiple retinoic acid isoform effects on cranial neural crest migration patterning

Within a few minutes of UV or white light exposure, at-RA is photo-converted to other retinoid isoforms, including the biologically-active 9-cis RA and 13-cis RA [175], eventually producing a mix of at--RA (25%), 9-cis-RA (10%), 11-cis-RA (10%), 13-cis-RA (30%) and 9,13-di-cis-RA (5%) after 30 mins of light exposure [176]. Therefore, it is likely that several isoforms of RA were present in previously published work using at-RA, even if in small amounts, since few studies state the lighting conditions under which the experiments were performed. Because these different RA isoforms can stimulate a wider repertoire of receptors than at-RA, they could potentiate the overall RA signal or produce a different array of phenotypes.

In this work, care was taken to use yellow filtered cold light at every stage of RA administration and live embryo manipulation, greatly reducing the possibility of photoconversion to different RA isoforms. A lower proportion of embryos with NCC mismigration phenotypes was found here than in published studies, which suggests that at-RA may not be the most effective RA isoform in initiating cNCC mismigration in r4 and that much of the mismigration effect could be caused by RA photoconversion products. In order to investigate whether photoconverted RA gave a more robust NCC mismigration phenotype, 50mM at-RA was exposed to strong daylight for 8 hours in order to cause breakdown into other forms. Light-exposed RA was used to inject r4 in 10ss embryos. It was found that the injections of 50mM light-exposed at-RA gave a much higher proportion

of embryos with a Type1 phenotype, 71.4% (n=7, not significant G-test), than had been observed using injections of 50mM at-RA (22.5%, 6/27 embryos).

4.2.1.3. Effects of the 9-cis retinoic acid isoform on the observed rate of a Type1 phenotype

As light-exposed RA showed a higher proportion of Type1 phenotypes when injected into r4, the question is if another isoform of RA could be involved in the mediation of a Type1 phenotype. There has been a lot of previously published work to show that the 9-cis retinoic acid isoform is biologically active [59]. Furthermore it is possible that different receptor activation may affect the frequency of a Type1 phenotype occurring, the 9-cis isoform of RA has been reported to bind with a high affinity to the RXR receptor, one that at-RA does not (see section 1.6.3). In order to investigate whether 9-cis RA could be more effective than at-RA in inducing a cNCC patterning defect, 9-cis RA was administered to r4, by either injection or beads, to give a comparison with the at-RA results.

It was found that the beads again gave better results than the injections, which gave only a 33.3% occurrence at best compared to 58.3% observed using the beads, both beads and injections at a 50mM concentration (**Figure 4-2**). At lower concentrations, 9-cis RA caused a phenotype in 23.5% of embryos at 1mM and in 20.0% of embryos at 1.6mM on formamide beads (**Figure 4-2**). This incidence was lower than that observed with the at-RA at the same concentration, however at higher concentrations 9-cis RA was much more effective. This difference may be due to 9-cis and at-RA having different receptors and/or different binding affinities to the RXR and RAR receptors. Furthermore at high concentrations it is possible that 9-cis RA has a greater effect on RAR receptors, as 9-cis can bind to both RXR and RAR, although its interaction with RAR is at a much lower affinity than with RXR [59].

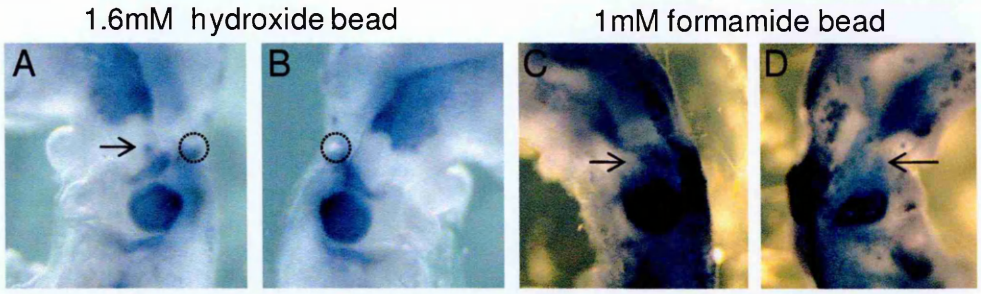

E

RA delivery method	Concentration of RA	Total number of sides with a phenotype (%)	Embryo sides with a partial type 1 phenotype (%)	G-test Significance
Injection	50mM	4/12 (33.3)	4/12 (33.3)	No
Injection	1.6mM	0/5 (0.0)	0/5 (0.0)	Yes
Bead – H	1.6mM	4/20 (20.0)	4/20 (20.0)	Yes
Bead – F	50mM	7/12 (58.3)	7/12 (58.3)	No
Bead – F	1mM	8/34 (23.5)	7/34 (20.6)	Yes

Figure 4-2. Neural Crest Cell Migration patterning following 9-cis retinoic acid exposure.

Rhombomere 4 exposure to 9-cis RA from hydroxide beads soaked in 1.6mM RA (**A,B**) or formamide beads soaked in 1mM RA (**C,D**) at the 10ss. The migration pattern of the NCCs were shown by ISH for the NCC marker Sox10 (Blue **A-D**). Table **E** shows the percentage occurrences of a Type1 mismigration phenotype in injected and bead-treated embryos G-test of association was used to determine significance. ($G=3.8$, $p<0.05$, d.f.=1). Dotted grey line – bead placement. Arrows indicate mismigrating cNCCs. Bead types, F-formamide, H-hydroxide.

4.2.2. Exposure of r4 cranial neural crest cells to retinoic acid affects their migration pattern

Although previous work has focused on the effect of RA on the neural tube, injections of RA can probably leak out of the injection site, therefore other neighboring tissues could be affected by RA, and so could be involved in cNCC migration patterning. The cNCCs themselves, the mesenchyme, or the surface ectoderm could each be responding to RA.

4.2.3. Cell autonomous control of cNCC migration pattern

As the cNCCs are the cell type showing a mismigration phenotype, an experiment to assess the effects of RA on cNCCs, rather than the neural tube was devised; this involved exposing just the cNCCs of r4 to RA. As 9-cis RA and at-RA both can cause a Type1 phenotype and both have different nuclear receptors, a mix of both isoforms of RA was used, in an attempt to achieve the highest impact on the cNCCs. The dorsal part of r4, containing the premigratory cNCCs, was removed at 10ss and then incubated in a mix of 1μM at-RA and 1μM 9-cis RA for 1 hour, before reimplantation back into a host embryo. The embryos were then incubated for 24 hours before viewing. The RA media in which the dorsal r4 tissue was incubated contained a green tracker dye, and the host embryo cNCCs were labelled with a red tracker dye 30 mins before removal of its dorsal r4 and implantation of the donor tissue, therefore the host neural tube and cNCCs appear red and the donor RA treated cNCCs green. Embryos that had the RA-treated tissue implanted showed a weak Type1 phenotype (3 out of 7 embryos). Furthermore not only had the green cells mismigrated, some of the red labelled donor cells had also followed the same migration pattern (**Figure 4-3**). The control embryos, transplanted with vehicle-only-treated r4, showed no migration patterning defects (4 out of 4 embryos). As RA has the ability to affect the identity of rhombomeres, embryos were further processed by ISH for the r3/r5 marker Krox20. Interestingly 4 out of 6 embryos that had been transplanted with at-RA-treated r4 showed reduced or absent Krox20 expression in r5, although r3 Krox20 expression was unaffected (**Figure 4-3**C). Embryos transplanted with vehicle-only-treated r4 showed no changes in Krox20 expression (**Figure 4-3**G). This raises the question of whether the RA-treated transplanted tissue acted like a slow-release bead and affected surrounding tissues, or whether the results were due to direct effects on the cNCCs. In relation to the bead experiments, the proportion of embryos displaying a Type1 phenotype was higher (42.8%) than the 1mM at-RA (37.5%) or 1mM 9-cis RA (23.5%) beads. Although the concentration used was 1000-fold lower (1μM as opposed to 1mM), the tissue was being incubated in it directly, therefore the RA, did not have far to

diffuse to reach all cells. Furthermore, the proportion of embryos with a phenotype could be higher because a mix of at-RA and 9-cis RA was used, meaning that the effect could also be more potent. Overall it is difficult to compare these results to the beads because different concentrations and a mix of isoforms were used.

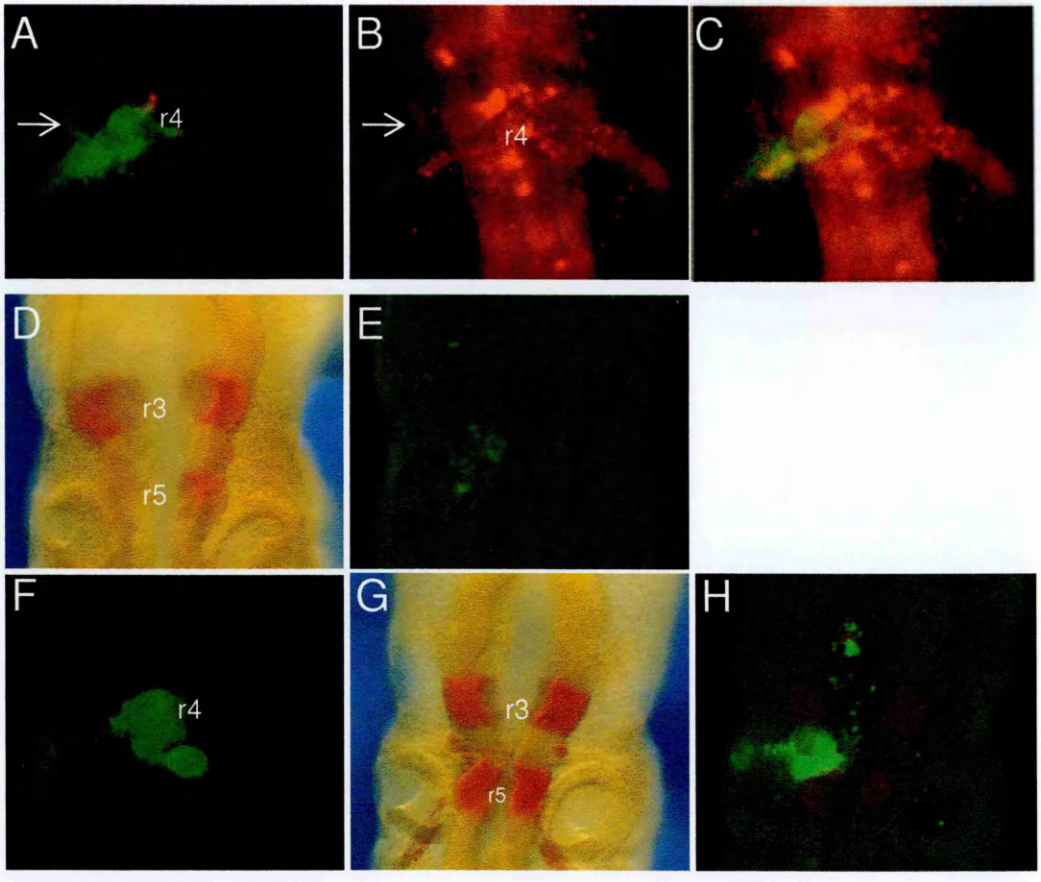

Figure 4-3. Effects on migration of neural crest cells exposed to retinoic acid.

The dorsal half of r4 was removed at 10ss and incubated in 1μM at-, 9-cis mixed RA, before reimplantation into a host 10ss embryo at the level of r4. **A-E** shows an embryo implanted with RA-treated r4, **F-H** shows an embryo implanted with a control non-RA-treated r4. The donor tissue was labelled with a green tracker dye (**A, F**) and the host tissue and NCCs with DiI (red, **B**), **C** shows an overlay of A and B. After 5 hours the green donor cells that were exposed to RA had migrated into the r3 mesenchyme (n=3/7). Embryos were subsequently processed by ISH for Krox20 (red-orange) on both the RA experimental embryo (**D,E**) and a control embryo (**G,H**), green shows residual green tracker dye indicating placement of the transplanted tissue. RA-treated r4 embryos showed a reduced or absent expression of Krox20 in r5(n=4/6). Arrows indicate mismigrating cNCCs. GFP controls n=4/4

4.3. Control of cranial neural crest migration patterning by the mesenchyme

The results described in the previous section indicate that it is possible that the cNCCs are directly affected by RA. If so, this evidence supports the theory that other tissues than the neural tube can be affected by RA to cause the Type1 phenotype. As the mesenchyme and surface ectoderm are situated adjacent to the neural tube, these could both be exposed to RA upon injections or bead placement. Both the mesenchyme and the surface ectoderm contain patterning information for r4 cNCCs and in the absence of these cues a Type1 phenotype is seen [7] (see section 1.5), and these tissues could be involved here by reacting to RA exposure. In order to further investigate which tissues respond to RA to give the cNCC mismigration phenotype, resin beads soaked in at-RA or 9-cis RA were placed in the mesenchyme at different locations (**Figure 4-4**). By placing the RA beads at different positions relative to the r4 cNCC stream, the effective dose of RA to different tissues could be investigated. First of all beads soaked in RA were placed in the r3 adjacent mesenchyme, as this is close to the r4 mesenchyme and r4 cNCCs without interfering with the cNCC migration physically. RA-soaked beads were also placed in the r5 adjacent mesenchyme, in theory RA that diffuses from beads in this position would mainly affect the cNCCs of the r4 stream and would not be able to affect the mesenchyme adjacent to r3 as efficiently. Beads were also placed in the r2 mesenchyme, the premise being that the RA would be able to affect the r3-adjacent mesenchyme, but not the r4 cNCCs as successfully (**Figure 4-4**).

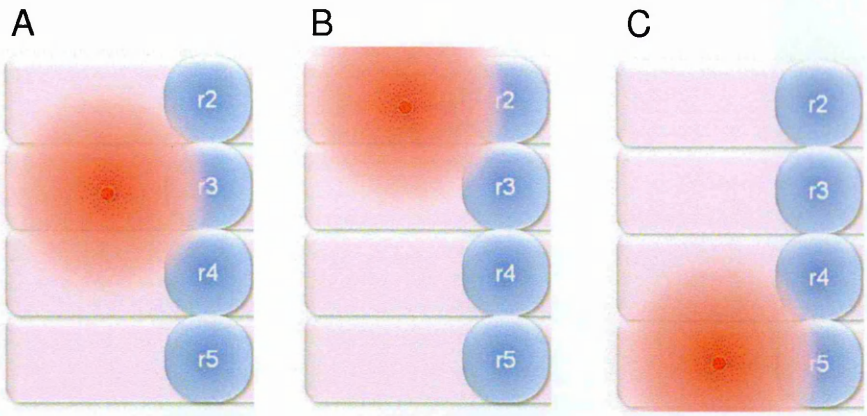

Figure 4-4. Schematic diagram depicting the different RA bead positions in the mesenchyme.

This diagram shows the hindbrain from rhombomeres 2 to 5 (blue) and the adjacent mesenchyme (pink). The hypothetical concentration gradient of RA from the bead (red) is shown by the hazed red area when the bead is placed in the r3 (**A**), r2 (**B**) and r5 (**C**) adjacent mesenchyme.

Embryos had either a hydroxide or formide RA-soaked bead implanted into the r3-adjacent mesenchyme at stage 10 and then were incubated for 24 hours, before processing by ISH for Sox10. When hydroxide ion exchange resin beads soaked in 1mM at-RA were placed in the r3 mesenchyme, an unusual cNCC migration pattern was observed (**Figure 1-1** A-C). The r4 stream of cNCC appeared to be split in two rostro-caudally (60%). However when the formide ion exchange resin beads soaked in 1mM at-RA were implanted into the r3 mesenchyme, a Type1 phenotype was observed (**Figure 1-1**,D 55.6%). This effect was still observed at lower concentrations of at-RA formide beads (**Figure 4-5**, E,F); at 10µM and 1µM the rate of incidence of a Type1 phenotype were 28.6% and 35.7% respectively. As 1µM 9-cis RA had shown to be effective at causing cNCC mismigration when the neuroepithelium was exposed to it, 1µM of 9-cis RA was also used to soak formamide beads and implanted into the r3 mesenchyme. Interestingly this gave a very robust phenotype with 80% occurrence (4/5 embryos), 60% of which were full Type1 phenotypes, compared to neural tube exposure of 7.1% of the

1μM at-RA on the same bead type (**Figure 4-5** K). These data suggests that the mesenchyme is actually the primary tissue responding to RA to give a Type1 phenotype. If this is the case, then the RA targeting to the neural tube gave better results at higher concentrations due to leakage of the RA into the mesenchyme, which then affected cNCC migration patterning, rather than the neural tube having a direct effect.

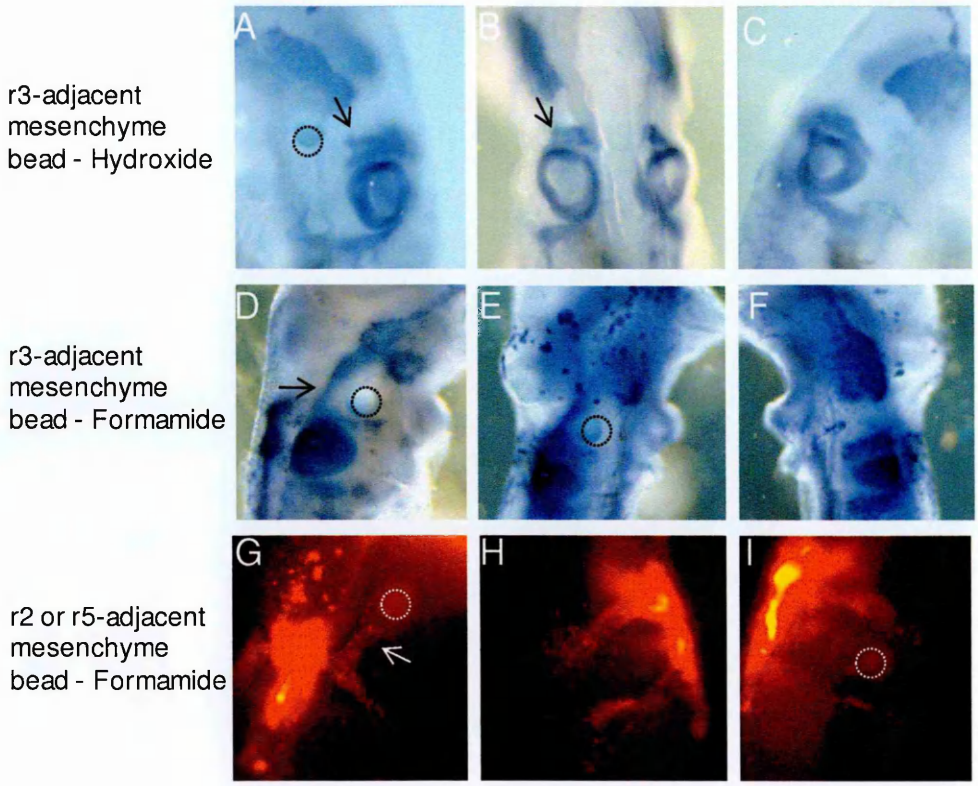

J

Mesenchyme Area	Concentration of 9-Cis RA	Total number of sides with a phenotype (%)	Embryo sides with a partial type 1 phenotype (%)	G-test Significance
r3	1µM (F)	4/5 (80.0)	1/5 (20.0)	No
r2	1µM (F)	0/5 (0.0)	0/5 (0.0)	No
r2	10µM (F) mix with all-trans RA	1/6 (16.7)	0/6 (0.0)	No
r5	1µM (F)	1/2 (50.0)	1/2 (50.0)	No

K

Mesenchyme Area	Concentration of all-trans RA	Total number of sides with a phenotype (%)	Embryo sides with a partial type 1 phenotype (%)	G-test Significance
r3	1mM (F)	5/9 (55.6)	4/9 (44.4)	No
r3	10µM (F)	2/7 (28.6)	2/7 (28.6)	No
r3	1µM (F)	5/14 (35.7)	4/14 (28.6)	No
r3	1mM (H)	3/5 (60.0) Type2 like	0/5 (00.0)	No
r2	1µM (F)	1/6 (16.7)	1/6 (16.7)	No
r5	1µM (F)	0/6 (0.0)	0/6 (0.0)	No

Figure 4-5. Neural Crest Cell Migration patterning following targeted exposure of the mesenchyme to retinoic acid.

The mesenchyme was targeted at different levels by implantation of a RA-soaked bead into the tissue at the 10 somite stage. Hydroxide beads soaked in 1mM at-RA implanted into the r3 mesenchyme (A-C) resulted in a unique cNCC migration phenotype, whereas formamide beads soaked in 1mM (D) or 1μM (E,F) at-RA gave the Type1 phenotype. F-control side of E. The r2 (10μM concentration of each at-- 9-cis RA mix, G) and r5 (1μM at-RA, H,I) were also targeted The NCCs were visualised by either ISH for sox10 (blue, A-F) or by DiI labelling at the time of bead implantation. Tables J and K show the frequency of a Type1 phenotype with either 9-Cis RA(J) or at-RA (K) and different bead placements, G-test of association was used to determine significance. ($G=3.8$, $p<0.05$, d.f.=1). Dotted circle – bead placement. Arrows indicate mismigrating cNCCs. Bead types, F-formamide, H-hydroxide.

When beads soaked in either 1μM 9-cis or at-RA were placed in the mesenchyme next to r5, the at-RA showed no effect in this position, whilst the 9-cis RA showed 1 out of 2 embryos with a weak Type1 phenotype (**Figure 4-5**). In the mesenchyme adjacent to r2 beads of 1μM at-RA showed a 16.7% Type1 occurrence, but beads soaked in 9-cis RA had no effect. As a preliminary experiment, a 10μM mix of at-RA and 9-cis RA was loaded onto formamide beads and placed into the r2-adjacent mesenchyme; this should theoretically activate both the RAR and RXR receptors, giving a more effective response. The rate of occurrence was not too high at 16.7% (n=6), but the migration pattern observed was extremely strong (**Figure 4-5** G), hence in order to get a more robust phenotype perhaps a mix of 9-cis and at-RA should be used. Although it is worth noting that the concentration of each RA isoform was 10 times higher than used on beads loaded with only one isoform. With regards to the bead placement, it appears as though the mesenchyme of r3 may respond most strongly to RA. Although it is possible that the cNCCs may still respond directly to the RA, to aid in producing a Type1 phenotype, their response is probably not as strong as the mesenchyme response.

4.4. Changes in Cyp26 expression patterns following removal of r3

The Cyp26 group of retinoic acid metabolising proteins, Cyp26A, Cyp26B and Cyp26C are all expressed in the developing head (See section 1.6.3.2). A study by Uehara in 2007 [68] showed that *Cyp26A-Cyp26C* double knockouts have a Type1 phenotype. Cyp26C, which is expressed in the r3 mesenchyme, is down-regulated by at-RA, whereas Cyp26A is upregulated by at-RA [165]. As Cyp26A and Cyp26C expression can be altered by at-RA, and Cyp26C is expressed in the r3 mesenchyme, it follows that they and other mesenchyme-expressed genes could be involved in maintenance of the r3 mesenchyme cNCC free zone. If, in the absence of r3, Cyp26C expression is no longer maintained in r3-adjacent mesenchyme, then the local level of RA would increase. The data presented here indicate that locally high levels of RA in r3-adjacent mesenchyme cause a Type1 phenotype. Therefore, Cyp26 expression in response to unilateral r3 removal was investigated, in order to determine if Cyp26 might be the mediator between r3-specific cues and NCC migration patterning cues in the adjacent mesenchyme.

Embryos were processed by double ISH for expression of the Sox10 and Cyp26C at 5, 8 and 24 hours following unilateral r3 removal. Five hours was chosen as the first time point to be examined, as this is when cNCCs have been observed to begin migrating into the r3 mesenchyme following r3 removal [7]. Any strong changes in Cyp26C gene expression at 5 hours would suggest that Cyp26C acts upstream or in parallel with the cNCC barrier cues. By 8 hours following r3 removal, the Type1 phenotype will be quite strong [7], so any changes in Cyp26C gene expression at this time would imply an involvement of Cyp26C in either reinforcement of the phenotype or downstream to disruption of the NCC barrier. Taking embryos at 24 hours allows the analysis of any longer term changes in gene expression. If changes in Cyp26C expression are causing cNCC mismigration, it would be expected that at this 5 hour time point Cyp26C changes would have already

occurred in the lead up to the cNCC mismigration. At the 5 hour time point, by eye, there seems to be no change in the expression of Cyp26C in the r3 adjacent mesenchyme on the operated side in comparison to the control side of the embryo (**Figure 4-6**). By 8 hours, a slight reduction in Cyp26C expression can be observed in the r4 mesenchyme area. All other expression of Cyp26C at the 8 hour time point appears to be the same on both sides of the embryos. At 24hours the expression pattern of Cyp26C looks even. In all cases the Sox10 staining confirms that the cNCCs have shown a Type1 phenotype (**Figure 4-6**).

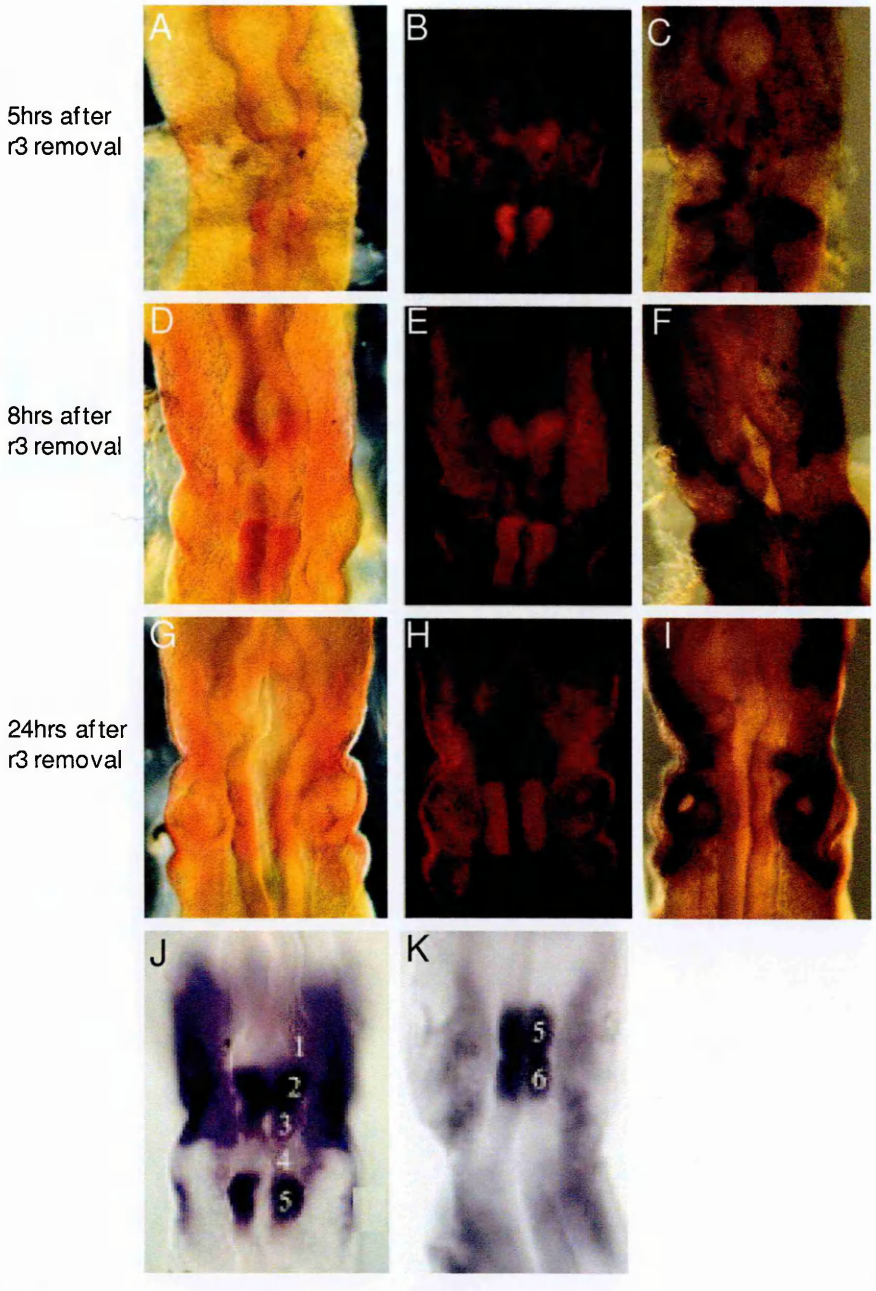

Figure 4-6. Expression pattern of Cyp26C following unilateral removal of r3.
Rhombomere 3 was removed unilaterally from embryos at the 10ss. Embryos were then incubated for 5 hours (**A-C**), 8 hours (**D-F**) and 24 hours (**G-I**). Embryos were processed by ISH for Cyp26C (orange bright field and red fluorescence) and Sox10 (Blue, **A-I** only). **J-K** Cyp26C expression at 16ss (J) and 22s (K), as published by Reijntjes 2004 [67]. Note that **J** is developmentally comparable to the +8hr embryos in D-F, whilst **K** is developmentally comparable to the +24hr embryos in G-I. These images are representative from 9 embryos per time point.

Although the previous hypothesis was that r3 regulates Cyp26C expression in r3 adjacent mesenchyme, it also could be that, as r3 expresses Cyp26C [67], r3 itself is a source of Cyp26C in the r3 adjacent mesenchyme; Cyp26C reaching the mesenchyme by diffusion. Therefore if r3 is removed from the hindbrain, a potential source of Cyp26C in the mesenchyme is also removed, thus leading to less RA degradation and so causing a higher local concentration of RA of r3 in the mesenchyme. So it is possible that removal of r3 mimics the implant of a RA soaked bead. However in the absence of an antibody against Cyp26Cor immunohistochemistry, this cannot be easily tested.

Similar experiments were also performed to look at any changes in the expression patterns of either Cyp26A or Cyp26B mRNA following unilateral r3 removal. Firstly, there was no change in Cyp26A expression at 5 and 8 hours post surgery, although Sox10 staining did show that the r4 cNCCs had mismigrated. By 24 hours there appeared to be increased expression of Cyp26A on the r3 removal side in comparison to the contralateral control side of the same embryo, at the level of the geniculate epibranchial placode at the top of the second arch (**Figure 4-7**). With regards to the Cyp26B expression pattern, at 5 hours post r3 removal the expression pattern does not seem to have been affected, however by 8 hours the expression at the tip of the tissue growth into the r3 void area shows stronger expression than the contralateral control side (**Figure 4-8**). At 24 hours the expression of Cyp26B looks slightly stronger in r4 on the experimental side, whereas the rest of the expression pattern looks even. It is possible that Cyp26**B** expression is increased upon removal of r3 in an attempt to compensate for the lack of Cyp26 proteins being produced by r3, which was removed, leading to less diffused Cyp26s in the mesenchyme. If Cyp26 protein levels become lowered in r3-adjacent mesenchyme, the regional RA concentration could be high, mimicking the RA r3 mesenchyme bead experiments. Therefore, if this is the case then a Type1 phenotype may be observed

following r3 removal, particularly close to the neural tube as this is the area which will be depleted of r3 derived Cyp26s the most.

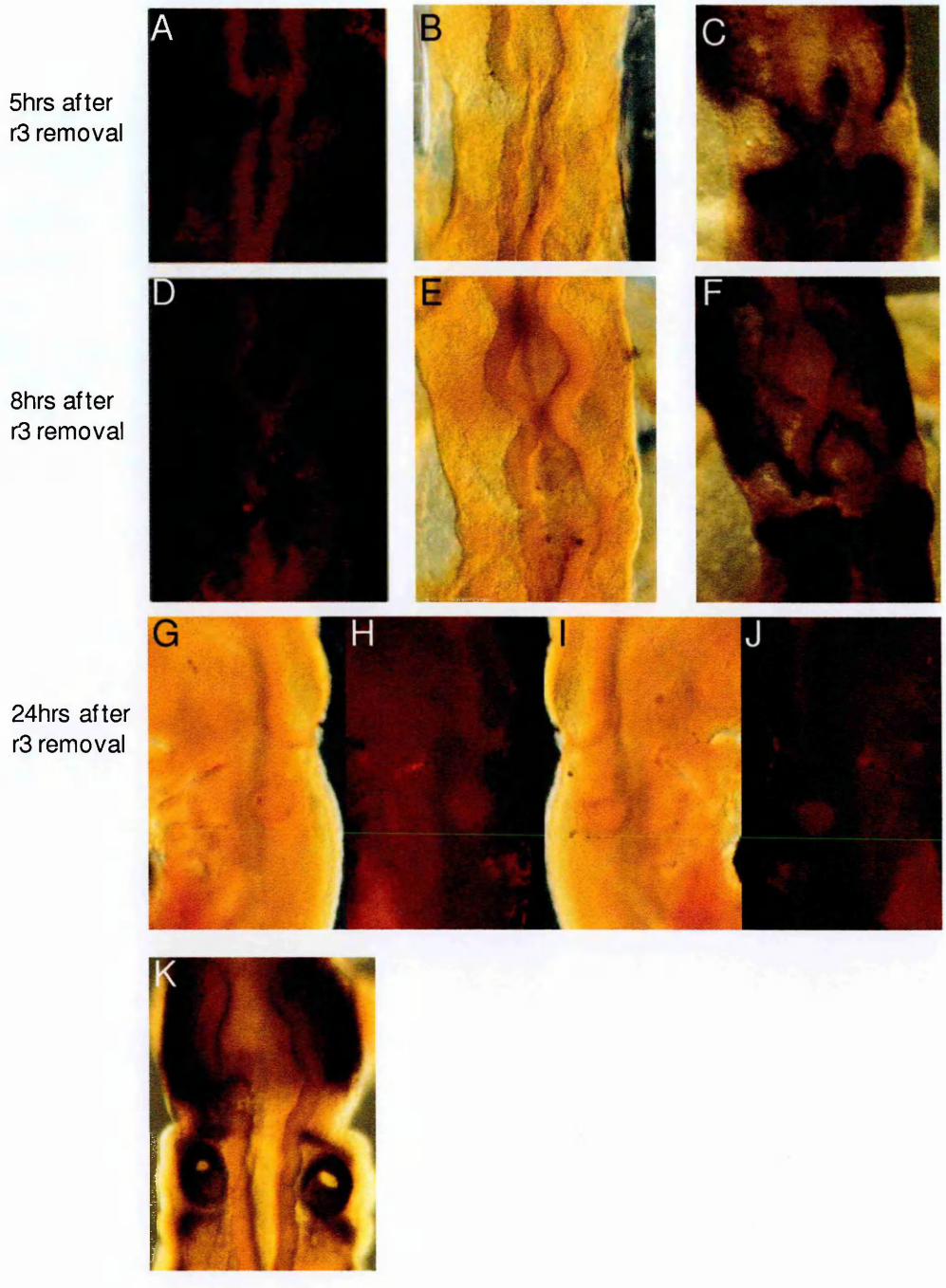

Figure 4-7. Expression pattern of Cyp26A following unilateral removal of r3.
Rhombomere 3 was removed unilaterally from embryos at the 10ss and incubated for 6 hours (**A-C,** n=6), 8 hours (**D-F,** n=6) and 24 hours (**G-K,** n=5). Embryos were processed by ISH for Cyp26A (orange bright field B,E,G and I and red fluorescence A,B,H and J) and Sox10 (Blue C,F and K).

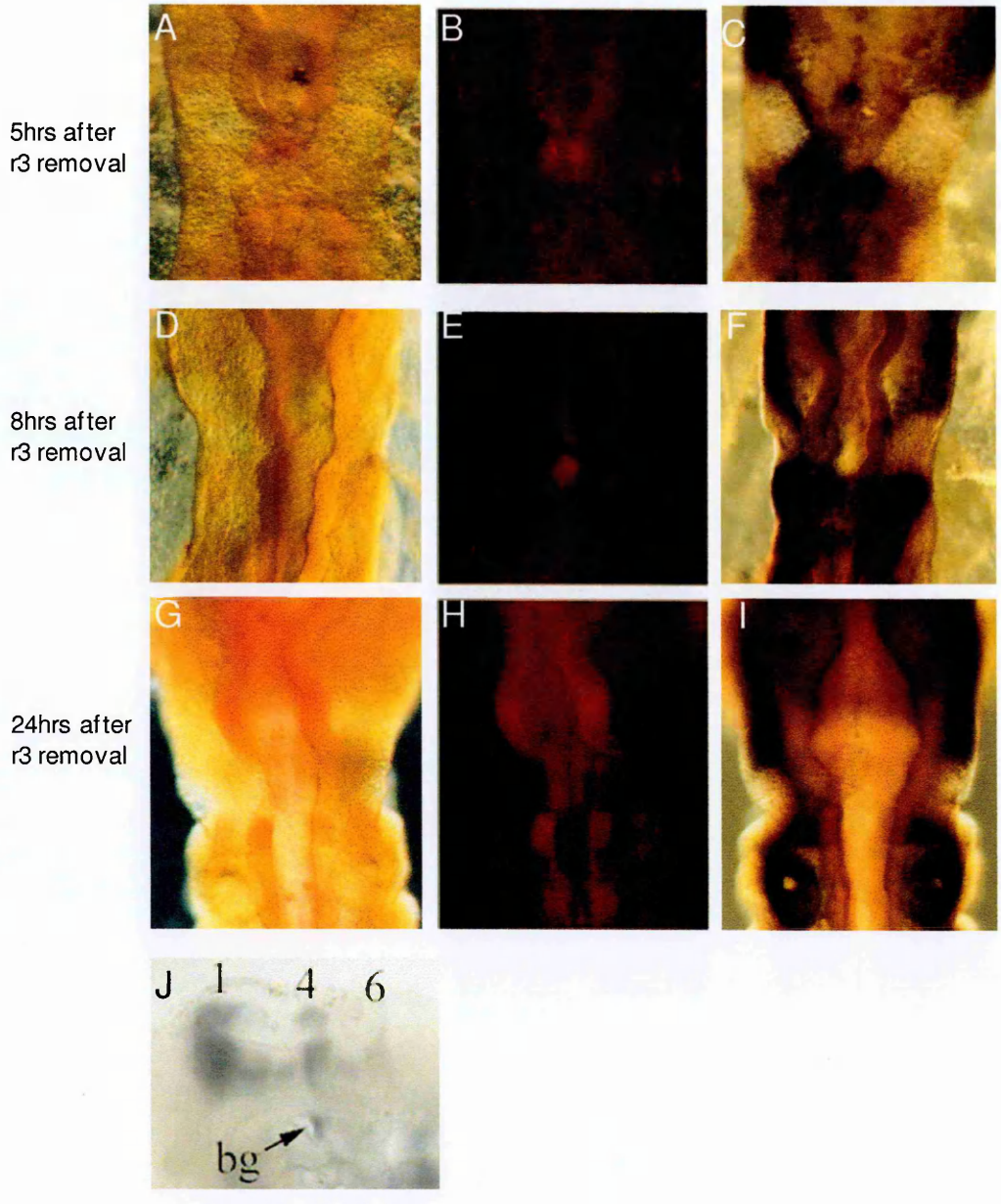

Figure 4-8. Expression pattern of Cyp26B following unilateral removal of r3.
Rhombomere 3 was removed unilaterally from embryos at the 10ss and incubated for 6 hours (**A-C**), 8 hours (**D-F**) and 24 hours (**G-I**). Embryos were processed by ISH for Cyp26B (orange bright field A,D,G and red fluorescence B,E,H) and Sox10 (Blue C,F,I). **J** - Cyp26B expression pattern (Blue) at 26ss, comparable to the +24hr embryos, as published by Reijntjes 2003 [66], showing the same expression pattern. These images are representative from 9 embryos per time point. Bg-branchial groove

4.5. Rhombomere to rhombomere signalling and its importance in maintaining correct cranial neural crest cell migration patterning

As a loss of ErbB4 signalling gives rise to a Type1 phenotype [17, 24], it is likely that ErbB4-NRG signalling is important in cNCC migration patterning. As ErbB4 is expressed in r3, and NRG is expressed in r4 (and to a lesser extent in r2), an impermeable barrier between the two would prevent signalling, and if the ErbB4-NRG signalling pathway is important, a Type1 phenotype should be seen. In order to investigate this possibility, an experiment was performed using 3 embryos, which had a piece of foil placed unilaterally between r3 and r4 as a barrier at stage 10 and then incubated for 24 hours before being processed by ISH for Sox10. Of these 3 embryos, 2 showed a Type1 phenotype (**Figure 4-9**). In order to ensure that the identity of the rhombomeres was not affected, additional embryos were processed by double ISH for Sox10 and either HoxB1 (n=3) or Krox20 (n=3). Unfortunately, although these embryos showed no changes in rhombomere identity, they also did not portray any cNCC mismigration. Overall the proportion of embryos depicting a Type1 phenotype was therefore 2 out of 9.

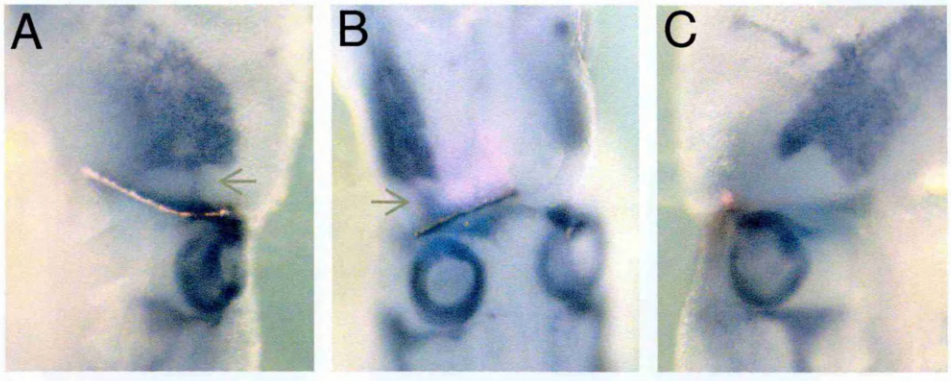

Figure 4-9. The affect of an impermeable barrier between r3 and r4 neuroepithelium on neural crest cell migration.

Foil barriers were placed between r3 and r4 unilaterally at the 10ss and embryos were then incubated for 24 hours. Neural crest cells were visualised by ISH for the NCC marker Sox10 (Blue, **A,B,C**), the migration pattern showed a Type1 phenotype (arrows) on the side with the barrier in place, the contralateral control side (**C**) showed normal crest migration (n=2/3).

4.6. Changes in ErbB4 expression and mismigration patterning

Studies by Golding et al [17, 24] have showed that ErbB4 is important in regulating the correct migration pattern of cNCCs. It has also be found in a separate study that RA exposure can alter the expression levels of ErbB4 in breast carcinoma cells *in vitro* [163]. Therefore it is possible that changes in the expression of ErbB4 may be linked to the mismigration of cNCCs upon exposure to RA. To test this, a preliminary experiment was set up in which embryos were injected with 50mM at-RA into r4 at stage 10 and then incubated for 24 hours before fixing and processing for ErbB4 and Sox10 expression by double ISH. Of these embryos 2 out of 3 showed discrete ectopic expression of ErbB4 around the area of RA delivery inr4, identified by residual DiI at the injection site (**Figure 4-10**). However in these embryos no cNCC phenotype was observed. As part of this preliminary experiment, beads of 1μM at-RA or 1μM 9-cis RA were implanted into the

neural tube at the level of r4 and incubated for 24 hours before double ISH processing for Sox10 and ErbB4 expression. For both conditions none of the 3 embryos in each experiment had any changes in ErbB4 expression, or showed any cNCC phenotype. As a high concentration of at-RA (50mM) was used when the ErbB4 ectopic expression was observed, there is a possibility that the identity of the rhombomere was being altered to be more like r3 or r5, where ErbB4 is expressed. The injections were repeated with a view to checking rhombomere identity by studying expression of Krox20 (r3,r5 marker) and HoxB1 (r4 marker), however out of the 6 embryos injected none showed the ectopic ErbB4 expression pattern, or changes in rhombomere identity. In-situ hybridisation was also performed for neuregulin, but the probe signal was too weak to allow any conclusions to be drawn. Overall it has been concluded that the ectopic ErbB4 expression observed following RA injections was probably due to changes in rhombomere identity, although this could not be confirmed here. Furthermore, the lack of ectopic ErbB4 expression in r4 following bead implantation could have been due to a lower initial dose of RA, rather than the high immediate does of RA required for changes in rhombomere identity.

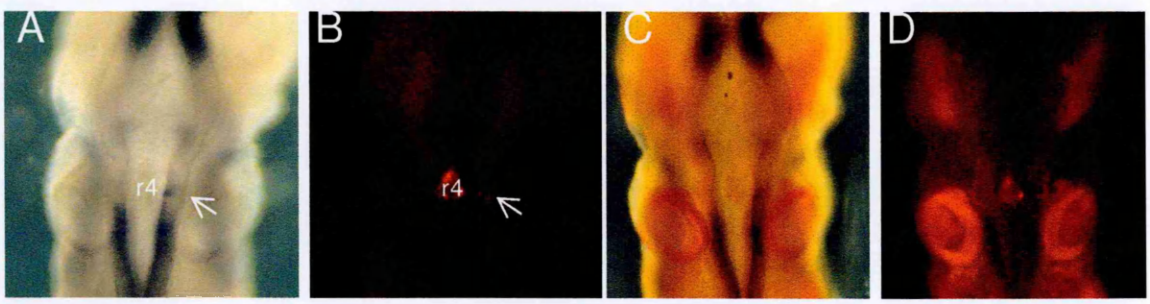

Figure 4-10. Expression pattern of ErbB4 following exposure of r4 to at-RA.
Embryos were injected with a 50mM at-RA –DiI mix and incubated for 24hours before fixation and processing by ISH for ErbB4 and Sox10. A-D shows the same embryo at different points of processing. A-ErbB4 (Blue), B- Residual DiI at the point of injection following ErbB4 ISH, C- Double ISH for Sox10 (Orange) and ErbB4 (blue), D- Fast red fluorescence of Sox10 ISH. Arrows indicate injection site. n=2/3

4.7. Discussion

The work shown here has helped to further the understanding of the complex mechanisms involved in controlling correct NCC migration patterning in head development. For the first time a novel role for the 9-cis RA isoform in the presentation of a Type1 phenotype has been shown, as well as the interaction of RA with the r3 adjacent mesenchyme in maintaining correct cNCC migration patterning. These data have also provided evidence that signalling between r3 and r4 neuroepithelium is important for maintenance of the r3 adjacent mesenchyme cNCC-free zone. Here possible mechanisms involved in initiating a Type1 phenotype are discussed.

Previous studies have shown that exposure of the hindbrain to at-RA causes cNCCs to mismigrate in a Type1 fashion. Lee and Osumi-Yamashita in 1995 showed that embryos incubated *in vitro* that were exposed globally to at-RA showed r1 and r2 cells migrating ectopically to the second branchial arch and geniculate ganglion [166]. The data presented here shows that a much higher proportion of embryos exhibiting aType1 phenotype are found when RA is used to target the mesenchyme adjacent to r3, instead of targeting the neural tube. Furthermore it was found that a lower concentration of RA was required in the mesenchyme to initiate a Type1 phenotype compared to r4 targeting. Therefore I have concluded that the mesenchyme is the tissue that is most affected by RA, not the neural tube. Although the neural tube, and the cNCCs directly, may respond to the RA to aid the Type1 phenotype, the mesenchyme is most likely the driving tissue involved.

Ion-exchange beads were used, in addition to injections, as a form of RA delivery as they have been shown to give a slow steady release of retinoids over a period of time [101]. Two forms of the ion-exchange resin beads were utilised, a hydroxide and formide form, the latter gave the better results, possibly due to its enhanced ability to release the RA

over the incubation time [173], therefore giving a higher effective dose in comparison to the hydroxide beads.

As many papers in this field do not state the lighting conditions used during preparation, surgery and incubation, it is possible that the at-RA used in many publications may have been exposed to light. This exposure could have significant effects, because it has been demonstrated that at-RA degrades upon exposure to normal room lighting conditions, giving a mix of at--RA (25%), 9-cis-RA (10%), 11-cis-RA (10%), 13-cis-RA (30%), 9,13-di-cis-RA (5%) and an unidentified compound (20%) after 30 mins of light exposure [176]. The effect of light is rapid; it only takes 15mins for photoconversion of the at-RA to other isoforms, [176, 177], the percentage of each RA isoform in solution then equilibrates by 30mins in room lighting conditions. Moreover it has been observed that 4.5% 9-cis RA can be obtained from a pure at-RA solution in just 0.6s of exposure to a 100W mercury lamp. Therefore it is feasible that previous studies involving use of at-RA could have unintentionally exposed their at-RA supply to room lighting and therefore have a significant amount of biologically active 9-cis, or other RA isoforms in their solutions. If this is the case a 16mM 'at-RA' solution, as used by Gale [45] could actually contain 0.75mM 9-cis RA, as well as low levels of other RA isoforms, if exposed to light for just 0.6s. As different isoforms of RA have been shown to be biologically active in other ways to at-RA, it has to be considered a possibility that in other studies other non-at-RA isoforms may well be contributing to any observations found. In this work, the cold light sources used during microsurgery had yellow light filters, in order to minimise photoconversion of the at-RA used.

At-RA and other isoforms of RA bind to their cognate receptors with different affinities. At-RA is best at binding to the RAR receptors and not the other retinoid receptors RXR [59]. For these reasons it would be expected that a mix of RA isoforms would give a higher proportion of the Type1 phenotype. Thus delivery of light-exposed RA to cells should

activate both RAR and RXR, in a multitude of homo and hetero-dimer forms, therefore giving a comprehensive RA response. Preliminary results using an at-RA and 9-cis RA mix also showed an enhanced effect on isolated cNCCs when transplanted *in ovo.* These results imply that the Type1 phenotypes observed when RA is added to the developing embryos could be the result of multiple hetero and homo-dimer activation therefore leading to the transactivation of their multiple gene targets (see section 1.6.3).

In order to investigate if signalling through the RXR instead of the RAR would make a difference to the cNCC mismigration phenotype, 9-cis RA was used in place of at-RA in the same experiments. As 9-cis has a stronger affinity for the RXR receptor, around 35-40x more than the RAR receptor [59, 178], it was an appropriate isoform to use here. Although 13-cis RA is also biologically active, it is only known to function through RAR receptors [175], and not RXR, and because of this similarity with at-RA, 13-cis RA was therefore not used in these experiments. The results showed that the 9-cis RA was more effective at inducing ectopic migration of the cNCCs under certain conditions. As the RXR receptor can both homodimerise and also heterodimerise with not only RAR but also other receptors such as the PPAR-γ receptor [60], it could be that the 9-cis RA is activating the RXR receptor either as a homodimer or as part of a heterodimer that does not include RAR (**Figure 4-11**). As RXR can be activated in other heterodimers, but cannot be activated in a RXR-RAR heterodimer without co-activation of the RAR receptor [60], it is possible that 9-cis RA is not acting in the same fashion as the at-RA. However some activation of the RXR-RAR heterodimers is possible as 9-cis RA is able to activate the RAR receptor, although it binds to it at a much lower affinity than to the RXR receptor [59]. Therefore it could be that upon exposure to 9-cis RA both the RXR-RAR and other RXR heterodimers are being activated, which is why 9-cis RA is more effective at causing ectopic cNCC migration.

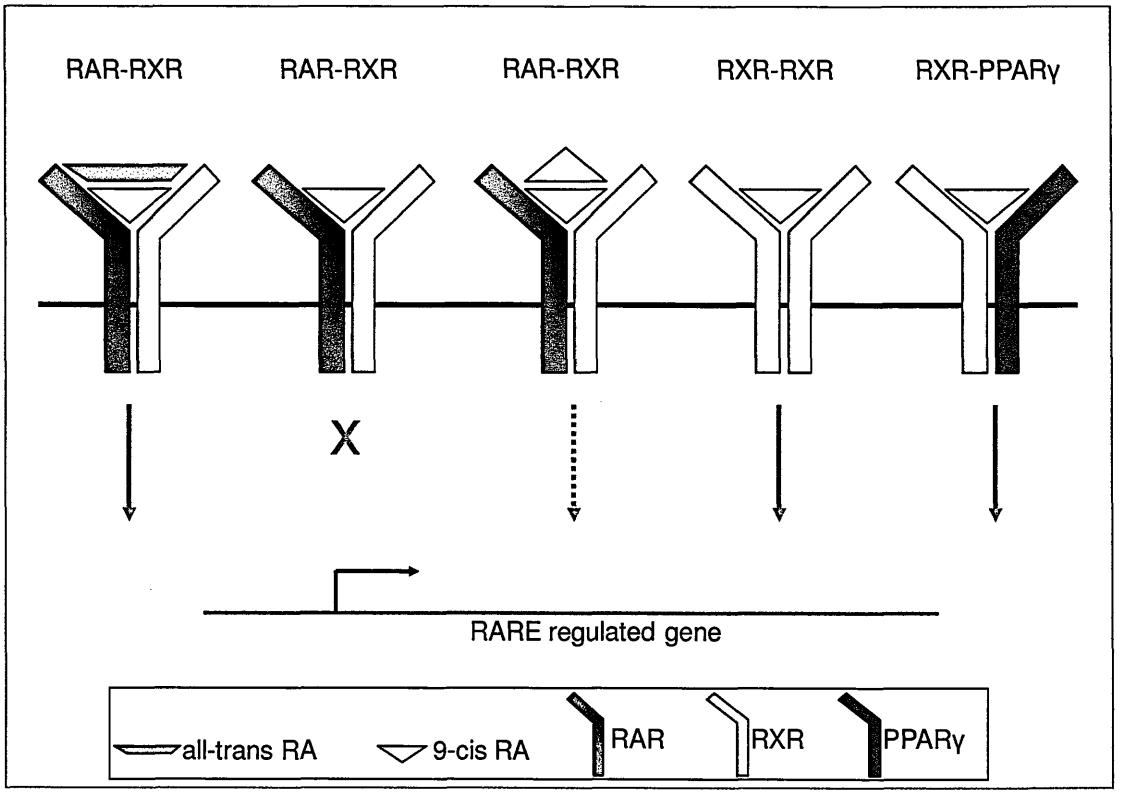

Figure 4-11. RXR activation by 9-cis RA

The schematic diagram demonstrates the conditions in which 9-cis RA is able to activate nuclear receptor activation. When hetero-dimerised with RAR, at-RA is normally required for activation, however 9-cis can activate RAR to a lesser extent. RXR homo-dimers are activated in the presence of 9-cis alone, and also when RXR is hetero-dimerised with other nuclear receptors such as PPARγ.

One more point that needs to be taken into consideration is that it has been previously reported that as time increases so does the isomerisation of at-RA to 13-cis RA upon release from the AG1-X2 resin beads used here [101]. The 13-cis isomer has not been shown to interact well with the RAR receptor [178]; therefore it could be acting through another, as yet undiscovered, mechanism. This possibility perhaps needs to be more of a consideration for the hydroxide bead experiments rather than the formamide bead experiments, because the hydroxide beads adsorb the RA more strongly and therefore

the RA is released more slowly. There have not yet been reports of at-RA isomerising when released from the formamide beads or of the 9-cis isomerising upon release from either type of bead.

These data provide further evidence that cNCCs can deviate from their normal path of migration when exposed to RA. However as the Krox20 ISH results demonstrate, there may be flaws in the experimental design, in that it is possible that the transplanted tissue was itself acting as a delivery vehicle for RA to the surrounding environment. As studies have shown that administration of RA to embryos or cells can change the expression level or pattern of Krox20 [45, 163], and changes in Krox20 mRNA expression were observed here, this has to be considered as a real possibility for the cause of the cNCC mismigration. Another interesting observation on the RA treated r4 transplanted embryos is that the host cNCCs also migrated with the transplanted RA-treated cNCCs. There are two possible explanations for this observation; firstly the donor RA-treated cNCCs may be using their cell-cell contacts with the host cNCCs to change their trajectory to a path of migration into the r3 mesenchyme. In support of this theory it has been observed that cNCCs can change direction to follow a neighbouring cell's path through its short range contacts of lamellipodia and short filopodia [14]. If this is the case, green donor cells would be at the forefront of the mismigrating cNCC stream leading the red host cNCCs. From the wholemount images it is difficult to see if the green labelled cells are indeed leading, in order to determine if this is the case, sections would need to be taken through the embryos in order to see individual cells. However it is possible that there are more green ectopically migrating cells than red, as the green stream of ectopic cells does look thicker and more substantial than the red stream of ectopic cells, implying that the RA was having an effect on the cNCCs directly. A second theory, as mentioned above, is that the transplanted tissue is releasing RA into the surrounding tissue and acting in a similar fashion to a bead of RA, acting on the neural tube or, as it has unobstructed access, also the r3 mesenchyme and thus causing a Type1 phenotype.

This is the first systematic study to specifically target the rhombomere adjacent mesenchyme of the developing head with retinoic acid to study its effects. The results show that, on an equimolar basis, 9-cis RA is more effective than at-RA at causing a Type1 phenotype (80% vs 35.7%) when r3 mesenchyme is targeted with formamide beads loaded with 1μM of either RA isoform. Alternate bead positioning in r2 adjacent mesenchyme or r5 adjacent mesenchyme gave a Type1 phenotype less frequently, implying that the r3 adjacent mesenchyme is indeed the tissue being affected (see **Figure 4-4** for schematic summary of RA targeting), as beads implanted into r5 mesenchyme would be expected to cause a phenotype just as frequently as beads implanted into the r3 mesenchyme, if the r4 cNCCs were the targets. However fewer embryos showed ectopic cNCCs, although experimental numbers were also low. When beads were placed into the r2 mesenchyme, there was also a low occurrence of mismigrating cNCCs, but when a phenotype was observed it was stronger than the r5 mesenchyme bead phenotypes, particularly when a mix of 9-cis-at-RA was used. These data are consistent with the hypothesis that the r3 adjacent mesenchyme is the affected tissue as the r5 adjacent beads had little effect and they are equidistant from the r4 cNCCs as the r3 adjacent mesenchyme beads, therefore if r4 cNCCs were the main target an equal proportion of Type1 phenotypes should have been observed. Furthermore as the r2 adjacent beads caused the cNCCs to show a stronger Type1 phenotype than the r5 adjacent beads, it supports the theory that the r3 adjacent mesenchyme is responsible, since r3 mesenchyme lies closer to r2 than r5.

The findings that an equal mix of 9-cis RA and at-RA can give such a strong Type1 phenotype further supports the hypothesis that the RXR nuclear receptor is important in cell migration patterning. Both the RXR and RAR receptors are found in the mesenchyme during cNCC migration [179], meaning that it is possible that a mix of RA isotypes could have a more potent effect, as both RAR and RXR are activated, as opposed to just one

RA isotype activating only one RA nuclear receptor. In addition it has previously been suggested that the mesoderm/mesenchyme has a role in cranial patterning, following observations that cNCCs show plasticity when transposed from one rhombomere to another, meaning that there is an environmental effect that maintains the rhombomere specific identity of isolated cNCCs [3]. As the surrounding environment has the ability to maintain correct rhombomere and cNCC identity following transplantation to another position it follows that it should also have the ability to affect migration patterning. One possible weakness of the experiments described here is that the concentration of the RA used for the r2 and r5 beads may not have been high enough to allow for diffusion to the r3 mesenchyme or the r4 cNCCs to give an effective concentration. In support of the mesenchyme being the actual target of RA in this situation is the observation that the rhombomeres need a much higher concentration of RA than the mesenchyme to have an effect on the cNCC migration pattern, therefore suggesting that a high concentration is needed in order to 'spill over' into the mesenchyme. Overall these results give a good basis for the theory that the mesenchyme actively directs cNCC patterning. This has been previously suggested following observations that transposition of small populations of cNCCs in the hindbrain observes local environmental patterning cues from the mesenchyme [3].

Another interesting observation from this set of results is the unique migration pattern of the neural crest following implantation with a hydroxide bead of at-RA. One possible explanation for this observation is that as the at-RA is released more slowly and therefore over a longer period of time, than from the formamide beads, there may well be increased isomerisation of the at-RA to 13-cis RA [101]. The 13-cis RA therefore could be the active form of RA that is causing this unique phenotype. 13-cis RA is an isotype that is present endogenously [180, 181], however its interactions with RAR receptors have been found to be very poor in comparison to 9-cis which has a weak binding affinity [178].

The embryos injected with RA showed an interesting gene expression pattern of ErbB4, with ectopic ErbB4 mRNA at the point of RA administration following injection with a high concentration of at-RA. A study by Gale and Prince in 1996 [45] proved that within 6 hours of exposure to RA there was ectopic expression of Krox20, a marker of r3 and r5 identity [182, 183]. Another study by Offerdinger and Schnieder in 1999 demonstrated that following incubation in RA, breast carcinoma cells *in vitro* reduced their protein expression of ErbB4 by 30-60% of the controls. Therefore it is feasible that in this case the identity of rhombomere 4 was altered to be more r3/r5 like, where ErbB4 is expressed during normal development [23], rather than the cells upregulating ErbB4 expression due to RA exposure. Further support for this hypothesis is that a Type1 phenotype occurs when *ErbB4* is either knocked out or the activity reduced through a dominant negative construct [17, 24], so a reduction in ErbB4 mRNA expression would be expected to contribute to cNCC mismigration and not an upregulation. RA can down-regulate ErbB4 protein [163], if this is also true of cells in the rhombomere then the RA could decrease the amount of ErbB4 protein in r3. Although no changes were observed in ErbB4 gene expression following RA injections, the protein level of ErbB4 may have been reduced by the RA through an unknown mechanism, which would not be reflected by the mRNA levels immediately.

If r4 becomes more r3-like, it is possible that the mesenchyme adjacent to r4 would become less hospitable to the cNCCs migrating through it, much like the r3 adjacent mesenchyme. In which case, the cNCCs could be expected to migrate away from the r4 adjacent mesenchyme and perhaps into the r5 adjacent mesenchyme. However this was not observed, as only a small proportion of the whole rhombomere was expressing ErbB4, it may be that the rest of the rhombomere 4 which was not expressing ErbB4 and therefore not r3-like is able to compensate for its presence, therefore maintaining normal cNCC migration. To summarise, as no abnormal cNCC migration phenotype was observed it is possible that this observation was a side-effect of the exposure to a high

concentration of RA changing the identity of the immediate surrounding tissue and not involved in patterning the migration of the cNCCs.

Results here also show that signalling between r3 and r4 is involved in the maintenance of the r3 mesenchyme cNCC-free zone by blocking signals between the two rhombomeres. It is possible that the barrier is preventing RA or RA metabolism-related molecules from diffusing from r3 to r4, thus leading to a Type1 phenotype. However another candidate is neuregulin (NRG), which is expressed in rhombomere 4 during hindbrain development [22, 23]. NRG is a ligand for the receptor ErbB4, which is expressed in rhombomeres 3 and 5 [23, 184] at the same point of development. *ErbB4* knockout embryos and embryos where ErbB4 activity was suppressed in r3 via a dominant-negative strategy display Type1 phenotypes [17, 24], demonstrating the importance of ErbB4 in maintenance of the neural crest free zone in the mesenchyme next to r3. Thus it is possible that the candidate protein, neuregulin, diffuses or is transported from rhombomere 4 to its neighbouring rhombomeres and then activates the ErbB4 receptor, which in turn maintains correct cNCC migration through its downstream responses.

At the same point of development other proteins are available for ErbB4 signalling, such as HB-EGF, which is expressed ubiquitously throughout the hindbrain [185], although it is unlikely that HB-EGF can compensate for the absence of neuregulin signalling. A study by Hoshino and Uchida in 2007 [185] has demonstrated that cNCC mismigration and cranial nerve defects in the absence of HB-EGF signalling, by use of siRNA for either HB-EGF or its transporter CNIL, cannot be rescued by neuregulin. It can therefore be concluded that perhaps both neuregulin and HB-EGF signalling are required to maintain correct cNCC migration and loss of signalling from either one cannot be compensated for by the other.

The RA metabolising proteins Cyp26A1 and Cyp26C1 have been documented to be involved in cNCC patterning and cranial nerve patterning, as *Cyp26A1-Cyp26C1* double knockouts show defects in both [68], while *Cyp26A1* knockouts show ectopic axon projections [164], much like those seen following a Type1 cNCC phenotype. The Cyp26 inhibitor Fluconazole has also been used to globally inhibit Cyp26s in rat embryos, which then developed Type1 phenotypes [162] further supporting their importance in cNCC patterning. Although experiments were tried targeting r3 with a saturated solution of Fluconazole on a bead at 10ss, no patterning defects were observed 6 or 24hours later. This result could be due to local compensating upregulation of Cyp26s, therefore perhaps a much higher concentration of Fluconazole would be required for local targeting than when the whole embryo is exposed to Fluconazole, as a low global presence of Fluconazole would prevent compensating Cyp26 activity.

The results reported here suggest that the Cyp26s, although involved in cNCC migration patterning, are most likely further down the signalling pathway than the immediate effector responsible for the cell's migration pattern, as changes in expression pattern, if any, are only observed after the cNCCs have begun to migrate into the r3 mesenchyme. Although the Cyp26A1 and Cyp26C1 are involved in cNCC migration patterning, in the event of removal of r3, they are probably not initiating the mechanism behind mismigration and changes in their expression levels are not necessary before mismigration can occur. Conversely the protein levels or activity of the Cyp26s may be altered before cNCC mismigration, and therefore could be involved, but mRNA expression may not be changed until later. This uncertainty could be resolved by analysis of protein activity and levels of the Cyp26s following r3 removal. Furthermore it still needs to be considered that r3 is itself a source of Cyp26s [67], therefore it could be that r3 expresses Cyp26s , which then are able to diffuse into the mesenchyme, which then aids in maintaining the r3 cNCC-free zone. So when r3 is removed, although the mRNA levels of Cyp26s in adjacent tissues may not change, a source of Cyp26 proteins (r3) has been removed, therefore lowering

available Cyp26 protein in the r3 adjacent mesenchyme. This change then could lead to an increase in local RA concentrations, which then leads to the Type1 phenotype, as observed when beads of RA are implanted into the r3 adjacent mesenchyme. In conclusion it is possible that in Type1 phenotypes, particularly with regards to the r3 removal and *Cyp26* knockouts, that the mechanism is indeed similar, both leading to increased local RA in r3 adjacent mesenchyme, which has been shown here to cause a Type1 phenotype.

4.8. Conclusions

The data presented here show a novel role for 9-cis RA in the presentation of a Type1 phenotype, and also demonstrate how a slow, long-term exposure to RA isoforms, either 9-cis or at-RA, is more effective at altering the pattern of cNCC migration than a single injection. In addition, the work shown here provides evidence for the involvement of the mesenchyme of r3 in maintaining correct cNCC migration patterning and perhaps the cNCCs themselves also.

Figure 4-12 gives an overall schematic summary of changes in Cyp26s following r3 removal and which tissues were affected the most by RA in order to initiate cNCC mismigration. The involvement of mesenchyme adjacent to r3 is shown not only by the RA experiments, but is also implied by the Cyp26 gene expression patterns observed following r3 removal, which could lead to an increase in local RA concentrations due to decreased RA metabolism. If both the r3 removal and Cyp26 gene expression data and the RA data are taken together, then the tissues involved in Type1 phenotypes are the r2, r4 and particularly the mesenchyme adjacent to r3 and also r2 and r4 neural tube. Finally it has been demonstrated that signalling between rhombomere3 and rhombomere 4 is also important in maintenance of the r3 mesenchyme cNCC barrier.

These data demonstrate a possible common mechanism through which changes in local RA concentration lead to a Type1 phenotype. The results presented here further elucidate the complex mechanisms controlling the migration patterning of the cranial neural crest cells during development and provide many directions for further study.

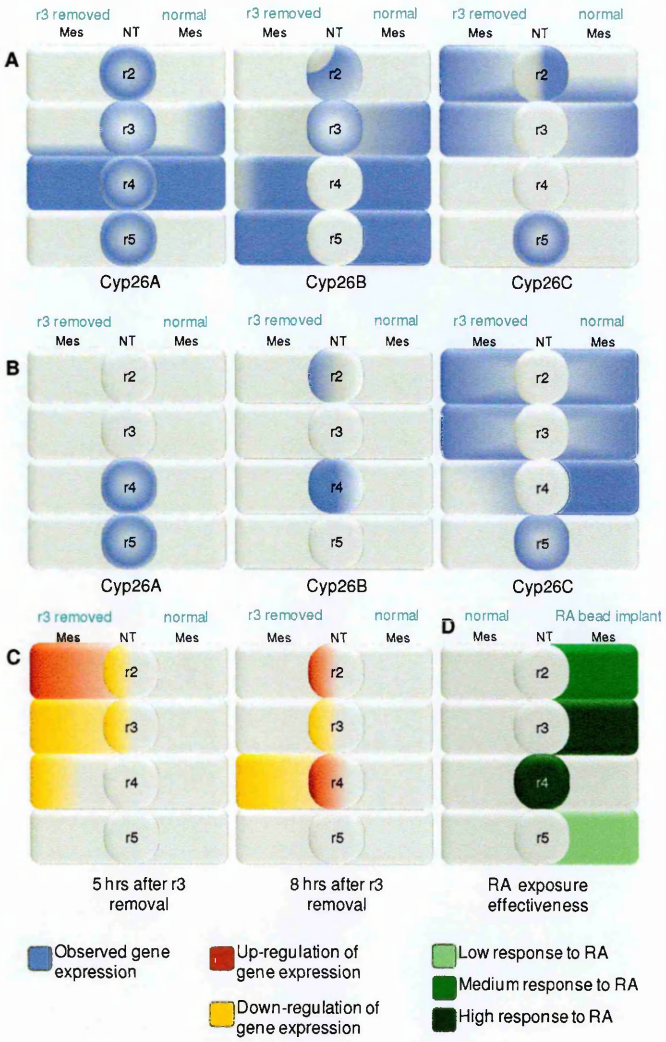

Figure 4-12. Schematic diagram representing the changes in gene expression of the Cyp26s following r3 removal and the effectiveness of RA exposure at the tissue to cause a cNCC mismigration phenotype.

The diagram represents the hindbrain from rhombomeres 2-5 and the adjacent mesenchyme area. Panels A and B shows the expression pattern observed when r3 is removed on the left side of the embryo and then incubated for a further 5 (**A**) or 8 (**B**) hours, the right side of the image shows normal gene expression when r3 has not been removed. Panel **C** represents the areas where gene expression was altered following r3 removal at both 5 and 8 hours after surgery, orange shading shows areas where gene expression has decreased and red shading shows areas which have increased gene expression. Panel **D** depicts the observed effectiveness of RA at initiating a Type1 phenotype, the deeper the shade of green, the more effective the RA was when applied to that tissue at causing cNCC mismigration. grey areas - there is no experimental data shown here for RA application to these areas. Mes- Mesenchyme, NT- Neural tube, r- rhombomere

4.9. Future Directions

These data have opened a number of interesting avenues for further investigation into the mechanisms controlling the migration pattern of the cranial neural crest. The finding that 9-cis RA is as effective, if not more so in some conditions, as at-RA at initiating a Type1 phenotype is novel in itself, however the preliminary results that imply that a mix of both the at-RA and 9-cis RA is even more effective begs further investigation. Initial experiments could be performed through delivery of the RA mix, by bead implants and injections, both to rhombomere 4 and also to the r3 mesenchyme. The finding that the r3 mesenchyme may also be involved in its own right as a control of cNCC patterning also provides an avenue for further work. It would be interesting to see if the expression of genes in the r3 mesenchyme is altered following RA administration. This possibility could be investigated by ISH, or perhaps it would also be useful to investigate the level and activity of r3 proteins by removing tissue at time points following RA bead implantation and using western blot analysis or 2D gel electrophoresis. This approach would allow study of changes in protein activity in addition to changes in gene expression, alterations in which may be delayed.

Further experiments to elucidate if cNCCs can also be affected by RA directly with regards to their migration pattern would also be interesting. Changes to the experimental design would probably be needed in order to reduce the possibility that RA might be transported with the cells. This could be achieved by either implanting only cells and not tissue, or perhaps using smaller tissue transplants and washing the tissue for longer periods, in all cases though the identity of the surrounding rhombomeres would need to be checked, particularly Krox20 expression. Another possible method would be to examine the migration pattern of RA treated cells on cryosections of hindbrain, similar to that used by Golding et al [184]. As patterning cues are still evident in cryosections, and furthermore they cannot respond to RA exposure as the tissue is dead, this approach

would allow the cNCCs to migrate following RA exposure without the question of affecting the environmental cues.

The present results indicate that activation of different RA receptors RAR and RXR or a combination of the two could be responsible for the variation in the number of embryos displaying a cNCC mismigration phenotype. In order to clarify this possibility, and allow specific identification of the receptors responsible for the Type1 phenotype, various agonists and inhibitors which are commercially available for specific RXR and RAR receptors could be used. These could be applied using the same bead implantation method.

Another interesting avenue for further investigation is the possible changes in ErbB4 protein expression following RA exposure. This analysis could be performed on embryos with r3 adjacent mesenchyme RA beads to see if ErbB4 protein levels could be involved in the Type1 phenotype. Although immunostaining of wholemount embryos would be a good way of studying this possibility, it was attempted unsuccessfully before the ISH for ErbB4 was chosen in the present study. Therefore in the event this problem could not be resolved, western blot or FACS analysis could be tried.

Finally, although no evident change in the expression pattern of the Cyp26s was observed before the cNCCs began mismigrating, it would still be useful to look at the protein levels and activity of the Cyp26s in order to make a successful conclusion with regards to their involvement in this situation. Changes in the protein activity may be occurring but the mRNA expression levels may not reflect that possibility.

5. Thesis Summary

The aims of this PhD were to study the tissues and molecules that regulate the migration of cranial neural crest cells in the chicken embryo, with particular focus on the roles of Mid1 and retinoic acid.

Mid1 is mutated in XLOS, causing congenital malformations of the midline, including cleft lip/palate, widely spaced eyes (hypertelorism) and broad nasal ridges, all of which could be caused by cNCC defects. To date studies have focused on the role of Mid1 in very early development or its role in cell biology. The main cellular functions of Mid1 identified so far are its ability to bind to microtubules, its ability to form multiprotein complexes and its ubiquitination of PP2A.

During development the role of Mid1 has not been widely studied, however some mRNA expression pattern work on Mid1 has shown that it is expressed from as early as 4 somites through to E16.5. Furthermore Mid1 is expressed in the hindbrain and adjacent mesenchyme of developing embryos at 10ss, leading to the possibility that Mid1 is involved in the developmental biology of the cNCC, defects in which could contribute to the craniofacial deformities as observed in XLOS.

Here I provide novel evidence that Mid1 is involved in several cNCC cell functions, including cell migration speed, protease secretions and initiation of placodal cell migration. These lead to premature geniculate ganglia development when cNCCs from r4 are made to over-express Mid1, the mechanism of which is shown here to be due to premature migration of cells from the placode, possibly due to changes in cNCC protease secretions.

This thesis has also focused on further elucidating the control of cNCC migration patterning. Several situations have been published to cause cNCC mismigration

phenotypes, here I have grouped all conditions which lead to a very similar phenotype of a thin stream of cNCCs migrating through the r3 adjacent mesenchyme into one common phenotype, termed Type 1. The conditions in which a Type 1 phenotype occur include exposure of the embryo to all-trans RA or removal of r3.

The work here has focused on the role of retinoic acid and has shown a novel role for the r3 adjacent mesenchyme as a potent responder to RA, needing only low concentrations of RA in comparison to the rhombomeres to cause a Type 1 mismigration phenotype. Furthermore I have shown that the cNCCs themselves may also be directly responding to RA exposure, leading to a disregard of local environmental cues which normally maintain the r3 adjacent mesenchyme cNCC free zone. I also provide evidence that the 9-cis RA isoform is more effective at causing a Type 1 phenotype than the traditionally used all-trans RA isoform, this is most likely due to the initiation of different RA nuclear receptors.

Overall, the data shown in this thesis provides several novel findings and therefore new avenues for study. Through further investigation, the role of Mid1 in regulating cNCC protease activity could provide insight into the mechanism behind not only the changes in placodal cell migration timings, but also the development of craniofacial abnormalities, as Mid1 is re-expressed later in development in the frontonasal prominence of embryos at a time when the geniculate structures are being formed.

The migration patterning data has also opened up some new leads for analysis. The finding that 9-cis RA is a more potent isoform than at-RA at initiating a Type1 phenotype leads to questions about how 9-cis RA causes different downstream signalling responses to at-RA. Furthermore it would be interesting to explore how cNCCs would respond to exposure to a cocktail of both 9-cis RA and at-RA, particularly when the r3 mesenchyme is targeted.

6. References

[1] M. B. Walker and P. A. Trainor, "Craniofacial malformations: intrinsic vs extrinsic neural crest cell defects in Treacher Collins and 22q11 deletion syndromes," *Clin Genet,* vol. 69, pp. 471-9, Jun 2006.

[2] L. Kochilas, S. Merscher-Gomez, M. M. Lu, V. Potluri, J. Liao, R. Kucherlapati, B. Morrow, and J. A. Epstein, "The role of neural crest during cardiac development in a mouse model of DiGeorge syndrome," *Dev Biol,* vol. 251, pp. 157-66, Nov 1 2002.

[3] P. Trainor and R. Krumlauf, "Plasticity in mouse neural crest cells reveals a new patterning role for cranial mesoderm," *Nat Cell Biol,* vol. 2, pp. 96-102, Feb 2000.

[4] G. Mellitzer, Q. Xu, and D. G. Wilkinson, "Eph receptors and ephrins restrict cell intermingling and communication," *Nature,* vol. 400, pp. 77-81, Jul 1 1999.

[5] D. L. Ellies, A. S. Tucker, and A. Lumsden, "Apoptosis of premigratory neural crest cells in rhombomeres 3 and 5: consequences for patterning of the branchial region," *Dev Biol,* vol. 251, pp. 118-28, Nov 1 2002.

[6] A. Graham, I. Heyman, and A. Lumsden, "Even-numbered rhombomeres control the apoptotic elimination of neural crest cells from odd-numbered rhombomeres in the chick hindbrain," *Development,* vol. 119, pp. 233-45, Sep 1993.

[7] J. P. Golding, M. Dixon, and M. Gassmann, "Cues from neuroepithelium and surface ectoderm maintain neural crest-free regions within cranial mesenchyme of the developing chick," *Development,* vol. 129, pp. 1095-105, Mar 2002.

[8] S. Kuriyama and R. Mayor, "Molecular analysis of neural crest migration," *Philos Trans R Soc Lond B Biol Sci,* vol. 363, pp. 1349-62, Apr 12 2008.

[9] A. Graham, "The neural crest," *Curr Biol,* vol. 13, pp. R381-4, May 13 2003.

[10] F. De Falco, S. Cainarca, G. Andolfi, R. Ferrentino, C. Berti, G. Rodriguez Criado, O. Rittinger, N. Dennis, S. Odent, A. Rastogi, J. Liebelt, D. Chitayat, R. Winter, H. Jawanda, A. Ballabio, B. Franco, and G. Meroni, "X-linked Opitz syndrome: novel mutations in the MID1 gene and redefinition of the clinical spectrum," *Am J Med Genet A,* vol. 120A, pp. 222-8, Jul 15 2003.

[11] M. D. Tapadia, D. R. Cordero, and J. A. Helms, "It's all in your head: new insights into craniofacial development and deformation," *J Anat,* vol. 207, pp. 461-77, Nov 2005.

[12] S. Kurosaka and A. Kashina, "Cell biology of embryonic migration," *Birth Defects Res C Embryo Today,* vol. 84, pp. 102-22, Jun 2008.

[13] K. Mikule, J. C. Gatlin, B. A. de la Houssaye, and K. H. Pfenninger, "Growth cone collapse induced by semaphorin 3A requires 12/15-lipoxygenase," *J Neurosci,* vol. 22, pp. 4932-41, Jun 15 2002.

[14] J. M. Teddy and P. M. Kulesa, "In vivo evidence for short- and long-range cell communication in cranial neural crest cells," *Development,* vol. 131, pp. 6141-51, Dec 2004.

[15] P. A. K. Rupp, P.M, "Chain migration of cranial neural crest cells, a dynamic *in vivo* analysis," *Developmental Biology,* vol. 283, pp. 705-705, 2005.

[16] K. Soo, M. P. O'Rourke, P. L. Khoo, K. A. Steiner, N. Wong, R. R. Behringer, and P. P. Tam, "Twist function is required for the morphogenesis of the cephalic neural tube and the differentiation of the cranial neural crest cells in the mouse embryo," *Dev Biol,* vol. 247, pp. 251-70, Jul 15 2002.

[17] J. P. Golding, D. Sobieszczuk, M. Dixon, E. Coles, J. Christiansen, D. Wilkinson, and M. Gassmann, "Roles of erbB4, rhombomere-specific, and rhombomere-independent cues in maintaining neural crest-free zones in the embryonic head," *Dev Biol,* vol. 266, pp. 361-72, Feb 15 2004.

[18] D. Orioli and R. Klein, "The Eph receptor family: axonal guidance by contact repulsion," *Trends Genet,* vol. 13, pp. 354-9, Sep 1997.

[19] A. Smith, V. Robinson, K. Patel, and D. G. Wilkinson, "The EphA4 and EphB1 receptor tyrosine kinases and ephrin-B2 ligand regulate targeted migration of branchial neural crest cells," *Curr Biol,* vol. 7, pp. 561-70, Aug 1 1997.

[20] D. O. Mellott and R. D. Burke, "Divergent roles for Eph and ephrin in avian cranial neural crest," *BMC Dev Biol,* vol. 8, p. 56, 2008.

[21] A. Davy, J. Aubin, and P. Soriano, "Ephrin-B1 forward and reverse signaling are required during mouse development," *Genes Dev,* vol. 18, pp. 572-83, Mar 1 2004.

[22] J. R. Barrow, H. S. Stadler, and M. R. Capecchi, "Roles of Hoxa1 and Hoxa2 in patterning the early hindbrain of the mouse," *Development,* vol. 127, pp. 933-44, Mar 2000.

[23] M. Dixon and A. Lumsden, "Distribution of neuregulin-1 (nrg1) and erbB4 transcripts in embryonic chick hindbrain," *Mol Cell Neurosci,* vol. 13, pp. 237-58, Apr 1999.

[24] J. P. Golding, P. Trainor, R. Krumlauf, and M. Gassmann, "Defects in pathfinding by cranial neural crest cells in mice lacking the neuregulin receptor ErbB4," *Nat Cell Biol,* vol. 2, pp. 103-9, Feb 2000.

[25] T. Takahashi, A. Fournier, F. Nakamura, L. H. Wang, Y. Murakami, R. G. Kalb, H. Fujisawa, and S. M. Strittmatter, "Plexin-neuropilin-1 complexes form functional semaphorin-3A receptors," *Cell,* vol. 99, pp. 59-69, Oct 1 1999.

[26] Q. Schwarz, C. H. Maden, J. M. Vieira, and C. Ruhrberg, "Neuropilin 1 signaling guides neural crest cells to coordinate pathway choice with cell specification," *Proc Natl Acad Sci U S A,* vol. 106, pp. 6164-9, Apr 14 2009.

[27] N. J. Osborne, J. Begbie, J. K. Chilton, H. Schmidt, and B. J. Eickholt, "Semaphorin/neuropilin signaling influences the positioning of migratory neural crest cells within the hindbrain region of the chick," *Dev Dyn,* vol. 232, pp. 939-49, Apr 2005.

[28] Q. Schwarz, J. M. Vieira, B. Howard, B. J. Eickholt, and C. Ruhrberg, "Neuropilin 1 and 2 control cranial gangliogenesis and axon guidance through neural crest cells," *Development,* vol. 135, pp. 1605-13, May 2008.

[29] J. Han, Y. Ito, J. Y. Yeo, H. M. Sucov, R. Maas, and Y. Chai, "Cranial neural crest-derived mesenchymal proliferation is regulated by Msx1-mediated p19(INK4d) expression during odontogenesis," *Dev Biol,* vol. 261, pp. 183-96, Sep 1 2003.

[30] G. Hu, H. Lee, S. M. Price, M. M. Shen, and C. Abate-Shen, "Msx homeobox genes inhibit differentiation through upregulation of cyclin D1," *Development,* vol. 128, pp. 2373-84, Jun 2001.

[31] Y. H. Liu, Z. Tang, R. K. Kundu, L. Wu, W. Luo, D. Zhu, F. Sangiorgi, M. L. Snead, and R. E. Maxson, "Msx2 gene dosage influences the number of proliferative osteogenic cells in growth centers of the developing murine skull: a possible mechanism for MSX2-mediated craniosynostosis in humans," *Dev Biol,* vol. 205, pp. 260-74, Jan 15 1999.

[32] G. Marazzi, Y. Wang, and D. Sassoon, "Msx2 is a transcriptional regulator in the BMP4-mediated programmed cell death pathway," *Dev Biol,* vol. 186, pp. 127-38, Jun 15 1997.

[33] S. J. Odelberg, A. Kollhoff, and M. T. Keating, "Dedifferentiation of mammalian myotubes induced by msx1," *Cell,* vol. 103, pp. 1099-109, Dec 22 2000.

[34] P. Woloshin, K. Song, C. Degnin, A. M. Killary, D. J. Goldhamer, D. Sassoon, and M. J. Thayer, "MSX1 inhibits myoD expression in fibroblast x 10T1/2 cell hybrids," *Cell,* vol. 82, pp. 611-20, Aug 25 1995.

[35] Y. Chen, M. Bei, I. Woo, I. Satokata, and R. Maas, "Msx1 controls inductive signaling in mammalian tooth morphogenesis," *Development,* vol. 122, pp. 3035-44, Oct 1996.

[36] J. A. Montero, Y. Ganan, D. Macias, J. Rodriguez-Leon, J. J. Sanz-Ezquerro, R. Merino, J. Chimal-Monroy, M. A. Nieto, and J. M. Hurle, "Role of FGFs in the control of programmed cell death during limb development," *Development,* vol. 128, pp. 2075-84, Jun 2001.

[37] S. Vainio, I. Karavanova, A. Jowett, and I. Thesleff, "Identification of BMP-4 as a signal mediating secondary induction between epithelial and mesenchymal tissues during early tooth development," *Cell,* vol. 75, pp. 45-58, Oct 8 1993.

[38] J. Willert, M. Epping, J. R. Pollack, P. O. Brown, and R. Nusse, "A transcriptional response to Wnt protein in human embryonic carcinoma cells," *BMC Dev Biol,* vol. 2, p. 8, Jul 2 2002.

[39] I. Satokata and R. Maas, "Msx1 deficient mice exhibit cleft palate and abnormalities of craniofacial and tooth development," *Nat Genet,* vol. 6, pp. 348-56, Apr 1994.

[40] M. Ishii, J. Han, H. Y. Yen, H. M. Sucov, Y. Chai, and R. E. Maxson, Jr., "Combined deficiencies of Msx1 and Msx2 cause impaired patterning and survival of the cranial neural crest," *Development,* vol. 132, pp. 4937-50, Nov 2005.

[41] J. G. Wilson and J. Warkany, "Malformations in the genito-urinary tract induced by maternal vitamin A deficiency in the rat," *Am J Anat,* vol. 83, pp. 357-407, Nov 1948.

[42] A. Gavalas and R. Krumlauf, "Retinoid signalling and hindbrain patterning," *Curr Opin Genet Dev,* vol. 10, pp. 380-6, Aug 2000.

[43] D. L. Young, R. A. Schneider, D. Hu, and J. A. Helms, "Genetic and teratogenic approaches to craniofacial development," *Crit Rev Oral Biol Med,* vol. 11, pp. 304-17, 2000.

[44] E. J. Lammer, D. T. Chen, R. M. Hoar, N. D. Agnish, P. J. Benke, J. T. Braun, C. J. Curry, P. M. Fernhoff, A. W. Grix, Jr., I. T. Lott, and et al., "Retinoic acid embryopathy," *N Engl J Med,* vol. 313, pp. 837-41, Oct 3 1985.

[45] E. Gale, V. Prince, A. Lumsden, J. Clarke, N. Holder, and M. Maden, "Late effects of retinoic acid on neural crest and aspects of rhombomere," *Development,* vol. 122, pp. 783-93, Mar 1996.

[46] R. J. Sessler and N. Noy, "A ligand-activated nuclear localization signal in cellular retinoic acid binding protein-II," *Mol Cell,* vol. 18, pp. 343-53, Apr 29 2005.

[47] E. J. Dekker, M. J. Vaessen, C. van den Berg, A. Timmermans, S. Godsave, T. Holling, P. Nieuwkoop, A. Geurts van Kessel, and A. Durston, "Overexpression of a cellular retinoic acid binding protein (xCRABP) causes anteroposterior defects in developing Xenopus embryos," *Development,* vol. 120, pp. 973-85, Apr 1994.

[48] J. F. Boylan and L. J. Gudas, "Overexpression of the cellular retinoic acid binding protein-I (CRABP-I) results in a reduction in differentiation-specific gene expression in F9 teratocarcinoma cells," *J Cell Biol,* vol. 112, pp. 965-79, Mar 1991.

[49] J. F. Boylan and L. J. Gudas, "The level of CRABP-I expression influences the amounts and types of all-trans-retinoic acid metabolites in F9 teratocarcinoma stem cells," *J Biol Chem,* vol. 267, pp. 21486-91, Oct 25 1992.

[50] P. Chambon, "A decade of molecular biology of retinoic acid receptors," *FASEB J,* vol. 10, pp. 940-54, Jul 1996.

[51] M. Leid, P. Kastner, and P. Chambon, "Multiplicity generates diversity in the retinoic acid signalling pathways," *Trends Biochem Sci,* vol. 17, pp. 427-33, Oct 1992.

[52] D. J. Mangelsdorf and R. M. Evans, "The RXR heterodimers and orphan receptors," *Cell,* vol. 83, pp. 841-50, Dec 15 1995.

[53] J. Bastien and C. Rochette-Egly, "Nuclear retinoid receptors and the transcription of retinoid-target genes," *Gene,* vol. 328, pp. 1-16, Mar 17 2004.

[54] P. J. Willy, K. Umesono, E. S. Ong, R. M. Evans, R. A. Heyman, and D. J. Mangelsdorf, "LXR, a nuclear receptor that defines a distinct retinoid response pathway," *Genes Dev,* vol. 9, pp. 1033-45, May 1 1995.

[55] S. A. Kliewer, K. Umesono, D. J. Mangelsdorf, and R. M. Evans, "Retinoid X receptor interacts with nuclear receptors in retinoic acid, thyroid hormone and vitamin D3 signalling," *Nature,* vol. 355, pp. 446-9, Jan 30 1992.

[56] X. K. Zhang, B. Hoffmann, P. B. Tran, G. Graupner, and M. Pfahl, "Retinoid X receptor is an auxiliary protein for thyroid hormone and retinoic acid receptors," *Nature,* vol. 355, pp. 441-6, Jan 30 1992.

[57] O. Bardot, T. C. Aldridge, N. Latruffe, and S. Green, "PPAR-RXR heterodimer activates a peroxisome proliferator response element upstream of the bifunctional enzyme gene," *Biochem Biophys Res Commun,* vol. 192, pp. 37-45, Apr 15 1993.

[58] S. A. Kliewer, K. Umesono, D. J. Noonan, R. A. Heyman, and R. M. Evans, "Convergence of 9-cis retinoic acid and peroxisome proliferator signalling pathways through heterodimer formation of their receptors," *Nature,* vol. 358, pp. 771-4, Aug 27 1992.

[59] R. A. Heyman, D. J. Mangelsdorf, J. A. Dyck, R. B. Stein, G. Eichele, R. M. Evans, and C. Thaller, "9-cis retinoic acid is a high affinity ligand for the retinoid X receptor," *Cell,* vol. 68, pp. 397-406, Jan 24 1992.

[60] A. I. Shulman, C. Larson, D. J. Mangelsdorf, and R. Ranganathan, "Structural determinants of allosteric ligand activation in RXR heterodimers," *Cell,* vol. 116, pp. 417-29, Feb 6 2004.

[61] K. Mehta, "Retinoids as regulators of gene transcription," *J Biol Regul Homeost Agents,* vol. 17, pp. 1-12, Jan-Mar 2003.

[62] F. Grignani, S. De Matteis, C. Nervi, L. Tomassoni, V. Gelmetti, M. Cioce, M. Fanelli, M. Ruthardt, F. F. Ferrara, I. Zamir, C. Seiser, M. A. Lazar, S. Minucci, and P. G. Pelicci, "Fusion proteins of the retinoic acid receptor-alpha recruit histone deacetylase in promyelocytic leukaemia," *Nature,* vol. 391, pp. 815-8, Feb 19 1998.

[63] T. Heinzel, R. M. Lavinsky, T. M. Mullen, M. Soderstrom, C. D. Laherty, J. Torchia, W. M. Yang, G. Brard, S. D. Ngo, J. R. Davie, E. Seto, R. N. Eisenman, D. W. Rose, C. K. Glass, and M. G. Rosenfeld, "A complex containing N-CoR, mSin3 and histone deacetylase mediates transcriptional repression," *Nature,* vol. 387, pp. 43-8, May 1 1997.

[64] C. K. Glass, M. G. Rosenfeld, D. W. Rose, R. Kurokawa, Y. Kamei, L. Xu, J. Torchia, M. H. Ogliastro, and S. Westin, "Mechanisms of transcriptional activation by retinoic acid receptors," *Biochem Soc Trans,* vol. 25, pp. 602-5, May 1997.

[65] S. Abu-Abed, P. Dolle, D. Metzger, B. Beckett, P. Chambon, and M. Petkovich, "The retinoic acid-metabolizing enzyme, CYP26A1, is essential for normal hindbrain patterning, vertebral identity, and development of posterior structures," *Genes Dev,* vol. 15, pp. 226-40, Jan 15 2001.

[66] S. Reijntjes, E. Gale, and M. Maden, "Expression of the retinoic acid catabolising enzyme CYP26B1 in the chick embryo and its regulation by retinoic acid," *Gene Expr Patterns,* vol. 3, pp. 621-7, Oct 2003.

[67] S. Reijntjes, E. Gale, and M. Maden, "Generating gradients of retinoic acid in the chick embryo: Cyp26C1 expression and a comparative analysis of the Cyp26 enzymes," *Dev Dyn,* vol. 230, pp. 509-17, Jul 2004.

[68] M. Uehara, K. Yashiro, S. Mamiya, J. Nishino, P. Chambon, P. Dolle, and Y. Sakai, "CYP26A1 and CYP26C1 cooperatively regulate anterior-posterior patterning of the developing brain and the production of migratory cranial neural crest cells in the mouse," *Dev Biol,* vol. 302, pp. 399-411, Feb 15 2007.

[69] Y. Saka and J. C. Smith, "Spatial and temporal patterns of cell division during early Xenopus embryogenesis," *Dev Biol,* vol. 229, pp. 307-18, Jan 15 2001.

[70] A. Graham, A. Blentic, S. Duque, and J. Begbie, "Delamination of cells from neurogenic placodes does not involve an epithelial-to-mesenchymal transition," *Development,* vol. 134, pp. 4141-5, Dec 2007.

[71] G. Schlosser, "Induction and specification of cranial placodes," *Dev Biol,* vol. 294, pp. 303-51, Jun 15 2006.

[72] A. D'Amico-Martel and D. M. Noden, "Contributions of placodal and neural crest cells to avian cranial peripheral ganglia," *Am J Anat,* vol. 166, pp. 445-68, Apr 1983.

[73] J. Begbie, M. Ballivet, and A. Graham, "Early steps in the production of sensory neurons by the neurogenic placodes," *Mol Cell Neurosci,* vol. 21, pp. 502-11, Nov 2002.
[74] I. Mason, "Initiation to end point: the multiple roles of fibroblast growth factors in neural development," *Nat Rev Neurosci,* vol. 8, pp. 583-96, Aug 2007.
[75] J. Begbie, J. F. Brunet, J. L. Rubenstein, and A. Graham, "Induction of the epibranchial placodes," *Development,* vol. 126, pp. 895-902, Feb 1999.
[76] S. Leger and M. Brand, "Fgf8 and Fgf3 are required for zebrafish ear placode induction, maintenance and inner ear patterning," *Mech Dev,* vol. 119, pp. 91-108, Nov 2002.
[77] D. Liu, H. Chu, L. Maves, Y. L. Yan, P. A. Morcos, J. H. Postlethwait, and M. Westerfield, "Fgf3 and Fgf8 dependent and independent transcription factors are required for otic placode specification," *Development,* vol. 130, pp. 2213-24, May 2003.
[78] H. Maroon, J. Walshe, R. Mahmood, P. Kiefer, C. Dickson, and I. Mason, "Fgf3 and Fgf8 are required together for formation of the otic placode and vesicle," *Development,* vol. 129, pp. 2099-108, May 2002.
[79] S. K. Sun, C. T. Dee, V. B. Tripathi, A. Rengifo, C. S. Hirst, and P. J. Scotting, "Epibranchial and otic placodes are induced by a common Fgf signal, but their subsequent development is independent," *Dev Biol,* vol. 303, pp. 675-86, Mar 15 2007.
[80] J. Begbie and A. Graham, "Integration between the epibranchial placodes and the hindbrain," *Science,* vol. 294, pp. 595-8, Oct 19 2001.
[81] D. Alfandari, T. G. Wolfsberg, J. M. White, and D. W. DeSimone, "ADAM 13: a novel ADAM expressed in somitic mesoderm and neural crest cells during Xenopus laevis development," *Dev Biol,* vol. 182, pp. 314-30, Feb 15 1997.
[82] D. H. Cai, T. M. Vollberg, Sr., E. Hahn-Dantona, J. P. Quigley, and P. R. Brauer, "MMP-2 expression during early avian cardiac and neural crest morphogenesis," *Anat Rec,* vol. 259, pp. 168-79, Jun 1 2000.
[83] V. Cantemir, D. H. Cai, M. V. Reedy, and P. R. Brauer, "Tissue inhibitor of metalloproteinase-2 (TIMP-2) expression during cardiac neural crest cell migration and its role in proMMP-2 activation," *Dev Dyn,* vol. 231, pp. 709-19, Dec 2004.
[84] T. A. Giambernardi, A. Y. Sakaguchi, J. Gluhak, D. Pavlin, D. A. Troyer, G. Das, U. Rodeck, and R. J. Klebe, "Neutrophil collagenase (MMP-8) is expressed during early development in neural crest cells as well as in adult melanoma cells," *Matrix Biol,* vol. 20, pp. 577-87, Dec 2001.
[85] R. J. Hall and C. A. Erickson, "ADAM 10: an active metalloprotease expressed during avian epithelial morphogenesis," *Dev Biol,* vol. 256, pp. 146-59, Apr 1 2003.
[86] M. Harrison, M. Abu-Elmagd, T. Grocott, C. Yates, J. Gavrilovic, and G. N. Wheeler, "Matrix metalloproteinase genes in Xenopus development," *Dev Dyn,* vol. 231, pp. 214-20, Sep 2004.
[87] D. H. Cai and P. R. Brauer, "Synthetic matrix metalloproteinase inhibitor decreases early cardiac neural crest migration in chicken embryos," *Dev Dyn,* vol. 224, pp. 441-9, Aug 2002.
[88] T. D. Duong and C. A. Erickson, "MMP-2 plays an essential role in producing epithelial-mesenchymal transformations in the avian embryo," *Dev Dyn,* vol. 229, pp. 42-53, Jan 2004.
[89] D. Alfandari, H. Cousin, A. Gaultier, K. Smith, J. M. White, T. Darribere, and D. W. DeSimone, "Xenopus ADAM 13 is a metalloprotease required for cranial neural crest-cell migration," *Curr Biol,* vol. 11, pp. 918-30, Jun 26 2001.
[90] H. Sato, T. Takino, Y. Okada, J. Cao, A. Shinagawa, E. Yamamoto, and M. Seiki, "A matrix metalloproteinase expressed on the surface of invasive tumour cells," *Nature,* vol. 370, pp. 61-5, Jul 7 1994.
[91] G. S. Butler, M. J. Butler, S. J. Atkinson, H. Will, T. Tamura, S. Schade van Westrum, T. Crabbe, J. Clements, M. P. d'Ortho, and G. Murphy, "The TIMP2

membrane type 1 metalloproteinase "receptor" regulates the concentration and efficient activation of progelatinase A. A kinetic study," *J Biol Chem,* vol. 273, pp. 871-80, Jan 9 1998.

[92] Y. Jo, J. Yeon, H. J. Kim, and S. T. Lee, "Analysis of tissue inhibitor of metalloproteinases-2 effect on pro-matrix metalloproteinase-2 activation by membrane-type 1 matrix metalloproteinase using baculovirus/insect-cell expression system," *Biochem J,* vol. 345 Pt 3, pp. 511-9, Feb 1 2000.

[93] A. Y. Strongin, I. Collier, G. Bannikov, B. L. Marmer, G. A. Grant, and G. I. Goldberg, "Mechanism of cell surface activation of 72-kDa type IV collagenase. Isolation of the activated form of the membrane metalloprotease," *J Biol Chem,* vol. 270, pp. 5331-8, Mar 10 1995.

[94] E. C. Swindell, C. Thaller, S. Sockanathan, M. Petkovich, T. M. Jessell, and G. Eichele, "Complementary domains of retinoic acid production and degradation in the early chick embryo," *Dev Biol,* vol. 216, pp. 282-96, Dec 1 1999.

[95] D. G. Wilkinson, S. Bhatt, P. Chavrier, R. Bravo, and P. Charnay, "Segment-specific expression of a zinc-finger gene in the developing nervous system of the mouse," *Nature,* vol. 337, pp. 461-4, Feb 2 1989.

[96] A. Granata and N. A. Quaderi, "The Opitz syndrome gene MID1 is essential for establishing asymmetric gene expression in Hensen's node," *Dev Biol,* vol. 258, pp. 397-405, Jun 15 2003.

[97] A. Granata, D. Savery, J. Hazan, B. M. Cheung, A. Lumsden, and N. A. Quaderi, "Evidence of functional redundancy between MID proteins: implications for the presentation of Opitz syndrome," *Dev Biol,* vol. 277, pp. 417-24, Jan 15 2005.

[98] Y. Cheng, M. Cheung, M. M. Abu-Elmagd, A. Orme, and P. J. Scotting, "Chick sox10, a transcription factor expressed in both early neural crest cells and central nervous system," *Brain Res Dev Brain Res,* vol. 121, pp. 233-41, Jun 30 2000.

[99] H. Acloque, A. Mey, A. M. Birot, H. Gruffat, B. Pain, and J. Samarut, "Transcription factor cCP2 controls gene expression in chicken embryonic stem cells," *Nucleic Acids Res,* vol. 32, pp. 2259-71, 2004.

[100] P. M. Voorhoeve, E. M. Hijmans, and R. Bernards, "Functional interaction between a novel protein phosphatase 2A regulatory subunit, PR59, and the retinoblastoma-related p107 protein," *Oncogene,* vol. 18, pp. 515-24, Jan 14 1999.

[101] G. Eichele, C. Tickle, and B. M. Alberts, "Microcontrolled release of biologically active compounds in chick embryos: beads of 200-microns diameter for the local release of retinoids," *Anal Biochem,* vol. 142, pp. 542-55, Nov 1 1984.

[102] M. D. Abramoff, Magelhaes, P.J., Ram, S.J., "Image Processing with ImageJ," *Biophotonics International,* vol. 11, pp. 36-42, 2004.

[103] T. C. Cox, L. R. Allen, L. L. Cox, B. Hopwood, B. Goodwin, E. Haan, and G. K. Suthers, "New mutations in MID1 provide support for loss of function as the cause of X-linked Opitz syndrome," *Hum Mol Genet,* vol. 9, pp. 2553-62, Oct 12 2000.

[104] S. Schweiger and R. Schneider, "The MID1/PP2A complex: a key to the pathogenesis of Opitz BBB/G syndrome," *Bioessays,* vol. 25, pp. 356-66, Apr 2003.

[105] J. Winter, T. Lehmann, S. Krauss, A. Trockenbacher, Z. Kijas, J. Foerster, V. Suckow, M. L. Yaspo, A. Kulozik, V. Kalscheuer, R. Schneider, and S. Schweiger, "Regulation of the MID1 protein function is fine-tuned by a complex pattern of alternative splicing," *Hum Genet,* vol. 114, pp. 541-52, May 2004.

[106] G. Meroni and G. Diez-Roux, "TRIM/RBCC, a novel class of 'single protein RING finger' E3 ubiquitin ligases," *Bioessays,* vol. 27, pp. 1147-57, Nov 2005.

[107] K. M. Short, B. Hopwood, Z. Yi, and T. C. Cox, "MID1 and MID2 homo- and heterodimerise to tether the rapamycin-sensitive PP2A regulatory subunit, alpha 4, to microtubules: implications for the clinical variability of X-linked Opitz GBBB syndrome and other developmental disorders," *BMC Cell Biol,* vol. 3, p. 1, 2002.

[108] J. Liu, T. D. Prickett, E. Elliott, G. Meroni, and D. L. Brautigan, "Phosphorylation and microtubule association of the Opitz syndrome protein mid-1 is regulated by

protein phosphatase 2A via binding to the regulatory subunit alpha 4," *Proc Natl Acad Sci U S A,* vol. 98, pp. 6650-5, Jun 5 2001.

[109] S. Schweiger, J. Foerster, T. Lehmann, V. Suckow, Y. A. Muller, G. Walter, T. Davies, H. Porter, H. van Bokhoven, P. W. Lunt, P. Traub, and H. H. Ropers, "The Opitz syndrome gene product, MID1, associates with microtubules," *Proc Natl Acad Sci U S A,* vol. 96, pp. 2794-9, Mar 16 1999.

[110] J. M. Richman, K. K. Fu, L. L. Cox, J. P. Sibbons, and T. C. Cox, "Isolation and characterisation of the chick orthologue of the Opitz syndrome gene, Mid1, supports a conserved role in vertebrate development," *Int J Dev Biol,* vol. 46, pp. 441-8, 2002.

[111] L. Dal Zotto, N. A. Quaderi, R. Elliott, P. A. Lingerfelter, L. Carrel, V. Valsecchi, E. Montini, C. H. Yen, V. Chapman, I. Kalcheva, G. Arrigo, O. Zuffardi, S. Thomas, H. F. Willard, A. Ballabio, C. M. Disteche, and E. I. Rugarli, "The mouse Mid1 gene: implications for the pathogenesis of Opitz syndrome and the evolution of the mammalian pseudoautosomal region," *Hum Mol Genet,* vol. 7, pp. 489-99, Mar 1998.

[112] L. Xu and X. Deng, "Suppression of cancer cell migration and invasion by protein phosphatase 2A through dephosphorylation of mu- and m-calpains," *J Biol Chem,* vol. 281, pp. 35567-75, Nov 17 2006.

[113] P. Cohen, C. F. Holmes, and Y. Tsukitani, "Okadaic acid: a new probe for the study of cellular regulation," *Trends Biochem Sci,* vol. 15, pp. 98-102, Mar 1990.

[114] A. H. Schonthal, "Role of PP2A in intracellular signal transduction pathways," *Front Biosci,* vol. 3, pp. D1262-73, Dec 15 1998.

[115] K. Murata, J. Wu, and D. L. Brautigan, "B cell receptor-associated protein alpha4 displays rapamycin-sensitive binding directly to the catalytic subunit of protein phosphatase 2A," *Proc Natl Acad Sci U S A,* vol. 94, pp. 10624-9, Sep 30 1997.

[116] A. Trockenbacher, V. Suckow, J. Foerster, J. Winter, S. Krauss, H. H. Ropers, R. Schneider, and S. Schweiger, "MID1, mutated in Opitz syndrome, encodes an ubiquitin ligase that targets phosphatase 2A for degradation," *Nat Genet,* vol. 29, pp. 287-94, Nov 2001.

[117] M. A. Massiah, J. A. Matts, K. M. Short, B. N. Simmons, S. Singireddy, Z. Yi, and T. C. Cox, "Solution structure of the MID1 B-box2 CHC(D/C)C(2)H(2) zinc-binding domain: insights into an evolutionarily conserved RING fold," *J Mol Biol,* vol. 369, pp. 1-10, May 25 2007.

[118] K. Takahashi, E. Nakajima, and K. Suzuki, "Involvement of protein phosphatase 2A in the maintenance of E-cadherin-mediated cell-cell adhesion through recruitment of IQGAP1," *J Cell Physiol,* vol. 206, pp. 814-20, Mar 2006.

[119] A. Ito, T. R. Kataoka, M. Watanabe, K. Nishiyama, Y. Mazaki, H. Sabe, Y. Kitamura, and H. Nojima, "A truncated isoform of the PP2A B56 subunit promotes cell motility through paxillin phosphorylation," *EMBO J,* vol. 19, pp. 562-71, Feb 15 2000.

[120] C. Berti, B. Fontanella, R. Ferrentino, and G. Meroni, "Mig12, a novel Opitz syndrome gene product partner, is expressed in the embryonic ventral midline and co-operates with Mid1 to bundle and stabilize microtubules," *BMC Cell Biol,* vol. 5, p. 9, Feb 29 2004.

[121] N. A. Quaderi, S. Schweiger, K. Gaudenz, B. Franco, E. I. Rugarli, W. Berger, G. J. Feldman, M. Volta, G. Andolfi, S. Gilgenkrantz, R. W. Marion, R. C. Hennekam, J. M. Opitz, M. Muenke, H. H. Ropers, and A. Ballabio, "Opitz G/BBB syndrome, a defect of midline development, is due to mutations in a new RING finger gene on Xp22," *Nat Genet,* vol. 17, pp. 285-91, Nov 1997.

[122] J. Winter, M. Kunath, S. Roepcke, S. Krause, R. Schneider, and S. Schweiger, "Alternative polyadenylation signals and promoters act in concert to control tissue-specific expression of the Opitz Syndrome gene MID1," *BMC Mol Biol,* vol. 8, p. 105, 2007.

[123] B. Aranda-Orgilles, A. Trockenbacher, J. Winter, J. Aigner, A. Kohler, E. Jastrzebska, J. Stahl, E. C. Muller, A. Otto, E. E. Wanker, R. Schneider, and S. Schweiger, "The Opitz syndrome gene product MID1 assembles a microtubule-associated ribonucleoprotein complex," *Hum Genet,* vol. 123, pp. 163-76, Mar 2008.

[124] A. D. Everett and D. L. Brautigan, "Developmental expression of alpha4 protein phosphatase regulatory subunit in tissues affected by Opitz syndrome," *Dev Dyn,* vol. 224, pp. 461-4, Aug 2002.

[125] G. Buchner, E. Montini, G. Andolfi, N. Quaderi, S. Cainarca, S. Messali, M. T. Bassi, A. Ballabio, G. Meroni, and B. Franco, "MID2, a homologue of the Opitz syndrome gene MID1: similarities in subcellular localization and differences in expression during development," *Hum Mol Genet,* vol. 8, pp. 1397-407, Aug 1999.

[126] P. Kang and K. K. Svoboda, "Epithelial-mesenchymal transformation during craniofacial development," *J Dent Res,* vol. 84, pp. 678-90, Aug 2005.

[127] N. M. Le Douarin, "The avian embryo as a model to study the development of the neural crest: a long and still ongoing story," *Mech Dev,* vol. 121, pp. 1089-102, Sep 2004.

[128] K. Gaudenz, E. Roessler, N. Quaderi, B. Franco, G. Feldman, D. L. Gasser, B. Wittwer, J. Horst, E. Montini, J. M. Opitz, A. Ballabio, and M. Muenke, "Opitz G/BBB syndrome in Xp22: mutations in the MID1 gene cluster in the carboxy-terminal domain," *Am J Hum Genet,* vol. 63, pp. 703-10, Sep 1998.

[129] M. P. Creyghton, G. Roel, P. J. Eichhorn, E. M. Hijmans, I. Maurer, O. Destree, and R. Bernards, "PR72, a novel regulator of Wnt signaling required for Naked cuticle function," *Genes Dev,* vol. 19, pp. 376-86, Feb 1 2005.

[130] Y. Xing, Y. Xu, Y. Chen, P. D. Jeffrey, Y. Chao, Z. Lin, Z. Li, S. Strack, J. B. Stock, and Y. Shi, "Structure of protein phosphatase 2A core enzyme bound to tumor-inducing toxins," *Cell,* vol. 127, pp. 341-53, Oct 20 2006.

[131] S. O. Wikstrom and M. Anniko, "Early development of the stato-acoustic and facial ganglia," *Acta Otolaryngol,* vol. 104, pp. 166-74, Jul-Aug 1987.

[132] R. O. Bellairs, M, *The Atlas of Chick Development,* 2nd ed.: Elsevier Academic Press, 2005.

[133] S. Chen, M. Ji, M. Paris, R. L. Hullinger, and O. M. Andrisani, "The cAMP pathway regulates both transcription and activity of the paired homeobox transcription factor Phox2a required for development of neural crest-derived and central nervous system-derived catecholaminergic neurons," *J Biol Chem,* vol. 280, pp. 41025-36, Dec 9 2005.

[134] F. Monier-Gavelle and J. L. Duband, "Control of N-cadherin-mediated intercellular adhesion in migrating neural crest cells in vitro," *J Cell Sci,* vol. 108 (Pt 12), pp. 3839-53, Dec 1995.

[135] R. Zakany, E. Bako, S. Felszeghy, K. Hollo, M. Balazs, H. Bardos, P. Gergely, and L. Modis, "Okadaic acid-induced inhibition of protein phosphatase 2A enhances chondrogenesis in chicken limb bud micromass cell cultures," *Anat Embryol (Berl),* vol. 203, pp. 23-34, Jan 2001.

[136] A. Garcia, X. Cayla, J. Guergnon, F. Dessauge, V. Hospital, M. P. Rebollo, A. Fleischer, and A. Rebollo, "Serine/threonine protein phosphatases PP1 and PP2A are key players in apoptosis," *Biochimie,* vol. 85, pp. 721-6, Aug 2003.

[137] N. Parameswaran, W. S. Spielman, D. P. Brooks, and P. Nambi, "Okadaic acid stimulates caspase-like activities and induces apoptosis of cultured rat mesangial cells," *Mol Cell Biochem,* vol. 260, pp. 7-11, May 2004.

[138] M. L. Xing, X. F. Wang, X. Zhu, X. D. Zhou, and L. H. Xu, "Morphological and biochemical changes associated with apoptosis induced by okadaic acid in human amniotic FL cells," *Environ Toxicol,* Oct 20 2008.

[139] M. Mumby, "PP2A: unveiling a reluctant tumor suppressor," *Cell,* vol. 130, pp. 21-4, Jul 13 2007.

[140] M. G. Del Barrio and M. A. Nieto, "Relative expression of Slug, RhoB, and HNK-1 in the cranial neural crest of the early chicken embryo," *Dev Dyn,* vol. 229, pp. 136-9, Jan 2004.
[141] M. G. del Barrio and M. A. Nieto, "Overexpression of Snail family members highlights their ability to promote chick neural crest formation," *Development,* vol. 129, pp. 1583-93, Apr 2002.
[142] J. P. Liu and T. M. Jessell, "A role for rhoB in the delamination of neural crest cells from the dorsal neural tube," *Development,* vol. 125, pp. 5055-67, Dec 1998.
[143] W. J. Lee, D. U. Kim, M. Y. Lee, and K. Y. Choi, "Identification of proteins interacting with the catalytic subunit of PP2A by proteomics," *Proteomics,* vol. 7, pp. 206-14, Jan 2007.
[144] Z. Baharians and A. H. Schonthal, "Autoregulation of protein phosphatase type 2A expression," *J Biol Chem,* vol. 273, pp. 19019-24, Jul 24 1998.
[145] Y. Nakaya, E. W. Sukowati, Y. Wu, and G. Sheng, "RhoA and microtubule dynamics control cell-basement membrane interaction in EMT during gastrulation," *Nat Cell Biol,* vol. 10, pp. 765-75, Jul 2008.
[146] L. Yan, V. A. Lavin, L. R. Moser, Q. Cui, C. Kanies, and E. Yang, "PP2A regulates the pro-apoptotic activity of FOXO1," *J Biol Chem,* vol. 283, pp. 7411-20, Mar 21 2008.
[147] B. L. Theriault, T. G. Shepherd, M. L. Mujoomdar, and M. W. Nachtigal, "BMP4 induces EMT and Rho GTPase activation in human ovarian cancer cells," *Carcinogenesis,* vol. 28, pp. 1153-62, Jun 2007.
[148] A. Cano, M. A. Perez-Moreno, I. Rodrigo, A. Locascio, M. J. Blanco, M. G. del Barrio, F. Portillo, and M. A. Nieto, "The transcription factor snail controls epithelial-mesenchymal transitions by repressing E-cadherin expression," *Nat Cell Biol,* vol. 2, pp. 76-83, Feb 2000.
[149] A. H. Monsoro-Burq, E. Wang, and R. Harland, "Msx1 and Pax3 cooperate to mediate FGF8 and WNT signals during Xenopus neural crest induction," *Dev Cell,* vol. 8, pp. 167-78, Feb 2005.
[150] C. Bialojan and A. Takai, "Inhibitory effect of a marine-sponge toxin, okadaic acid, on protein phosphatases. Specificity and kinetics," *Biochem J,* vol. 256, pp. 283-90, Nov 15 1988.
[151] A. Franchini, L. Casarini, D. Malagoli, and E. Ottaviani, "Expression of the genes siamois, engrailed-2, bmp4 and myf5 during Xenopus development in presence of the marine toxins okadaic acid and palytoxin," *Chemosphere,* Aug 13 2009.
[152] V. Quaranta, "Cell migration through extracellular matrix: membrane-type metalloproteinases make the way," *J Cell Biol,* vol. 149, pp. 1167-70, Jun 12 2000.
[153] J. Westermarck, J. Lohi, J. Keski-Oja, and V. M. Kahari, "Okadaic acid-elicited transcriptional activation of collagenase gene expression in HT-1080 fibrosarcoma cells is mediated by JunB," *Cell Growth Differ,* vol. 5, pp. 1205-13, Nov 1994.
[154] I. Shoval, A. Ludwig, and C. Kalcheim, "Antagonistic roles of full-length N-cadherin and its soluble BMP cleavage product in neural crest delamination," *Development,* vol. 134, pp. 491-501, Feb 2007.
[155] Y. A. De Clerck, T. D. Yean, B. J. Ratzkin, H. S. Lu, and K. E. Langley, "Purification and characterization of two related but distinct metalloproteinase inhibitors secreted by bovine aortic endothelial cells," *J Biol Chem,* vol. 264, pp. 17445-53, Oct 15 1989.
[156] F. J. Naya, C. Wu, J. A. Richardson, P. Overbeek, and E. N. Olson, "Transcriptional activity of MEF2 during mouse embryogenesis monitored with a MEF2-dependent transgene," *Development,* vol. 126, pp. 2045-52, May 1999.
[157] A. Buchberger and H. H. Arnold, "The MADS domain containing transcription factor cMef2a is expressed in heart and skeletal muscle during embryonic chick development," *Dev Genes Evol,* vol. 209, pp. 376-81, Jun 1999.

[158] S. Chang, B. D. Young, S. Li, X. Qi, J. A. Richardson, and E. N. Olson, "Histone deacetylase 7 maintains vascular integrity by repressing matrix metalloproteinase 10," *Cell,* vol. 126, pp. 321-34, Jul 28 2006.
[159] J. M. Sontag and E. Sontag, "Regulation of cell adhesion by PP2A and SV40 small tumor antigen: an important link to cell transformation," *Cell Mol Life Sci,* vol. 63, pp. 2979-91, Dec 2006.
[160] D. L. Brautigan, "Flicking the switches: phosphorylation of serine/threonine protein phosphatases," *Semin Cancer Biol,* vol. 6, pp. 211-7, Aug 1995.
[161] A. C. Wilcock, J. R. Swedlow, and K. G. Storey, "Mitotic spindle orientation distinguishes stem cell and terminal modes of neuron production in the early spinal cord," *Development,* vol. 134, pp. 1943-54, May 2007.
[162] E. Menegola, M. L. Broccia, F. Di Renzo, V. Massa, and E. Giavini, "Relationship between hindbrain segmentation, neural crest cell migration and branchial arch abnormalities in rat embryos exposed to fluconazole and retinoic acid in vitro," *Reprod Toxicol,* vol. 18, pp. 121-30, Jan-Feb 2004.
[163] M. Offterdinger, S. M. Schneider, H. Huber, and T. W. Grunt, "Expression of c-erbB-4/HER4 is regulated in T47D breast carcinoma cells by retinoids and vitamin D3," *Biochem Biophys Res Commun,* vol. 258, pp. 559-64, May 19 1999.
[164] Y. Sakai, C. Meno, H. Fujii, J. Nishino, H. Shiratori, Y. Saijoh, J. Rossant, and H. Hamada, "The retinoic acid-inactivating enzyme CYP26 is essential for establishing an uneven distribution of retinoic acid along the anterio-posterior axis within the mouse embryo," *Genes Dev,* vol. 15, pp. 213-25, Jan 15 2001.
[165] S. Reijntjes, A. Blentic, E. Gale, and M. Maden, "The control of morphogen signalling: regulation of the synthesis and catabolism of retinoic acid in the developing embryo," *Dev Biol,* vol. 285, pp. 224-37, Sep 1 2005.
[166] Y. M. Lee, N. Osumi-Yamashita, Y. Ninomiya, C. K. Moon, U. Eriksson, and K. Eto, "Retinoic acid stage-dependently alters the migration pattern and identity of hindbrain neural crest cells," *Development,* vol. 121, pp. 825-37, Mar 1995.
[167] L. Wang, J. P. Mear, C. Y. Kuan, and M. C. Colbert, "Retinoic acid induces CDK inhibitors and growth arrest specific (Gas) genes in neural crest cells," *Dev Growth Differ,* vol. 47, pp. 119-30, Apr 2005.
[168] H. Watabe, Y. Soma, M. Ito, Y. Kawa, and M. Mizoguchi, "All-trans retinoic acid induces differentiation and apoptosis of murine melanocyte precursors with induction of the microphthalmia-associated transcription factor," *J Invest Dermatol,* vol. 118, pp. 35-42, Jan 2002.
[169] S. Guidato, C. Barrett, and S. Guthrie, "Patterning of motor neurons by retinoic acid in the chick embryo hindbrain in vitro," *Mol Cell Neurosci,* vol. 23, pp. 81-95, May 2003.
[170] N. D. Afonso and M. Catala, "Sonic hedgehog and retinoic acid are not sufficient to induce motoneuron generation in the avian caudal neural tube," *Dev Biol,* vol. 279, pp. 356-67, Mar 15 2005.
[171] S. Golz, T. Muhleisen, D. Schulte, and J. Mey, "Regulation of RALDH-1, RALDH-3 and CYP26A1 by transcription factors cVax/Vax2 and Tbx5 in the embryonic chick retina," *Int J Dev Neurosci,* vol. 26, pp. 435-45, Aug 2008.
[172] J. Mey, P. McCaffery, and M. Klemeit, "Sources and sink of retinoic acid in the embryonic chick retina: distribution of aldehyde dehydrogenase activities, CRABP-I, and sites of retinoic acid inactivation," *Brain Res Dev Brain Res,* vol. 127, pp. 135-48, Apr 30 2001.
[173] Bio-Rad, "AG® 1, AG MP-1 and AG 2 Strong Anion Exchange Resin Instruction Manual," LIT212 Rev C ed, B.-R. Laboratories, Ed.
[174] J. Li, J. D. Molkentin, and M. C. Colbert, "Retinoic acid inhibits cardiac neural crest migration by blocking c-Jun N-terminal kinase activation," *Dev Biol,* vol. 232, pp. 351-61, Apr 15 2001.
[175] W. S. Blaner, "Cellular metabolism and actions of 13-cis-retinoic acid," *J Am Acad Dermatol,* vol. 45, pp. S129-35, Nov 2001.

[176] A. Murayama, T. Suzuki, and M. Matsui, "Photoisomerization of retinoic acids in ethanol under room light: a warning for cell biological study of geometrical isomers of retinoids," *J Nutr Sci Vitaminol (Tokyo),* vol. 43, pp. 167-76, Apr 1997.

[177] H. J. Cahnmann, "A fast photoisomerization method for the preparation of tritium-labeled 9-cis-retinoic acid of high specific activity," *Anal Biochem,* vol. 227, pp. 49-53, May 1 1995.

[178] J. J. Repa, K. K. Hanson, and M. Clagett-Dame, "All-trans-retinol is a ligand for the retinoic acid receptors," *Proc Natl Acad Sci U S A,* vol. 90, pp. 7293-7, Aug 1 1993.

[179] M. Romeih, J. Cui, J. J. Michaille, W. Jiang, and M. H. Zile, "Function of RARgamma and RARalpha2 at the initiation of retinoid signaling is essential for avian embryo survival and for distinct events in cardiac morphogenesis," *Dev Dyn,* vol. 228, pp. 697-708, Dec 2003.

[180] M. A. Kane, N. Chen, S. Sparks, and J. L. Napoli, "Quantification of endogenous retinoic acid in limited biological samples by LC/MS/MS," *Biochem J,* vol. 388, pp. 363-9, May 15 2005.

[181] G. W. Tang and R. M. Russell, "13-cis-retinoic acid is an endogenous compound in human serum," *J Lipid Res,* vol. 31, pp. 175-82, Feb 1990.

[182] S. Schneider-Maunoury, P. Topilko, T. Seitandou, G. Levi, M. Cohen-Tannoudji, S. Pournin, C. Babinet, and P. Charnay, "Disruption of Krox-20 results in alteration of rhombomeres 3 and 5 in the developing hindbrain," *Cell,* vol. 75, pp. 1199-214, Dec 17 1993.

[183] P. J. Swiatek and T. Gridley, "Perinatal lethality and defects in hindbrain development in mice homozygous for a targeted mutation of the zinc finger gene Krox20," *Genes Dev,* vol. 7, pp. 2071-84, Nov 1993.

[184] J. P. Golding, H. Tidcombe, S. Tsoni, and M. Gassmann, "Chondroitin sulphate-binding molecules may pattern central projections of sensory axons within the cranial mesenchyme of the developing mouse," *Dev Biol,* vol. 216, pp. 85-97, Dec 1 1999.

[185] H. Hoshino, T. Uchida, T. Otsuki, S. Kawamoto, K. Okubo, M. Takeichi, and O. Chisaka, "Cornichon-like protein facilitates secretion of HB-EGF and regulates proper development of cranial nerves," *Mol Biol Cell,* vol. 18, pp. 1143-52, Apr 2007.